

SYNTHESIS OF DONOR-ACCEPTOR-DONOR MOLECULES FOR PREPARATION  
OF STABLE n-DOPING POLYMERS

THESIS

Presented to the Graduate Council of  
Texas State University-San Marcos  
in Partial Fulfillment  
of the Requirements

for the Degree

Master of SCIENCE

by

Makda T. Araya, B.S.

San Marcos, Texas  
December 2012

SYNTHESIS OF DONOR-ACCEPTOR-DONOR MOLECULES FOR PREPARATION  
OF STABLE n-DOPING POLYMERS

Committee Members Approved:

---

Jennifer Irvin, Chair

---

Gary Beall

---

Benjamin Martin

Approved:

---

J. Michael Willoughby  
Dean of the Graduate College

**COPYRIGHT**

by

Makda T. Araya

2012

## **FAIR USE AND AUTHOR'S PERMISSION STATEMENT**

### **Fair Use**

This work is protected by the Copyright Laws of the United States (Public Law 94-553, section 107). Consistent with fair use as defined in the Copyright Laws, brief quotations from this material are allowed with proper acknowledgement. Use of this material for financial gain without the author's express written permission is not allowed.

### **Duplication Permission**

As the copyright holder of this work I, Makda Araya, authorize duplication of this work, in whole or in part, for educational or scholarly purposes only.

## ACKNOWLEDGEMENTS

This thesis would not be possible if it were not for Dr. Jennifer Irvin's tireless help and guidance. Not only has she allowed me to work in her lab but also spent hours teaching me valuable organic synthesis techniques, edited all of my writings and presentations and encouraged my work by holding many one-to-one progress meetings. I would also like to acknowledge the rest of my committee members, Dr. Gary Beall and Dr. Benjamin Martin, for editing my thesis and training me on the X-ray diffraction instrument and helping solve crystal structures.

When I joined the Irvin Lab, I had no experience with organic chemistry. The Irvin lab members were all helpful. Katie Winkel showed me all of the basic techniques from flame drying to Schlenk line operation and set up of complicated apparatus. I really appreciate her taking the time to thoroughly answer all of my questions and allowing me to shadow her for weeks. Jamie Carberry was kind enough to teach me how to use the glovebox and actually close the big antechamber every time I use it. I would also like to thank Blake Bowden, Leslie Wood, James Warren and Adrian Bergia for sharing their knowledge and welcoming me to the group. I am thankful to Dr. Charles J. Neef for his expertise advice and demonstration of column packing. I had the pleasure of guiding the research efforts of two undergraduate students, Raddiete Ghion and Derek Medellin, whose precursor syntheses saved me countless hours. Also, I am thankful for Sarah Stammnitz and Brad Rodier for adding to the Irvin Lab ambiance.

The Texas State Chemistry and Biochemistry department is a supportive group. I thank Dr. Todd Hudnall, Dr. David Irvin, Grant Bemis and Jingfang Yu for training me in NMR, Photo-reactor, crystal isolation and mounting, and microwave reaction, respectively. I thank Laurie Ellis was for keeping my paperwork in order and David Fehlis for letting me borrow chemicals from the stock room.

Lastly, I would like to acknowledge my supportive mom, sister, uncle, the rest of my family in Asmara, Eritrea and my wonderful friends. I could not have done it without their encouragement and prayers.

This manuscript was submitted on July 18th, 2012.

## TABLE OF CONTENTS

ACKNOWLEDGMENTS.....	v
LIST OF FIGURES.....	ix
LIST OF SCHEMES .....	xi
LIST OF TABLES.....	xiii
ABSTRACT.....	xiv
CHAPTER	
I. INTRODUCTION TO ELECTROACTIVE POLYMERS.....	1
Electroactive Polymer Background .....	1
Doping Processes in Electroactive Polymers.....	2
Band Gap.....	4
Approaches to Stable n-Doping Polymers .....	6
Coupling Strategies for Use in Monomer Synthesis.....	7
Polymerization Methods .....	10
Applications .....	11
Motivation for Research .....	12
II. SYNTHESIS OF BISTHIENYLPYRIMIDINES, BISTHIENYLBIPYRIMIDINES, AND BISTHIENYLPYRAZINES.....	13
Background.....	13
Experimental .....	14
Materials .....	14
Instrumentation.....	15
Synthesis.....	15
2,2'-Bipyrimidine.....	15
5,5'-Dibromo-2,2'-bipyrimidine.....	16
3-Chloropyrazine 1-oxide .....	17
Dichloropyrazines .....	17

Results and Discussion .....	20
Bisthienylpyrimidine Structural Determination.....	21
Attempted Synthesis of Bisthienylbipyrimidines .....	26
Bisthienylpyrazines.....	28
Conclusions.....	32
III. SYNTHESIS OF BISTHIENYLFLUOROPYRAZINES.....	33
Background.....	33
Experimental.....	34
Materials.....	34
Instrumentation.....	34
Synthesis .....	35
2-Fluoro-3,6-(thien-2-yl)-pyrazine (BTFPz) .....	36
2-Bromo-3,4-ethylenedioxythiophene .....	37
2-Fluoro-3,6-(3,4-ethylenedioxythien-2-yl)-pyrazine (BEFPz).....	37
Results and Discussion .....	38
Conclusions.....	41
IV. SYNTHESIS OF BISTHIADIAZOLYL BENZENES.....	42
Background.....	42
Experimental.....	44
Materials .....	44
Instrumentation .....	44
Synthesis .....	44
1,4-Bis-1,3,4-thiadiazolyl benzene (BTdB).....	44
2,5-Dibromohydroquinone (DBrHq) .....	45
1,4-Bis-1,3,4-thiadiazolyl-2,5-bis(hexadecyloxy)benzene (BTdB <sub>16</sub> ).....	47
Results and Discussion .....	48
Conclusions .....	50
V. CONCLUDING REMARKS .....	51
Conclusions.....	51
Future Work.....	51
APPENDIX A.....	54
APPENDIX B.....	76
REFERENCES .....	81

## LIST OF FIGURES

Figure	Page
1. Common heteroatomic rings.....	2
2. From left to right, examples of polymers that have been doped: polythiophene (pT), poly(3,4-ethylenedioxythiophene) (pEDOT), poly(phenylenevinylene) (pPV), polyaniline (pANI), and polypyrrole (pPy) .....	3
3. Doping chromatics of poly[2,5-bis(3,4-ethylenedioxythien-2-yl)pyridine] .....	4
4. Band gap decreases as conjugation increases .....	5
5. General mechanism for palladium catalyzed C-C formation .....	9
6. Oxidative polymerization of thiophene .....	11
7. Proposed monomers for stable n-doping polymers .....	12
8. 2,5-Bis(thien-2-yl)pyrimidine (BTPm, left) and 2,5-bis(3,4-ethylenedioxythien-2-yl)pyrimidine (BEPm, right).....	21
9. Resolved structure of BTPm (yellow=sulfur, blue=nitrogen, black=carbon and white=hydrogen).....	22
10. Ring flipping disorder of BTPm .....	23
11. Planarity of BTPm .....	24
12. Unit cell packing of BTPm (left); donors and acceptors are aligned for maximum $\pi$ - $\pi$ stacking .....	25
13. 2,5-Bis(thien-2-yl)-2,2'-bipyrimidine (BTPm, left) and 2,5-bis(3,4-ethylenedioxythien-2-yl)-2,2'-bipyrimidine (BEPm, right) .....	26
14. Bisthienylpyrazines.....	28

15. Possible bithienylpyrazine isomers .....	30
16. Bithienylfluoropyrazines .....	34
17. Bithiadiazolylbenzenes.....	43

## LIST OF SCHEMES

Schemes	Page
1. Doping processes of polythiophene .....	2
2. Non-redox doping of polyaniline (pANI) .....	3
3. Heck coupling synthesis of styrene .....	8
4. General reaction scheme of Sarandeses coupling .....	9
5. Synthesis of 2,2'-bipyrimidine .....	27
6. Bromination of 2,2'-bipyrimidine .....	28
7. Synthesis of 3-chloropyrazine 1-oxide .....	29
8. Synthesis of dichloropyrazines .....	29
9. Sarandeses coupling of dichloropyrazine isomers with thiophene to yield 2,3-bis(thien-2-yl)pyrazine (2,3-BTPz) and 2,5-bis(thien-2-yl)pyrazine (2,5-BTPz) .....	31
10. Sarandeses coupling of dichloropyrazine isomers with EDOT to yield 2,3-bis(3,4-ethylenedioxythien-2-yl)pyrazine (2,3-BEPz) and 2,5-bis(3,4-ethylenedioxy thien-2-yl)pyrazine (2,5-BEPz) .....	31
11. Aromatic nucleophilic substitution of 2-chloropyrazine .....	39
12. Stannylation of 2-fluoropyrazine .....	39
13. Stille coupling of 2-fluoro-3,6-bis(tributylstannyl)pyrazine with 2-bromothiophene .....	40
14. Bromination of EDOT .....	41
15. Stille coupling of 2-fluoro-3,6-bis(tributylstannyl)pyrazine with BrEDOT .....	41
16. Synthesis of 1,4-bis-(1,3,4-thiadiazol-2-yl)benzene (BTdB) .....	48

17. Bromination of hydroquinone.....	49
18. Etherification of 1,4-dibromohydroquinone .....	49
19. Synthesis of 1,4-bis-(1,3,4-thiadiazol-2-yl)-2,5-bis-hexadecyloxybenzene (BTdBC <sub>16</sub> ).....	49

## LIST OF TABLES

<b>Tables</b>	<b>Page</b>
1. Selected crystallographic data for BTPm .....	22
2. Recrystallization of BEPm.....	26

## ABSTRACT

### SYNTHESIS OF DONOR-ACCEPTOR-DONOR MOLECULES FOR PREPARATION OF STABLE n-DOPING POLYMERS

by

Makda T. Araya, B.S.

Texas State University-San Marcos

December 2012

SUPERVISING PROFESSOR: JENNIFER A. IRVIN

Electroactive polymers are polymers that switch reversibly between insulating and conducting states. Their unique properties enable them to be used in a wide range of applications including electrochemical capacitors, sensors and electrochromics. This research is focused on conjugated, high-nitrogen content, heterocyclic monomers for stable n-doping polymers. To minimize band gap, compounds of significantly different electronic properties are coupled. Pyrimidines, pyrazines and benzenes will be used as precursors to couple with thien-2-yl, 3,4-ethylenedioxythien-2-yl and 1,3,4-thiadiazolyl rings. The mixing of electron-rich rings with high electron affinity heterocycles facilitates efficient electron mobility and stabilizes n-doping of resultant polymers.

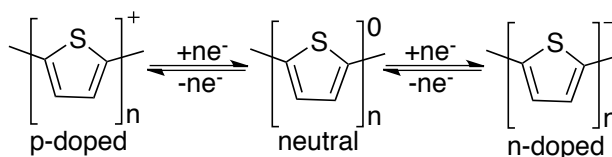
## CHAPTER I

### INTRODUCTION TO ELECTROACTIVE POLYMERS

#### Electroactive Polymer Background

In the late 1970s, it was discovered that conjugation and doping increased the conductivity of polymers.<sup>1</sup> The resultant electroactive polymers (EAPs) switch reversibly between insulating and conducting states. These intrinsically conductive polymers are easier to process and offer cheap alternatives to inorganic conductors. Their unique properties enable them to be used in a wide range of applications including electrochemical capacitors, photovoltaics, sensors and electrochromics.<sup>1,2</sup> With greater demand for nanoscaling and efficiency, EAPs are drawing much attention.

Conjugated, heterocyclic monomers are oxidatively polymerized either chemically or electrochemically. The resultant conjugated polymers can be repeatedly reduced and oxidized, switching between conducting and insulating states. Upon positive doping (p-doping), electrons are removed from a polymer yielding positive charges along the polymer chain.<sup>1</sup> During negative doping (n-doping), electrons are added to the neutral polymer yielding negative charges along the polymer chain. Thus, neutral polymers are converted to oxidized or reduced states via p-doping or n-doping, respectively (Scheme1). Suitable electrolyte media are used to provide counter ions.



**Scheme 1:** Doping processes of polythiophene

### Doping Processes in Electroactive Polymers

EAPs are insulators or semiconductors in the neutral state; metallic level conductivity is achieved via doping. As doping level increases, conductivity increases from insulating to semiconducting to metallic.<sup>3</sup> Such polymers usually contain multiple aromatic rings in conjugation with each other in the backbone to stabilize charge transfer. Conjugated polymers can be subjected to both p- and n-doping.

Many conjugated aromatic polymers contain heterocyclic rings (Figure 1) incorporating sulfur, nitrogen, or oxygen. Polythiophene (pT, Figure 2) and its derivatives have been found to be highly stable with and without p-doping.<sup>3</sup> p-Doped polymers are the more stable and studied polymers. Other examples of stable p-type polymers (Figure 2) are polyaniline (pANI), poly(phenylenevinylene) (pPV), and polypyrrole (pPy).

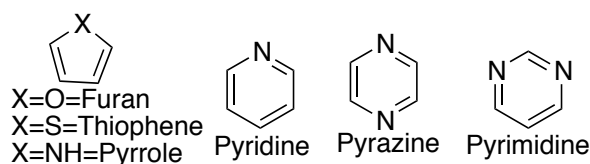


**Figure 1:** Common heteroatomic rings

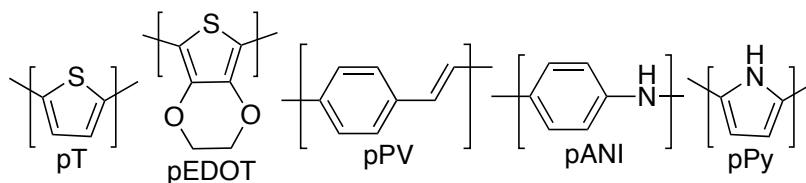
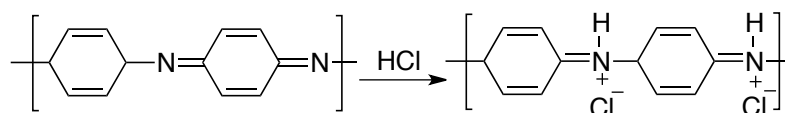


**Figure 2:** From left to right, examples of polymers that have been doped: polythiophene (pT), poly(3,4-ethylenedioxythiophene) (pEDOT), poly(phenylenevinylene) (pPV), polyaniline (pANI), and polypyrrole (pPy)

Either chemical or electrochemical methods can be used to affect redox doping.

Redox doping is when  $\pi$  electrons are mobilized to and from the polymer. Conversely, non-redox doping employs the use of protonic aqueous acids to introduce charges.<sup>3</sup> This type of doping is shown in Scheme 2. The amount of doping is relevant to the pH of the solution. While many stable p-doped polymers have been synthesized, current researchers are faced with instability, highly negative reduction potentials and air-sensitivity of n-doping polymers.<sup>3,4,5,6,7,9</sup>



**Scheme 2:** Non-redox doping in polyaniline (pANI)

Figure 3 shows an example of a polymer that undergoes non-redox doping as well as p-doping and n-doping. Note that each state of the polymer has a distinct color; differences in color as a result of doping state have led researchers to pursue electrochromic applications of EAPs.<sup>16</sup> In 1995, Arbizzani *et al.*<sup>22</sup> effectively n- and p-doped polydithieno [3,4-B: 3',4'-D]thiophene (pDTT). Two years earlier, Zotti and company<sup>4</sup> discovered that the n-type polydithienylvinylene (pDTV) is 10-100 times less electroactive than the p-type. This was thought at the time to be due to the large cation

counter ions (tetra-n-alkyl ammonium dopant) used hindering electron mobility by increasing interchain distances.<sup>4</sup> Small alkali metal ions such as  $\text{Li}^+$ ,  $\text{Na}^+$ ,  $\text{K}^+$  and  $\text{Cs}^+$  stabilize n-doping of polythiophene (pT) for capacitors.<sup>3</sup> This is supported by Eiji and coworkers' comparative study of lithium perchlorate and tetraethyl ammonium perchlorate as electrolytes.<sup>8</sup>

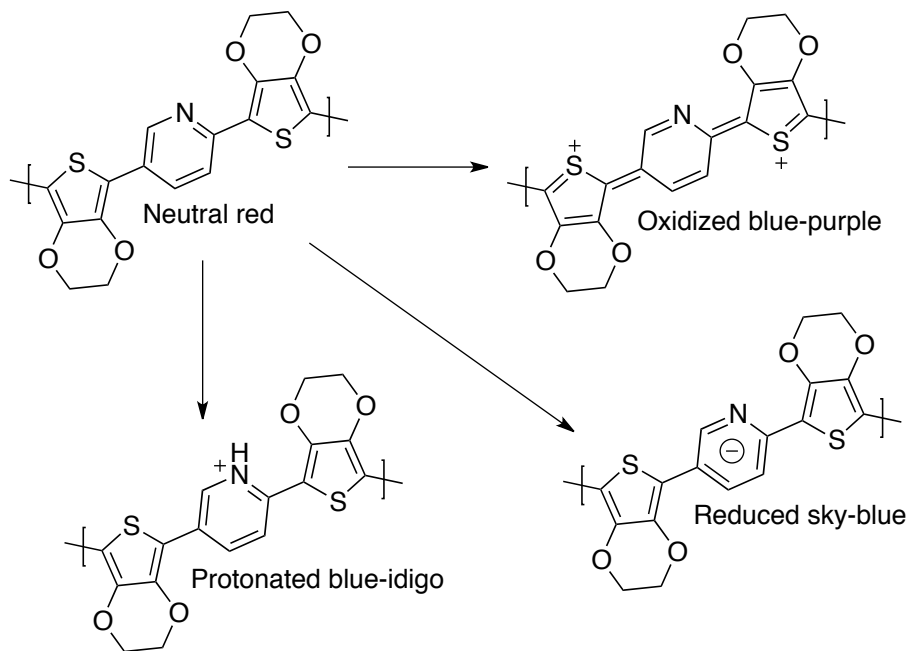


**Figure 3:** Doping chromatics of poly[2,5-bis(3,4-ethylenedioxythien-2-yl)pyridine]<sup>17</sup>

### Band Gap

The band gap,  $E_g$ , is the energy difference between the highest occupied molecular orbital (HOMO) and the lowest unoccupied molecular orbital (LUMO). For a material to be conductive,  $E_g$  must be low enough for electrons to hop from the valence band to the conducting band. Although organic materials have higher band gaps than inorganic materials, modifying organic structures offers ways of lowering band

gap.<sup>3,6,7,9,21,22,23,24,32,34</sup> Generally, band gap can be lowered by increasing conjugation<sup>1,3</sup>, increasing planarity<sup>2-15</sup> and doping.<sup>4</sup>

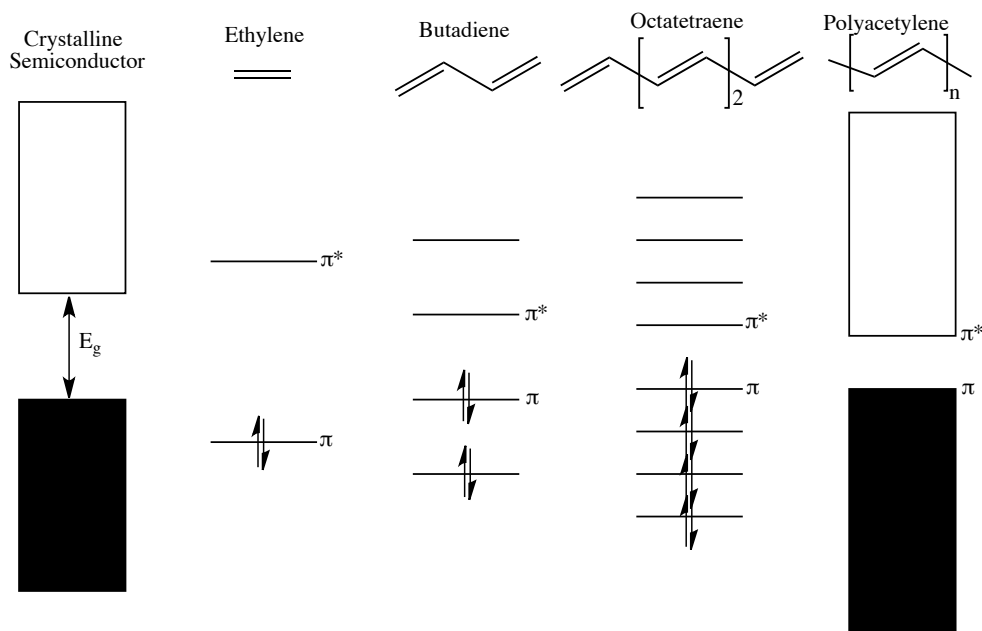


**Figure 4:** Band gap decreases as conjugation increases

Conjugation is important to conductivity since  $\pi$  orbitals are required for electron mobility.<sup>9</sup>  $\sigma$ - $\sigma^*$  Electron hopping is impossible since the energy difference between the  $\sigma$  orbitals is too large.<sup>9</sup> In contrast,  $\pi$ - $\pi^*$  energies are shorter and optimal for conductivity. The higher the degree of conjugation, the greater the number of  $\pi$  orbitals are available for overlap, and the lower the  $E_g$ . Aromatic rings in polymer backbones increase conjugation and planarity of electroactive polymers, increasing electron mobility along the polymer chain.<sup>2-9,10,11</sup> Lastly, doping decreases  $E_g$  by creating intermediate bands between the HOMO and LUMO to act as stepping-stones for electrons. These energy bands are created through the high energy charged states of polymers upon doping. The stability of n-doping EAPs is typically poor due to the instability of carbanions formed during the reductive processes.<sup>12</sup>

### Approaches to Stable n-Doping Polymers

p-Doped polymers dominate electroactive polymer research. Cations and anions are highly reactive species but cations are intrinsically more stable than anions. Cations and anions are highly reactive species, but cations are more stable than anions.<sup>13</sup> Thus, stable p-doped polymers are abundant, while stable n-doped polymers have remained elusive.

According to Arbizzani and coworkers,<sup>31</sup> the highly negative potentials needed to n-dope polymers cause “high self-discharge and low electrode life-cycle,” making n-doping not ideal. To battle the instability of n-doped polymers, polymers with an electron-withdrawing group on aromatic rings have been synthesized. The race to manufacture ambient environmentally safe n-doped polymers continues to broaden applications of conductive polymers to light emitting diodes and transistors.<sup>13</sup>

For battery and capacitor applications, n-doped polymers have been shown to be stable with small alkali metals such as  $\text{Li}^+$ ,  $\text{Na}^+$ ,  $\text{K}^+$  and  $\text{Cs}^+$ .<sup>14</sup> Small metals are better able to penetrate and counter the negative charges than bigger ions. One way to stabilize any charge, positive or negative, is to have a highly conjugated system where charge is delocalized through resonance. Pendant electron withdrawing groups have been incorporated<sup>15</sup> to stabilize negative charges by withdrawing electron density from the polymer backbone. A drawback to this method is the reduction of conductivity due to charge trapping and increase in interchain distances. Short interchain distances are required for  $\pi$ - $\pi$  stacking to allow bidirectional electron mobility.<sup>4</sup> Conductivity and stability are further optimized by carefully choosing conjugated systems with donating

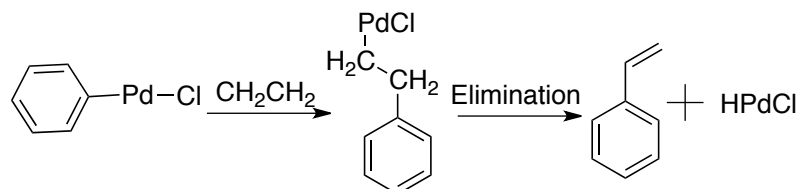
and accepting capabilities within a given monomer. The acceptors' high affinity for electrons lowers the LUMO.<sup>8,16</sup>

Heteroatoms of sulfur, oxygen and nitrogen have been utilized as acceptors;  $sp^2$  hybridized nitrogen-containing heteroatoms are particularly electron deficient, lowering the LUMO.<sup>8,16</sup> Since the LUMO energy level is governed by the electron acceptor and the HOMO energy level is governed by the electron donor, electron donors are designed to be stable, electron rich conjugated systems that have low oxidization potential.<sup>17</sup> Donor rings are integrated as terminal moieties to facilitate a low potential electropolymerization, giving rise to donor-acceptor-donor monomers. Manipulating the donor-acceptor ratios and attaching various functional groups to the polymer enhances n-doping stability. Usually, conjugated systems (heterocyclic or not) are added as acceptors to thiophene or similar donating groups. Acceptor groups are chosen to be heteroatomic, conjugated rings that are electron poor and have higher oxidization potential.

### Coupling Strategies for Use in Monomer Synthesis

Coupling reactions include reactions that form C-C bonds from an organohalide and organometallic in the presence of transition metal catalyst. Heck and co-workers pioneered cross-coupling reactions in the late 1960s.<sup>18</sup> Heck successfully prepared styrene by reacting ethylene with phenyl palladium chloride at room temperature (Scheme 3). Since then, this synthetic breakthrough has been optimized and referred to as the Heck cross-coupling reaction. Almost a decade later, in 1976, Negishi was able to incorporate organozinc compounds in palladium-catalyzed couplings to introduce functionality to simple aromatic substrates.<sup>19,20</sup> Around the same time, Suzuki<sup>11,21</sup> perfected organoboron

reagents as nucleophiles in a palladium catalyzed cross coupling while Migita<sup>11,22</sup> and Stille<sup>11</sup> discovered organotin reagent nucleophiles. More recently, Sarandeses et al. broadened palladium-induced chemistry with the incorporation of organoindium reagents.<sup>16</sup>



**Scheme 3:** Heck coupling synthesis of styrene

Advances in coupling chemistry have been recognized in Chemistry Nobel Prizes in 1912 (Grignard Reaction), 1963 (Ziegler-Natta Polymerization), 1979 (Wittig reaction), 1990 (Corey-House Reaction), 2005 (Grubbs/Schrock/Shauvin Metathesis) and 2010 (Heck/Negishi/Suzuki Pd catalysis).<sup>23</sup> Over the decades, many new synthetic discoveries have led to efficient functionalization of aryls. Although Grignard, Diels–Alder and Wittig reactions have been instrumental in the advancement of organic chemistry, cross-coupling reactions have dominated polymer and biological chemistry. These palladium-initiated reactions consist of four basic steps (Figure 5): oxidative addition of the arylhalide to palladium via the insertion of palladium between an aryl carbon and the adjacent halide, transmetalation during which a second aryl group replaces the halide on palladium, trans/cis isomerization, and lastly, reductive elimination of the tetravalent palladium and its two ligands and the formation of the desired aryl-aryl bond.

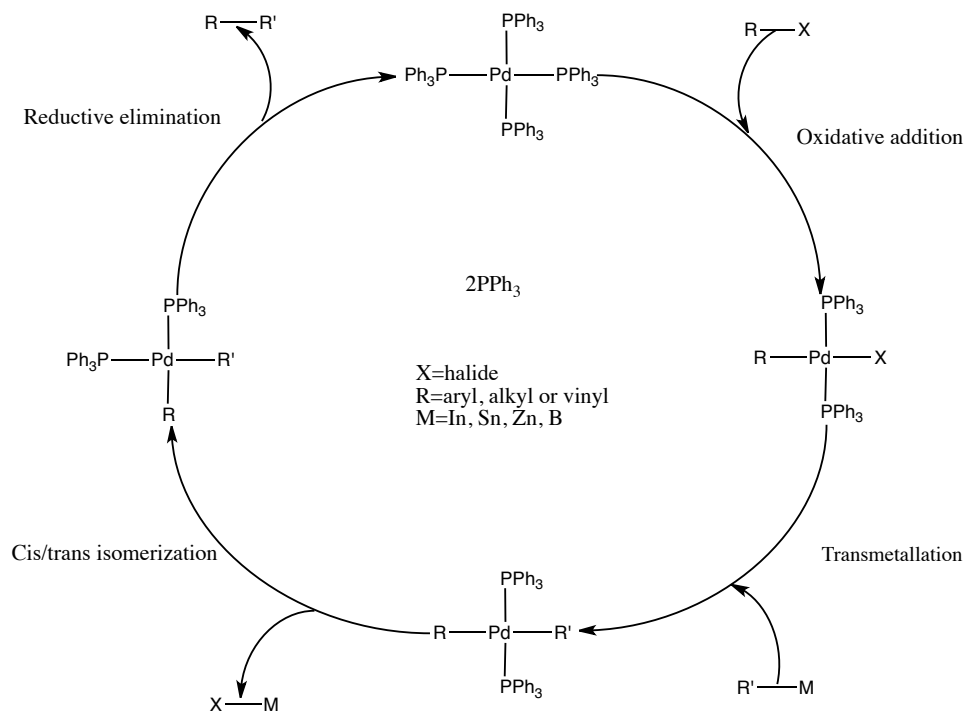
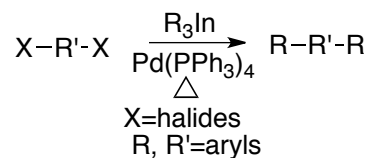


**Figure 5:** General mechanism for palladium catalyzed C-C formation

These coupling reactions are fairly efficient and offer good yields. Due to their simplicity, such reactions are utilized in both organic synthesis and pharmaceutical manufacturing.<sup>20</sup> Sarandeses<sup>52</sup> (Scheme 4) and Toudic<sup>24</sup> and their respective coworkers demonstrated organoindium and organotin reagents, respectively, in effecting C-C formation with high-nitrogen heterocycles.



**Scheme 4:** General reaction scheme of Sarandeses coupling

### Polymerization Methods

Polymers are produced via oxidative (chemical or electrochemical) or non-oxidative routes. Non-oxidative polymerizations include chemical or thermal elimination of precursors as well as coupling reactions.<sup>25,26,27</sup> Non-oxidative polymerizations produce reduced, regioregular, higher molecular weight soluble polymers while oxidative polymerization tends to give simple, oxidized and slightly insoluble and lower molecular weight polymers, depending on the monomer. Since regioirregularity is problematic, decreasing conjugation and tensile strength of the polymer, symmetric monomers and regioregular polymerizations are sometimes preferred.<sup>7</sup> Regioirregularity in polymer films affects charge mobility and absorption ability.<sup>28</sup>

Electrochemical oxidative polymerization uses an electrode and current to grow polymers on a conductive substrate while chemical oxidative polymerization uses oxidizing salts such as ferric chloride. Both polymerization techniques remove a single electron from a monomer to create a radical cation. The radical cation combines with neutral monomers creating other radical cations as the polymer grows or radical cations combine to create dicationic dimers (Figure 6).<sup>51</sup> Chemical oxidation faces over-oxidation and solubility limitations.

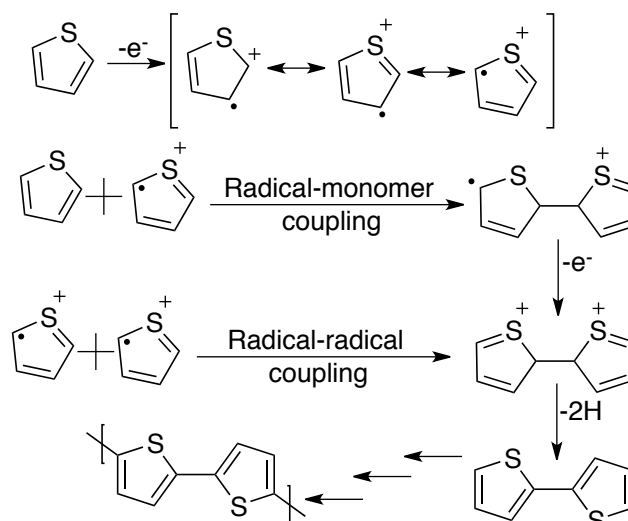


**Figure 6:** Oxidative polymerization of thiophene

### Applications

Electroactive polymers are great candidates for use in electrochemical capacitors (also known as supercapacitors or ultracapacitors)<sup>29</sup> due to the intrinsic versatility of electrochemical processes. Polymers' conductivity can reach metallic status when doped; doping is necessary for battery and capacitor applications of EAPs. Electroactive polymer-based electrochemical capacitors (EPECs) use an EAP as at least one electrode. Using a p-doped polymer as the anode and an n-doped polymer as the cathode produces a so-called "Type IV" EPEC.<sup>30</sup> EPECs with the latter conformation have shown to have greater power and charge mobility than conventional capacitors.<sup>31</sup> Such systems are usually achieved by engineering a push and pull of electron donor-acceptor structures in the monomer.

Doping is also necessary for photovoltaics/solar cells. There are three types of organic solar cell structures. The bulk heterojunction is a polymer electron donor-acceptor blend that addresses both the surface area and thickness of films increasing

electron mobility, charge separation and exciton diffusion. Bulk heterojunction uses high electron affinity and ionization potential compounds as electron donors and fullerene or its derivatives as electron acceptors. Conductivity is further optimized by carefully choosing conjugated systems with donating and accepting capabilities within a given blend.<sup>32,33</sup>

### Motivation for Research

The demand for efficiency and green-friendly source of energy has driven the last couple of decades' research. Conductive polymers offer a wide range of applications in solar cells, capacitors and LEDs. The motivation for this research is to make stable n-doping polymers with high electron mobility. The syntheses of seven novel donor-acceptor-donor molecules and a known molecule (2,5-bisthien-2-ylpyrazine, BTPz)<sup>34</sup> are discussed herein (Figure 7). High-nitrogen, conjugated heterocyclic compounds are chosen to increase the mobility of electrons by decreasing the  $E_g$  through  $\pi$ - $\pi$  stacking and stabilization of the HOMO energy levels, yielding stable n-doping polymers.

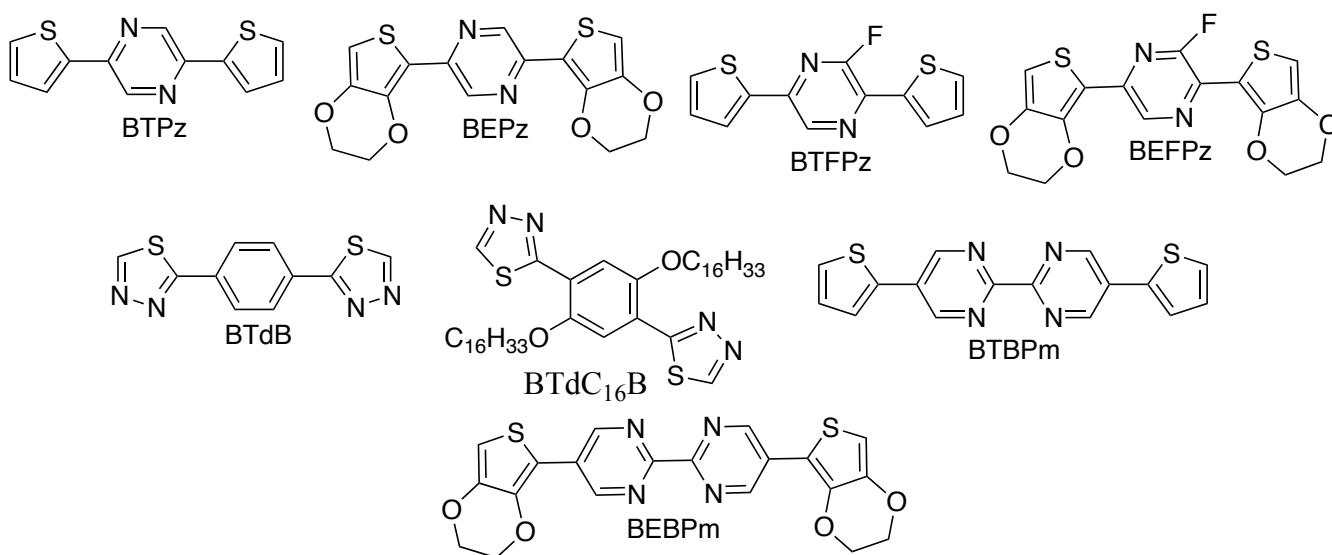


**Figure 7:** Proposed monomers for stable n-doping polymer

## CHAPTER II

### SYNTHESIS OF BISTHIENYLPYRIMIDINES, BISTHIENYLBIPYRIMIDINES, AND BISTHIENYLPYRAZINES

#### Background

As the amount of nitrogen content increases, a broad range of optical properties are observed in donor-acceptor moieties.<sup>16</sup> “Higher chemical and electrochemical reducibility” is reached going from poly(p-phenylene) to poly(pyridine-2,5-diyl) to poly(pyrimidine-2,5-diyl) and lastly to poly(pyrazine-2,5-diyl).<sup>35</sup> Reducibility, n-doping ability, is increased with increasing nitrogen-content and by increasing the number of carbons between nitrogens. Bisthienylpyridines<sup>36,37</sup> have been used to prepare n-doping polymers, but long term stability is not sufficient for use in desired applications. Acceptor ability is directly related to electron affinity. Electron affinity increases from -0.62eV for pyridine to 0eV for pyrimidine to +0.25eV for pyrazine.<sup>49</sup> Therefore, replacing the pyridine acceptor with pyrimidine or pyrazine should significantly improve stability of n-doped polymers.

Since electron affinity and an acceptors’ strength increases with increasing number of nitrogens, incorporation of high-nitrogen content acceptors within a monomer is expected to stabilize n-doping. To make stable n-doped donor-acceptor molecules,

high-nitrogen content heterocycles of pyrazines and pyrimidines were assembled as acceptor moieties. High-nitrogen content acceptors were coupled with known good donors, 3,4-ethylenedioxythiophene (EDOT) and thiophene.

## Experimental

### Materials

EDOT was purchased from Aldrich and purified as follows: dissolved in dichloromethane, washed thrice with 0.1M HCl, neutralized in saturated sodium bicarbonate, dried over anhydrous MgSO<sub>4</sub>, filtered through neutral alumina, evaporated under reduced pressure, vacuum distilled and stored in the freezer under argon. EDOT, n-butyl lithium (n-BuLi, 2.5M in hexanes), and anhydrous tetrahydrofuran (THF) were purchased from Aldrich and used as received.

Tetrakis(triphenylphosphine) palladium(0), 2-bromothiophene, indium chloride, 2-chloropyrazine, phosphoryl oxychloride, triphenyl phosphine, calcium chloride, N,N-dimethylformamide (DMF), ethylenediaminetetraacetic acid (EDTA), bromine and toluene were purchased from Acros and used as received. Diethyl ether, ethyl acetate, hexanes, ethanol (95%), dichloromethane, hydrochloric acid, glacial acetic acid, ammonium chloride, methanol, hydrogen peroxide (30%), sodium bicarbonate and anhydrous magnesium sulfate were purchased from Fisher Scientific and used as received. Column chromatography was accomplished using Selecto Scientific 32-63  $\mu\text{m}$  silica gel purchased from Fisher Scientific. 5-Chloropyrimidine was purchased from Acros and purified via sublimation prior to use. Nickel chloride hexahydrate

(NiCl<sub>2</sub>·6H<sub>2</sub>O) and zinc metal were purchased from Alfa Aesar and used as received. Ammonium hydroxide was purchased from EMD Chemicals Incorporation and used as received. 2,5-Bis(thien-2-yl)pyrimidine (BTPm) and 2,5-bis(3,4-ethylenedioxythien-2-yl)pyrimidine (BEPm) were synthesized by Winkel<sup>40</sup> and used as received.

### Instrumentation

Single crystal X-ray diffraction measurements were performed at the Texas State University—San Marcos X-ray laboratory, using a Rigaku SCX-Mini diffractometer, equipped with a Mo tube and SHINE optics. Crystals were mounted on a glass fiber for measurement. Data collection and data integration were completed using Process-Auto.<sup>38</sup> Solutions were generated by direct methods using SHELXS-97, and refined by full-matrix least squares on *F*<sup>2</sup> using SHELXL-97.<sup>39</sup>

Compounds were characterized using melting point determination (MP) and nuclear magnetic resonance (NMR) spectroscopy. <sup>1</sup>H and <sup>13</sup>C NMR were accomplished with Varian INOVA 400 MHz NMR and a Bruker Avance III 400 MHz NMR while MPs were determined using Mel-Temperature Electrochemical with Fluke 51 thermometer detector. Structure drawing and estimation of <sup>1</sup>H and <sup>13</sup>C NMR chemical shifts was accomplished using CS ChemDraw NMR Pro Version 6.0.

### Synthesis

**2,2'-Bipyrimidine:** This molecule was synthesized according to literature procedure.<sup>46</sup> A flame dried 1000mL 3-neck round bottom flask was fitted with gas-inlet adapter, condenser and septum. DMF (493.4mL) was added to the flask via cannula

transfer and bubbled with argon for 18 hours. Triphenyl phosphine (34.4g, 131mmol), Zn (4.28g, 65.5mmol) and  $\text{NiCl}_2 \cdot 6\text{H}_2\text{O}$  (7.78g, 32.8mmol) were dried for 20-30 minutes in a vacuum desiccator prior addition to the reaction flask under positive argon flow. The reaction mixture turned black/red from dark green upon stirring. 2-Chloropyrimidine (15g, 131mmol) was added to the flask and stirred at room temperature for 1 hour. The reaction was heated at  $50^\circ\text{C}$  for 74 hours. After cooling, the reaction mixture was filtered through Celite® and washed with chloroform. Evaporation under reduced pressure yielded a glassy dark red solid. The solid was suspended in a solution of EDTA (75g) in 7% ammonia, extracted 8 times with diethyl ether to remove the yellow triphenyl phosphine and extracted 8 more times with chloroform to yield fluorescent orange organic layers. The orange organic layers were combined, dried over  $\text{MgSO}_4$  and evaporated under reduced pressure to yield a pale yellow solid. 2,2'-Bipyrimidine was purified by sublimation to yield white solid (4.63g, 22.4%). Experimental MP range of  $109.6\text{-}111.1^\circ\text{C}$  was consistent with literature<sup>52</sup> MP range of  $113\text{-}115^\circ\text{C}$ .  $^1\text{H NMR}$  ( $\text{CDCl}_3$ , 400 MHz)  $\delta$  9.0 (s, 2H), 7.4 (t, 4H). (Lit:<sup>52</sup> ( $\text{CDCl}_3$ , 300 MHz)  $\delta$  9.02 (d, 2H), 7.44 (t, 4H)).

**5,5'-Dibromo-2,2'-bipyrimidine:** 5,5'-Dibromo-2,2'-bipyrimidine was attempted via a modification of Song and coworkers' protocol.<sup>53</sup> Reactions of 2,2'-bipyrimidine (200mg, 1.27mmol) and 2.2 equivalents of bromine (0.143mL, 7.79mmol) were subjected to microwave and photo reaction using  $\text{CCl}_4$  (10mL) or dichloromethane/acetic acid (1:1; 10mL) as reaction solvents. Microwave reactions of  $155^\circ\text{C}$  for 5 minutes,  $75^\circ\text{C}$  for 5 minutes,  $75^\circ\text{C}$  for 10 minutes and  $155^\circ\text{C}$  for 10 minutes

were carried out with and without the presence of FeBr<sub>3</sub> (3.7mg). Photo reactions of 12, 24 and 48 hours at temperature cycling range of 146-154°C were also carried out. Reaction mixtures were washed with 1M Na<sub>2</sub>CO<sub>3</sub> and NaOH and extracted with CH<sub>2</sub>Cl<sub>2</sub> ten times, and solvent was evaporated under reduced pressure to yield off-white solid. NMR analysis of solids obtained revealed the decomposition of the 2,2'-bipyrimidine and failure of bromination reactions.

**3-Chloropyrazine 1-oxide:** 3-Chloropyrazine 1-oxide was prepared according to a literature procedure,<sup>50</sup> with reaction time increased to 24 hours in an attempt to improve yield. A flame-dried 100mL 3-neck round bottom flask fitted with gas-inlet adapter, condenser and septum was charged with 2-chloropyrazine (5.0g, 43.7mmol), glacial acetic acid (13.09mL, 227.2mmol) and 30% hydrogen peroxide (8.4mL, 275.3mmol) under positive argon flow. The mixture was stirred at 70°C for 24 hours. Approximately half the volume of the liquid was removed under reduced pressure, and the remaining mixture was poured into water and re-concentrated. The mixture was extracted with chloroform (15mL, three times), washed with water (45mL), dried over anhydrous calcium chloride, and evaporated under reduced pressure to yield pale yellow crystals. Recrystallization from ethanol afforded crystalline white solid (2.64, 46.3%) with a melting point range of 92.4-94.8°C. Experimental MP is comparable to the published MP of 95-96 °C.<sup>28</sup> <sup>1</sup>H NMR (CDCl<sub>3</sub>) δ 8.23 (d, 1H), 8.15 (s, 1H), 8.01 (d, 1H).

**Dichloropyrazines:** Dichloropyrazine was synthesized according to a literature procedure.<sup>50</sup> Under positive argon flow, 3-chloropyrazine 1-oxide (2.64g, 20.2mmol) was

added in small amounts to warm phosphoryl chloride (5.47mL, 58.58mmol) with stirring in a dry 50-mL 3-neck round bottom flask. The flask was heated at reflux for 1.5 hours until the reaction darkened. The mixture was cooled to room temperature, poured on to 100g of ice and stirred vigorously. After extraction with chloroform (10mL, three times), the organic layer was washed with water (30mL), neutralized with sodium bicarbonate (30mL), washed with water (30mL) and dried over anhydrous MgSO<sub>4</sub>. Solvent was evaporated under reduced pressure to yield 2.29g (76%) dichloropyrazine isomers as dark reddish-orange liquid, which solidified upon freezing as reported in the literature. <sup>1</sup>H NMR (CDCl<sub>3</sub>) δ 8.39 (s, 2H) and 8.20 (s, 2H).

**2,5-Bis-(thien-2-yl)-pyrazine (BTPz):** The mixture of dichloropyrazine isomers was coupled with two equivalents of thiophene to yield 2,5-bis-(thien-2-yl)-pyrazine (BTPz) following a literature procedure for the preparation of a donor-acceptor-donor monomer.<sup>52</sup> A dry 1000mL 3-neck round bottom flask was fitted with an gas-inlet adapter and two septa and flame dried under vacuum. 2-Bromothiophene (6.74mL, 69mmol) and THF (67.4mL, 10 wt. %) were added with positive argon flow and stirring. The solution was chilled to -78°C using acetone/dry ice bath, and n-BuLi (2.5M in hexanes; 30.64mL, 76.56mmol) was added drop-wise. The mixture was stirred at -78°C for 1 hour to yield a pale orange solution of lithiated thiophene. A second dry 1000mL 3-neck round bottom flask was fitted with an air inlet adapter and two septa. InCl<sub>3</sub> (5.65g, 76.56mmol) was added to this flask and dissolved in THF, and the resultant 0.05M solution was slowly added to the lithiated thiophene solution via cannula transfer. The mixture was stirred at -78°C for 1 hour and cooled to room temperature for another hour to afford trithienyl

indium. A third dry 1000mL 3-neck round bottom flask was fitted with an air inlet adapter, a septum and a condenser and flame dried under vacuum. The mixture of dichloropyrazine isomers (2.29g, 15.37mmol) in THF (22.9mL, 10 wt.%) and Pd(PPh<sub>3</sub>)<sub>4</sub> (344mg, 0.0130mM) was added to the flask under positive argon flow with stirring. The trithienyl indium solution was added dropwise to the dichloropyrazine solution via cannula transfer and heated at 80°C. Reaction progress was monitored using TLC until the consumption of the starting material was apparent after 5 days. At that point, 2mL of methanol was added to quench the reaction. Solvent was evaporated under reduced pressure and the resultant solid was dissolved in dichloromethane, washed with 5% HCl and the aqueous layer extracted with ethyl acetate (3 times). The combined organic layers were washed with saturated ammonium chloride and sodium chloride, dried over anhydrous MgSO<sub>4</sub> and solvent evaporated under reduced pressure to yield brown oil. Silica gel column chromatography using toluene/hexanes yielded 24.3mg (6.48%) yellow powder with a melting range of 289.8-291.6°C. <sup>1</sup>H NMR (CDCl<sub>3</sub>) δ 8.89 (s, 1H), 7.71 (s, 1H), 7.50 (s, 1H) and 7.18 (s, 1H) comparable to published<sup>34</sup> <sup>1</sup>H NMR (CDCl<sub>3</sub>) δ 7.48 (d, 2H), 7.68 (d, 2H) and 8.88 (s, 2H).

**2,5-Bis-(3,4-ethylenedioxythien-2-yl)-pyrazine (BEPz):** 2,5-Bis-(3,4-ethylenedioxythien-2-yl)-pyrazine (BEPz) was prepared in a similar manner as 2,5-bis-(thien-2-yl)-pyrazine (BTPz). Instead of thiophene, EDOT was coupled to dichloropyrazines. A dry 1000mL 3-neck round bottom flask was fitted with an air inlet adapter and two septa and flame dried under vacuum. EDOT (4.19mL, 39mmol) in THF (41.9mL, 10 wt. %) was added under positive argon flow with stirring. The solution was

chilled to  $-78^{\circ}\text{C}$  using acetone/dry ice bath and n-BuLi (2.5M in hexanes; 17.26mL, 43.1mmol) was added drop-wise. The mixture was stirred at  $-78^{\circ}\text{C}$  for 1 hour to yield a pale orange solution of lithiated EDOT. A second dry 1000mL 3-neck round bottom flask was fitted with an air inlet adapter and two septa and flame dried under vacuum. 0.05M  $\text{InCl}_3$  solution in THF (3.18g, 14.3mmol) was added to the lithiated EDOT solution via cannula transfer. The mixture is stirred at  $-78^{\circ}\text{C}$  for 1 hour and warmed to room temperature for another hour to afford  $(\text{EDOT})_3\text{In}$ . A third dry 1000mL 3-neck round bottom flask was fitted with an air inlet adapter, a septum and a condenser and flame dried under vacuum. The mixture of dichloropyrazine isomers (1.3g, 87.3mmol) in THF (13mL, 10 wt.%) and  $\text{Pd}(\text{PPh}_3)_4$  (195.3mg, 0.013mM) were added under positive argon flow and stirred.  $(\text{EDOT})_3\text{In}$  was added to the dichloropyrazine solution dropwise via cannula transfer and heated at  $80^{\circ}\text{C}$ . Reaction progress was monitored with TLC until the consumption of the starting material was observed. At that point, 2mL of methanol was added to quench the reaction. Solvent was evaporated under reduced pressure and the resultant solid was dissolved in dichloromethane, washed with 5% HCl and the aqueous layer extracted three times with ethyl acetate. The combined organic layers were washed with saturated ammonium chloride and sodium chloride, dried over anhydrous  $\text{MgSO}_4$  and solvent evaporated under reduced pressure to yield brown oil. Silica gel column chromatography using ethyl acetate/hexanes yielded 46.78mg (16.4%) brown powder with a melting range of  $247.8\text{-}248.9^{\circ}\text{C}$ .  $^1\text{H}$  NMR ( $\text{CDCl}_3$ )  $\delta$  8.93 (s, 1H), 6.56 (s, 1H), 4.42 (s, 2H) and 4.30 (s, 2H).  $^{13}\text{C}$  NMR ( $\text{CD}_2\text{Cl}_2$ )  $\delta$  146.85 (s, 1C), 142.54 (s, 1H), 141.62 (s, 1C) 138.59 (s,1C), 116.36 (s,1C), 103.32 (s,1C), 65.66 (s, 1C) and 64.84 (s, 1C).

## Results and Discussion

### Bisthienylpyrimidine Structural Determination

The bisthienylpyrimidines, 2,5-bis(thien-2-yl)pyrimidine (BTPm) and 2,5-bis(3,4-ethylenedioxythien-2-yl)pyrimidine (BEPm, Figure 8) were synthesized by Winkel<sup>40</sup> for stable n-doping polymers. Katie Winkel was a previous Irvin Research Group member.

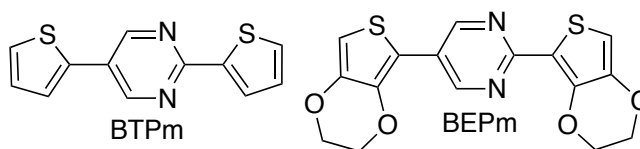


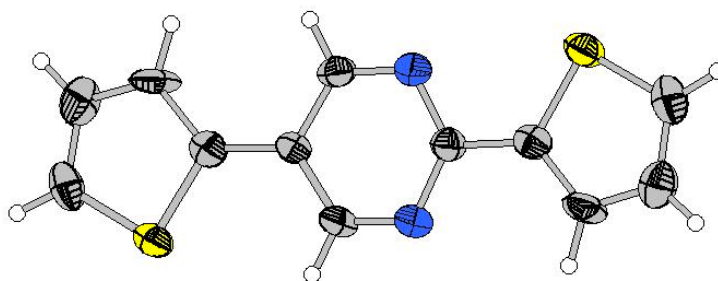
**Figure 8:** 2,5-Bis(thien-2-yl)pyrimidine (BTPm, left) and 2,5-bis(3,4-ethylenedioxythien-2-yl)pyrimidine (BEPm, right)

Single-crystal X-ray diffraction (XRD) analysis was attempted on both bisthienylpyrimidines (Figure 8). A single crystal of BTPm was selected, 5509 (2444 independent) reflections were collected, and an analytical absorption correction was applied ( $R_{\text{int}} = 0.0551$ ). Data were collected within a  $\theta$  range of  $3.52 - 27.48^\circ$  to a completeness of 100.0% with a data index range of  $-13 \leq h \leq 13$ ,  $-6 \leq k \leq 6$ ,  $-14 \leq l \leq 14$ . The initial solution was calculated using direct methods in space group  $P21$ . All nonhydrogen atoms were refined anisotropically on  $F^2$  for 171 variables with final electron density residuals of 0.222 and  $-0.313 \text{ e}\text{\AA}^{-3}$ . The results of the solution are displayed in Figure 9 and Table 1.

**Table 1:** Selected crystallographic data for BTPm

Space group	P21
Formula weight	244.32
<i>a</i> , Å	10.734(6)
<i>b</i> , Å	5.037(3)
<i>c</i> , Å	10.881(6)
<i>b</i> , (deg)	115.255(11)
<i>Z</i>	2
<i>V</i> , Å <sup>3</sup>	532.1(5)
$\rho$ , calc, g/cm <sup>3</sup>	1.525
radiation wavelength, Å	0.71073
linear abs. coeff., mm <sup>-1</sup> (calculated)	0.9121
collection temp, K	223
R1 <sup>a</sup> ( <i>I</i> >2 $\sigma$ )	0.0476
wR2 <sup>b</sup> ( <i>I</i> >2 $\sigma$ )	0.0956

<sup>a</sup>  $R1 = S(|F_o| - |F_c|)/\sum |F_o|$    <sup>b</sup>  $wR2 = [S[w(F_o^2 - F_c^2)^2]/\sum (w(F_o^2)^2)]^{1/2}$

**Figure 9:** Resolved structure of BTPm (yellow=sulfur, blue=nitrogen, black=carbon and white=hydrogen)

Determining the position of sulfur on the thiophene ring was difficult. Ring flipping occurs about the sigma bond between thiophene and pyrimidine (Figure 10). To model the disorder, the thiophene rings were restrained to be planar, and anisotropic displacement parameters for equivalent atoms were set to be equivalent. Bond distances in the disordered rings were also set to be equivalent in both conformers.

In the disordered model, the thiophene rings favored a conformation in which the sulfur atoms are trans relative to each other on opposite sides of the pyrimidine ring. The thiophene closest to the pyrimidine nitrogens adopted the favored conformation 71.0% of the time, while the other thiophene ring adopted this conformation 76.4% of the time. Since these values are similar, it is likely that the structure adopts two alternate trans conformations.

Published C-S lengths in thiophene are 1.73 and 1.77 Å.<sup>41</sup> Comparatively, C-S lengths for BTPm were 1.68 and 1.71 Å for the thiophene ring away from the nitrogens and 1.67 and 1.71 Å for the thiophene close to the nitrogens. BTPm thiophenes' C-C bonds were found to be about 0.10 Å lower than reported by Jenks *et al.*<sup>41</sup> while the pyrimidine ring's C-N and C-C bonds were 1.34 and 1.40 Å, respectively. The BTPm pyrimidine bonds' lengths are comparable to reported pyrimidine bonds' length of Amaral *et al.*<sup>42</sup>

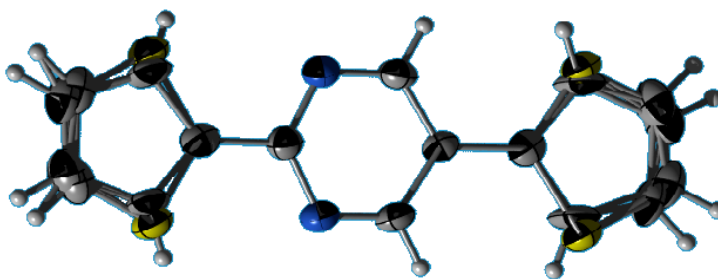


**Figure 10:** Ring flipping disorder of BTPm

The highest torsion angle between the rings is less than 5°, making the structure planar (Figure 11). This planarity is somewhat surprising, because it was feared that electron-electron repulsion between S and nearby N would tilt the thiophene ring closest to the nitrogen atoms out of the plane of the pyrimidine ring. Given the small torsion angles in the monomer, resultant polymer backbone is predicted to exhibit similar

features. Increased planarity decreases stabilization energy of oxidized polymers and lowers  $\pi$ - $\pi^*$  transition in the neutral polymer.<sup>44</sup> Oxidized polymers are stabilized by the extended conjugation a planar polymer offers.

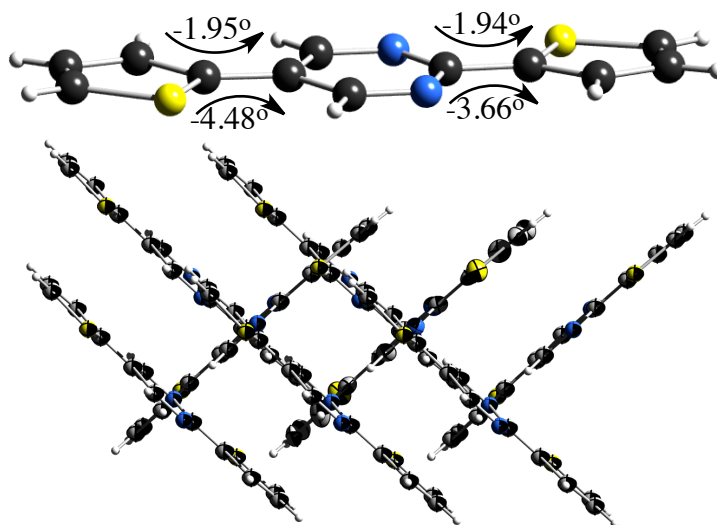


**Figure 11:** Planarity of BTPm

Within a unit cell, thiophene rings from one monomer are stacked with pyrimidine rings from monomers above and below them. As seen in Figure 12, donor-acceptor alignments are observed in two orthogonal directions. Estimated stacking distances between thiophene and pyrimidine rings are as low as 3.35Å. Such low distances are known to allow for  $\pi$ - $\pi$  stacking,<sup>43</sup> which in this case should allow for sharing of donor electron density with acceptor groups.

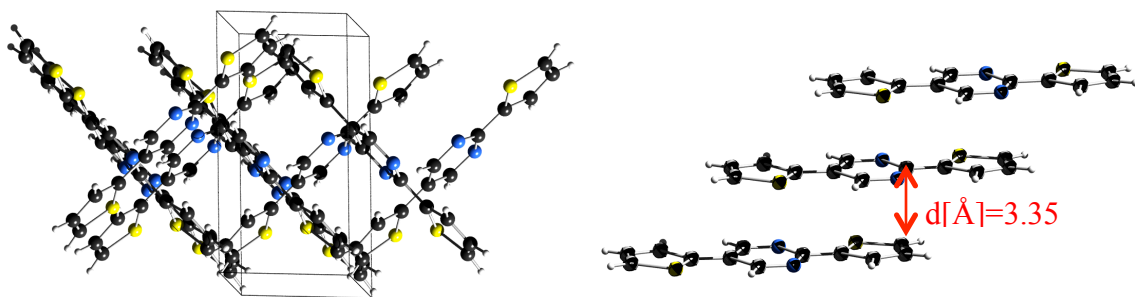


**Figure 12:** Unit cell packing of BTPm (left); donors and acceptors are aligned for maximum  $\pi$ - $\pi$  stacking

The ring flipping observed in BTPm is expected to have an even more pronounced effect in BEPm. BEPm's dioxy bridges are expected to further increase the entropic disorder expected with respect to the  $180^\circ$  rotation of the EDOT rings, preventing crystalline packing of the molecule. While the dioxy bridge of BEPm is expected to be in a half-chair confirmation,<sup>44</sup> it is still likely that the thiophene and pyrimidine rings will be coplanar.<sup>45</sup> BEPm recrystallization was attempted using various solvents (Table 1). Mixed solvents of saturated BEPm dissolved in appropriate solvent was diluted with excess insoluble solvents of Table 1 and allowed to slowly crystallize over days. Fibrous, small crystals from acetonitrile and small, fragile, clumped sheets were obtained from chloroform/isopropyl. These crystals were too small and imperfect to yield enough reflections for XRD.

**Table 2:** Recrystallization of BEPm

<b>Attempted recrystallization of BEPm for X-ray structure determination</b>			
Solvent	Soluble	Soluble with heat	Crystals
Hexane	slightly	yes	no
Toluene	slightly	yes	no
Dichloromethane	yes	yes	no
THF	yes	yes	no
Ethyl acetate	yes	yes	no
Acetonitrile	slightly	yes	yes
Chloroform	yes	yes	no
Methanol	slightly	yes	no
Ethanol	slightly	yes	no
Isopropanol	slightly	yes	no
Dichloroethane	slightly	yes	no

#### Attempted Synthesis of Bisthienylbipyrimidines

According to Fu and coworkers' Density Function Theory (DFT) findings,<sup>5</sup> donor-acceptor ratios are important in designing EAPs. DFT estimations showed a 1:1 ratio of donor:acceptor is optimal for efficient electron mobility. While the BTPm and BEPm structures reported in the previous chapter each have a 2:1 donor:acceptor ratio, replacing pyrimidine with bipyrimidine would result in a 1:1 ratio while still providing easily oxidized donor groups on both ends of the molecule. For this reason, synthesis of bisthienylbipyrimidines was attempted.

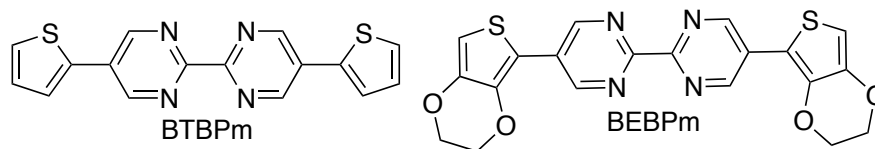
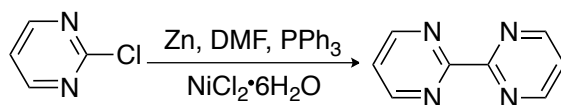


**Figure 13:** 2,5-Bis(thien-2-yl)-2,2'-bipyrimidine (BTBPm, left) and 2,5-bis(3,4-ethylenedioxythien-2-yl)-2,2'-bipyrimidine (BEBPm, right)

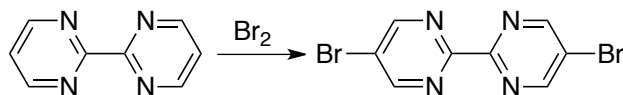
2,2'-Bipyrimidine was synthesized using Schwab and coworkers' procedure.<sup>46</sup> 2-chloropyrimidine was reductively coupled in the presence of zinc catalyst to yield 2,2'-

bipyrimidine (Scheme 5). In order to remove triphenyl phosphine contaminants, it was necessary to extract the crude product with diethyl ether 8 times instead of 3 times as reported by Schwab. Sublimation yielded pure product as indicated by  $^1\text{H}$  NMR and melting point.



**Scheme 5:** Synthesis of 2,2'-bipyrimidine

In order to prepare bisthienylbipyrimidines, it was first necessary to prepare 5,5'-dibromobipyrimidine for use in coupling reactions. While 5,5'-dibromobipyrimidine has been reported previously,<sup>47,48</sup> the conditions used were extremely vigorous and impossible to replicate in our laboratory. Additionally, reported yields were very low (40%). In attempts to identify a more feasible route to 5,5'-dibromobipyrimidine, bipyrimidine was exposed to a series of bromination conditions (Scheme 6). The bromination protocol of Song *et al.*<sup>48</sup> was modified to afford various reactions conditions and methods. The published protocol called for harsh conditions and provided low yields. Using carbon tetrachloride and dichloromethane/acetic acid as solvents, microwave reactions with varying reaction time and temperature and with/ without ferric bromide and photoreactions at  $\sim 155^\circ\text{C}$  for 12, 24 and 48 hours were carried out. None of the brominations yielded significant results. Due to the inability to prepare 4,4'-dibromobipyrimidine, it was not possible to synthesize the desired bisthienylbipyrimidines.



**Scheme 6:** Bromination of 2,2'-bipyrimidine.

### Bisthienylpyrazines

The properties of bisthienylpyrazines became of interest upon the discovery of the stable p and n-doping capabilities of bisthienyl pyridines.<sup>34</sup> Unlike pyridines and pyrimidines, pyrazines are symmetrical, less basic and offer new optical and chemical possibilities. Electron affinities of pyrazines are much higher than those of pyridines or pyrimidines,<sup>49</sup> so it is possible they would produce even better donor-acceptor-donor molecules. Pyrazines in this work were functionalized as acceptors following the work of Klein *et al.*<sup>50</sup> While bis thienyl pyrazine (BTPz) was successfully synthesized previously by Chiagnaud<sup>34</sup> *et al.*, its chemical properties have not been previously reported. Using Sarandeses' coupling, 2,5-dichloropyrazine was coupled to two thienyl groups to form 2,5-bis(thien-2-yl)pyrazine (BTPz) and to two 3,4-ethylenedioxythienyl groups to form 2,5-bis(3,4-ethylenedioxythiophene-2-yl)pyrazine (BEPz, Figure 14). BEPz was synthesized to compare the effects of thienyl versus 3,4-ethylenedioxythienyl (EDOT) donor groups, because EDOT is known to have a lower oxidation potential than thiophene.<sup>51</sup>

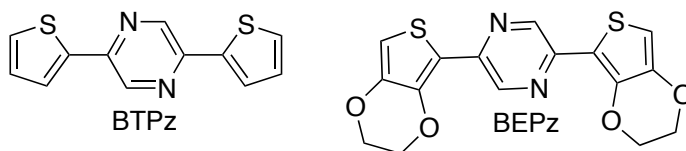
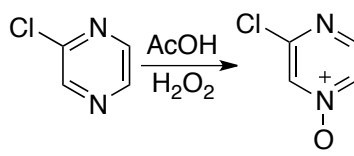


**Figure 14:** Bisthienylpyrazines

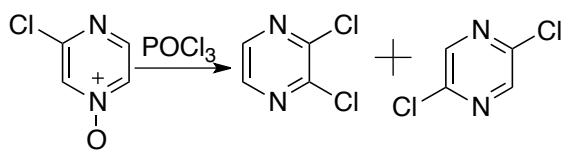
Following Klein and co-workers' method,<sup>50</sup> 2-chloropyrazine was oxidized to form 3-chloropyrazine 1-oxide (Scheme 7). Stirring time was increased until complete

consumption of 2-chloropyrazine was confirmed using thin layer chromatography (TLC). This process is likely to occur via the transfer of oxygen to the pyrazine from the newly formed peracetic acid in the presence of acetic acid and hydrogen peroxide. Upon the creation of the 1-oxide salt, the nitrogen carries the positive charge while the more electronegative oxygen bears the negative charge.<sup>50</sup> The expected three pyrazine peaks between 8-9ppm are observed along with solvent peaks below 2ppm (Spectrum 2).



**Scheme 7:** Synthesis of 3-chloropyrazine 1-oxide

2,5-Dichloropyrazine was achieved upon refluxing 3-chloropyrazine 1-oxide in phosphoryl chloride (Scheme 8). The mechanism of 2,5-dichloropyrazine is not understood.<sup>50</sup> Unfortunately, NMR revealed that two isomers of dichloropyrazine were formed. Peaks at 8.4 and 8.2 suggest the presence of two types of hydrogens.



**Scheme 8:** Synthesis of dichloropyrazines

Klein and co-workers described 2,5-dichloropyrazine as a brown residue that freezes at 0°C. When this report was published (1963), NMR would not have been available for them to determine that a mixture of isomers was formed. Separation of isomers was attempted using silica gel and various solvents, but no conditions were identified that would separate the two isomers. After elution from column, aliphatic peaks

emerged on  $^1\text{H}$  spectrum, indicating degradation of isomers (Spectrum 3). Synthesis continued with coupling of the mixture of isomers to thiophene donating groups. Since two thienyl rings, one on each side, were to be added, separation of isomers was expected to be easier (Figure 15).

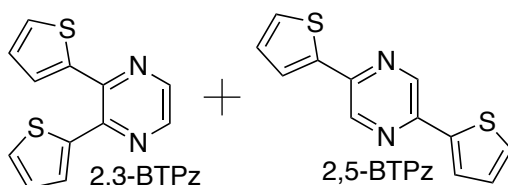
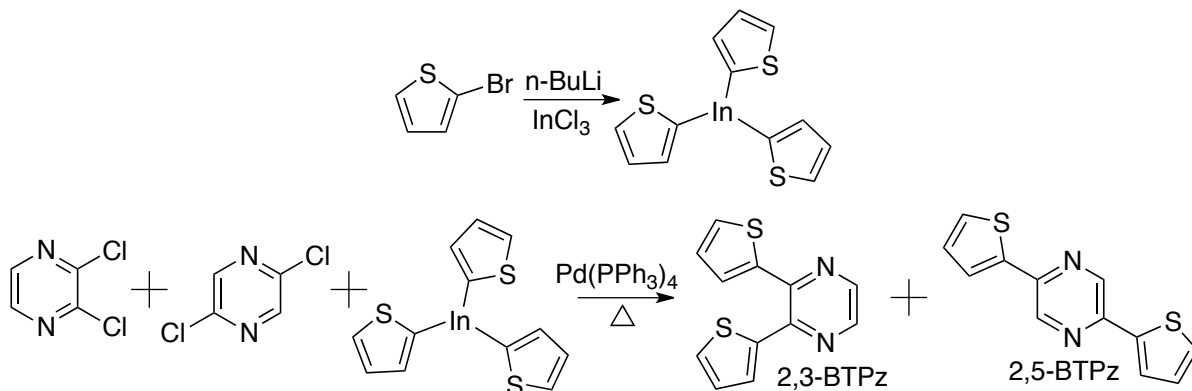


**Figure 15:** Possible bithienylpyrazine isomers

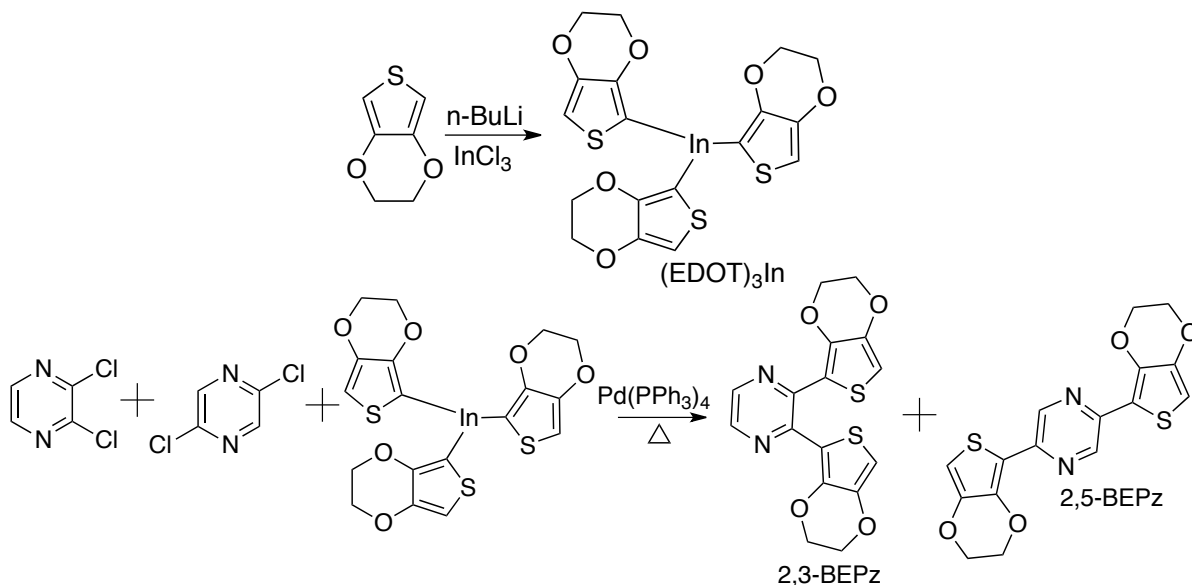
The mixture of dichloropyrazine isomers were coupled to thiophene and EDOT using the Mosquera *et al.* protocol.<sup>52</sup> BTPz was prepared from the palladium catalyzed coupling of dichloropyrazine and trithienyl indium (Scheme 9). BEPz was synthesized in a similar manner (Scheme 10). In both cases column chromatography was used to separate the two isomers (ortho- and para-substituted pyrazines) from each other and from other byproducts.

The 2,5-bis(thien-2-yl)pyrazine was successfully isolated from the 2,3-bis(thien-2-yl)pyrazine as evidenced by the  $^1\text{H}$  NMR (Spectrum 4): only one pyrazine hydrogen can be seen around 8ppm. Three thiophene hydrogens are evident around 7ppm along with contaminants below 2ppm. The 2,3-bis(thien-2-yl)pyrazine can not be isolated. The 2,3- and 2,5- bisEDOT pyrazines were successfully isolated. A comparison of the two isomers reveals that their spectra are remarkably different (spectra 4 and 5). NMR prediction software (CS ChemDraw NMR Pro Version 6.0) was unable to predict significant differences in either the  $^1\text{H}$  or  $^{13}\text{C}$  NMR spectra of the two isomers. Based on

NMR data (spectra 4-7), it is obvious that the isomers are different but 2D NMR or single crystal structure determination is necessary to discern which is which.



**Scheme 9:** Sarandese coupling of dichloropyrazine isomers with thiophene to yield 2,3-bis(thien-2-yl)pyrazine (2,3-BTPz) and 2,5-bis(thien-2-yl)pyrazine (2,5-BTPz)



**Scheme 10:** Sarandese coupling of dichloropyrazine isomers with EDOT to yield 2,3-bis(3,4-ethylenedioxythien-2-yl)pyrazine (2,3-BEPz) and 2,5-bis(3,4-ethylenedioxythien-2-yl)pyrazine (2,5-BEPz)

### Conclusions

To improve on the optical properties of known n-dopable EAPs,<sup>36,37</sup>

bisthienylpyrazines were synthesized. Bisthienylpyrimidines' single crystal X-ray

structure determination was attempted to estimate the extent of resultant polymers' conjugation and stabilization upon doping. BTPm's crystal structure was successfully determined. A 1:1 ratio of donor:acceptor moieties was targeted to improve electron mobility, but unsuccessful synthesis of precursor discouraged synthesis of target monomers. Thiophene- and EDOT- disubstituted pyraines were prepared as mixtures of isomers, but separation was accomplished.

## CHAPTER III

### SYNTHESIS OF BISTHIENYLFLUOROPYRAZINES

#### Background

n-Doped polymers are typically unstable due to the presence of anions in the polymer. Such anions can be stabilized by pendant electron withdrawing groups like fluorine that delocalize the electron density away from the backbone.<sup>53</sup> It is possible that electron mobility along the polymer backbone could be hindered due to localization of electrons on the pendant fluorine, effectively decreasing conductivity relative to the non-fluorinated pyrazine-based molecules discussed in Chapter II. However, it is also possible that the high electron affinity of pyrazine might counteract that effect.

Bisthienylfluoropyrazine monomers were prepared to test the difference in properties induced by incorporating the electronegative fluorine atom pendant to the acceptor group.

Thienyl and EDOT fluoropyrazines are expected to have efficient charge mobility and reducibility due to the competition for anions between the acceptor moiety and the withdrawing fluorine group. EDOT donor groups were incorporated to lower monomer oxidation potentials relative to the thienyl analogues. These novel donor-acceptor-donor moiety monomers should produce stable n and p-doping polymers (Figure 15); conductivity measurements will be used to discern the effect of the F substituents on electron mobility.

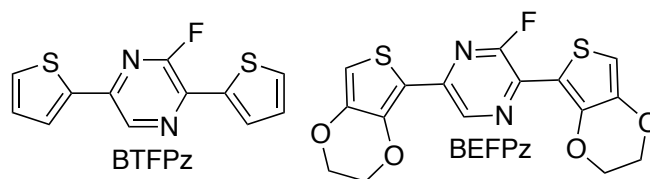


**Figure 16:** Bisthienylfluoropyrazines

## Experimental

### Materials

EDOT was purchased from Aldrich and purified as described in Chapter II. *n*-Butyl lithium (*n*-BuLi, 2.5M in hexanes), and anhydrous tetrahydrofuran (THF) were purchased from Aldrich and used as received. Anhydrous dimethyl sulfoxide (DMSO, AcroSeal™), anhydrous tetrahydrofuran (THF, AcroSeal™), 2,2,6,6-tetra methyl piperidine hydride (TMPH), and tributyltin chloride were purchased from Acros and used as received. Sodium bicarbonate and anhydrous magnesium sulfate were purchased from Fisher Scientific and used as received. Sodium carbonate and tetrabutylammonium fluoride (TBAF) was purchased from Aldrich Chemical and used as received. *N*-bromosuccinimide was purchased from Acros, recrystallized from water, dried under vacuum over phosphorus pentoxide and stored at 2-8°C prior use. All other reagents were procured and purified as described in Chapter 2.

### Instrumentation

Compounds were characterized using melting point determination (MP) and nuclear magnetic resonance (NMR). <sup>1</sup>H and <sup>13</sup>C NMR were accomplished using a Varian

INOVA 400 MHz NMR or a Bruker Avance III 400 MHz NMR while MPs were determined using Mel-Temperature Electrochemical with Fluke 51 thermometer detector.

### Synthesis

**2-Fluoropyrazine (FPz):** Synthesis of this compound followed a report by Sun *et al.*<sup>55</sup> with minor modifications. A 250mL 3-neck round bottom flask fitted with a gas-inlet adapter and 2 septa was charged with a stir bar and flame dried under vacuum and filled with argon. DMSO (85mL) was added via cannula transfer before addition of 2-chloropyrazine (3.0 mL, 33.9mmol) to make a 0.4M solution under positive argon flow. TBAF (44.08mL, 44.1mmol) was added with stirring under positive argon flow. The mixture was stirred for 1 hour. After quenching of the reaction with 1M HCl, the product was isolated via distillation. The collected organic was then washed with water three times and extracted with dichloromethane three times. The aqueous layer was extracted with dichloromethane three times, and combined organics were washed with water four times, neutralized with 5% sodium bicarbonate, washed with water three times, dried over anhydrous MgSO<sub>4</sub> and evaporated under reduced pressure to yield a pale liquid (1.2mL, 36.5%). <sup>1</sup>H NMR (acetone-d<sub>6</sub>) δ 8.50 (s, 1H), 8.40 (d, 1H) and 8.28 (s, 1H) close to the published <sup>1</sup>H NMR (CDCl<sub>3</sub>) δ 8.37 (dd, 1H), 8.32 (dd, 1H) and 8.09 (m, 1H).<sup>55</sup>

**2-Fluoro-3,6-bis(tributylstannyl)pyrazine ((SnBu<sub>3</sub>)<sub>2</sub>FPz):** Synthesis of this compound followed a report by Toudic and co workers<sup>24</sup> with minor modifications. A 100mL 3-neck round bottom flask was fitted with a stir bar, a gas-inlet adapter and two septa and flame dried under vacuum. Under positive argon flow, THF (22mL) was added

and the flask was cooled to  $-50^{\circ}\text{C}$  using acetonitrile/dry ice bath for 20 minutes. n-BuLi (23.12mL, 57.8mmol; 2.5M in hexanes) was added drop wise using a syringe, and then TMPH (9.98mL, 59.1mmol) was added drop wise using a syringe. The reaction mixture was warmed to  $0^{\circ}\text{C}$  for 20 minutes and then cooled to  $-100^{\circ}\text{C}$  using a diethyl ether/dry ice bath. Under positive argon flow,  $\text{SnBu}_3\text{Cl}$  (19.71g, 60.5mmol) and 2-fluoropyrazine (2mL, 27.5mmol) were dissolved in THF (26.7mL, 10 wt%) and added simultaneously to the reaction mixture under positive argon flow. The reaction mixture was stirred at  $-100^{\circ}\text{C}$  for two hours until it turned dark, allowed to warm to room temperature.

Hydrolysis was accomplished by addition of a 1:4:5 solution of 35% HCl:ethanol:THF. After neutralization with sodium bicarbonate, the aqueous layer was extracted three times with dichloromethane and dried over  $\text{MgSO}_4$ . Solvent was evaporated under reduced pressure to give a dark reddish-orange liquid. A silica gel column using dichloromethane/cyclohexane produced a colorless liquid (17.2g, 92%). Reported  $^1\text{H}$  NMR ( $\text{CDCl}_3$ ) 8.56 (d, 1H) and 1.8-0.53 (m, 54H)<sup>24</sup> is comparable to experimental  $^1\text{H}$  NMR ( $\text{CD}_2\text{Cl}_2$ ) of 8.76 and 2.5-0.5 (m, 54H).

**2-Fluoro-3,6-(thien-2-yl)-pyrazine (BTFPz):** This novel compound was synthesized via a Stille coupling using a modification of the method reported by Toudic et al.<sup>24</sup> A 100mL 3-neck round bottom flask was fitted with a stir bar, gas-inlet adapter, a condenser and a septum and flame dried under vacuum. Under positive argon flow,  $(\text{SnBu}_3)_2\text{FPz}$  (4.6g, 6.79mmol) dissolved in anhydrous toluene (46mL, 10 wt%) was added to the flask. Under positive argon flow, 2-bromothiophene (1.05mL, 10.86mmol) and  $\text{Pd}(\text{PPh}_3)_4$  (390mg, 0.34mmol) were added to the flask and heated at reflux for 96

hours. Reaction completion was monitored via TLC. Upon completion, the flask was allowed to cool to room temperature, and 1:1 water:dichloromethane was added. The aqueous layer was extracted 3 times with dichloromethane and dried over  $\text{MgSO}_4$ . Solvent evaporation under reduced pressure yielded a dark brown suspension. The suspension was first added to acetone and filtered to remove impurities, concentrated and then added to methanol to filter out further impurities, resulting in a yellow-brown liquid. Column chromatography using hexanes/dichloromethane yielded a yellow liquid, which was stored under argon in the presence of 2-3mL of isopropanol to crystallize catalyst impurities. Passing the mixture through a short silica column in dichloromethane afforded (76.2mg, 42.6%).  $^1\text{H}$  NMR ( $\text{CD}_2\text{Cl}_2$ ) 8.90 (d, 1H), 7.38 (s, 2H), 7.31 (s, 2H) and 7.29 (s, 2H).

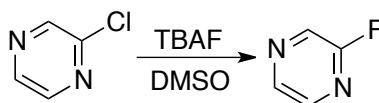
**2-Bromo-3,4-ethylenedioxythiophene:** Bromination of EDOT was accomplished via a modification of the method reported by Belletête *et al.*<sup>54</sup> A 100mL 3-neck round bottom flask fitted with a gas-inlet adapter and two septa was flame dried under vacuum. The flask was charged with EDOT (3.0mL, 28.08mmol) in THF (39.9mL, 10 wt%). While stirring, NBS (2.49g, 14mmol) was added under positive argon flow. The reaction mixture was stirred for 1 hour and washed with water. The organic layer was extracted three times with diethyl ether, washed with brine, dried over  $\text{MgSO}_4$  and evaporated under reduced pressure to yield a colorless liquid mixture of 2-BrEDOT and EDOT 3.34g.  $^1\text{H}$  NMR (acetone- $\text{d}_6$ )  $\delta$  6.50 (s, 1H), 6.35 (s, H), 4.29 (s, H), 4.24 (s, H), 4.18 (s, H) and 4.15 (s, H).  $^{13}\text{C}$  NMR (acetone- $\text{d}_6$ )  $\delta$  142.4, 126.4, 125.9, 123.7, 27.04 and 13.73.

**2-Fluoro-3,6-(3,4-ethylenedioxythiophen-2-yl)-pyrazine (BEFPz):** A 100mL 3-neck round bottom flask was fitted with a stir bar, gas inlet adapter, a condenser and a septum and flame dried under vacuum. Under positive argon flow,  $(\text{SnBu}_3)_2\text{FPz}$  (4.6g, 6.79mmol) dissolved in anhydrous toluene (46mL, 10 wt%) was added to the flask. Under positive argon flow, BrEDOT (1.05mL, 10.86mmol) and  $\text{Pd}(\text{PPh}_3)_4$  (390mg, 0.34mmol) were added to the flask and heated at reflux for 96 hours. Reaction completion was monitored via TLC. Upon completion, the flask was allowed to cooled to room temperature, and 1:1 water:dichloromethane was added. The aquesout layer was extracted three times with dichloromethane and dried over  $\text{MgSO}_4$ . Solvent evaporation under reduced pressure yielded a dark brown liquid (1.86g).

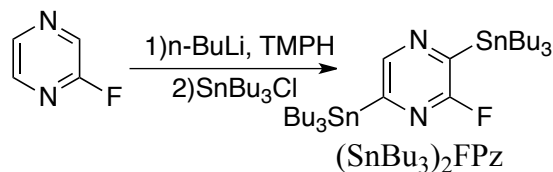
### Results and Discussion

Synthesis of 2-fluoropyrazine (Scheme 11) was accomplished according to a procedure reported by Sun *et al.*<sup>55</sup> 2-Chloropyrazine was stirred at room temperature in the presence of a high boiling solvent and fluorine source (tetrabutylammonium fluoride, TBAF) to afford 2-fluoropyrazine in a simple nucleophilic aromatic substitution with a fluoride nucleophile. 2-Fluoropyrazine was verified by  $^1\text{H}$  NMR results (Spectrum 9) of three pyrazine peaks around 8ppm and solvent peaks below 2.5ppm. Then, stannylation of 2-fluoropyrazine (Scheme 12) was accomplished following Toudic and co-workers' method.<sup>24</sup> Fluorine acts as an ortho/para director during the stannylation process but *ortho* lithiation is encouraged since those positions are stabilized by the lone pairs on the fluoro group in the formation of the positively charged intermediate. First, n-BuLi is used

to lithiate the positions *ortho* to the fluorine substituent. In order to prevent competitive acid/base reactions, TMPH is used to coordinate lithium ions and provide protons for the basic butyl group. As TMPH dissociates to  $\text{TMP}^-$ ,  $\text{Li}^+$  combines to form  $\text{TMPLi}$ . Next, an aromatic nucleophilic substitution mechanism takes over as the nucleophile (tributyltin) attacks the lithiated carbon, to form  $\text{LiCl}$ , which precipitates and drives the reaction to completion. This process creates 2-fluoro-3,6-bis(tributylstannyl)pyrazine ( $(\text{SnBu}_3)_2\text{FPz}$ ). This structure has a pyrazine  $^1\text{H}$  doublet at 8.9ppm and butyl group multiplets from 1.7-0.8ppm (Spectrum 10).



**Scheme 11:** Aromatic nucleophilic substitution of 2-chloropyrazine

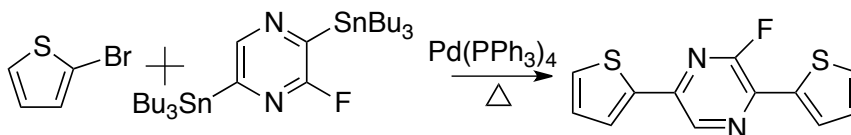


**Scheme 12:** Stannylation of 2-fluoropyrazine

Regioselective arylation of fluoropyrazines was accomplished using a palladium catalyzed Stille coupling of the organotin reagent ( $(\text{SnBu}_3)_2\text{FPz}$ ) with aryl halides. The organotin precursor ( $(\text{SnBu}_3)_2\text{FPz}$ ) was then used to prepare 2-fluoro-3,6-(thien-2-yl)pyrazine (BTFPz, Scheme 13) and 2-fluoro-3,6-(3,4-ethylenedioxythien-2-yl)pyrazine (BEFPz, Scheme 15).

Two equivalents of 2-bromothiophene were coupled ( $(\text{SnBu}_3)_2\text{FPz}$ ) using stille coupling conditions to yield BTFPz. While the expected chemical shifts are apparent in

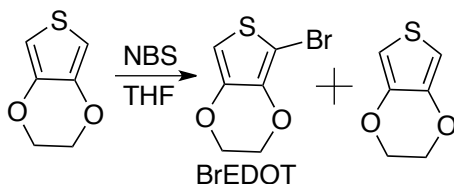
the  $^1\text{H}$  NMR of the product (Spectrum 11). The spectrum also reveals aliphatic contaminants, likely solvent and tributyltin by-products. Additional purification is needed before  $^{13}\text{C}$  NMR and electrochemical characterization can be accomplished.



**Scheme 13:** Stille coupling of 2-fluoro-3,6-bis(tributylstannyl)pyrazine with 2-bromothiophene

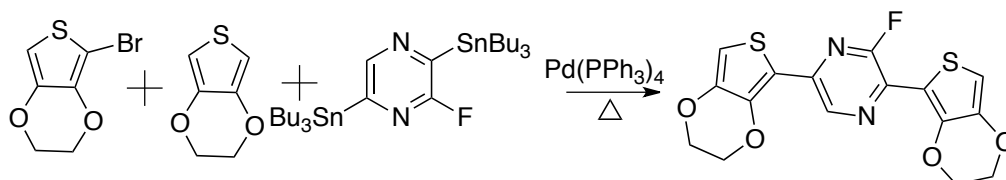
While 2-bromothiophene is commercially available, BrEDOT is not. However, the synthesis of BrEDOT via reaction of EDOT with *N*-bromosuccinimide (NBS, Scheme 14) has been previously reported<sup>48</sup> The authors found that only 50% of the desired product was formed, with the rest of the reaction mixture being unreacted EDOT; no separation of the two species was reported. In fact, the relatively poor stability of BrEDOT (decomposes rapidly in air, stored in the dark under argon in the freezer) makes separation impractical. Instead, the mixture of EDOT and BrEDOT could be used; since Stille reactions are selective for aryl halides, the brominated EDOT was expected to react. Note that the ratio of EDOT:BrEDOT could be determined by NMR and used to calculate the amount of EDOT/BrEDOT to use in the subsequent reaction. Bromination of EDOT<sup>48</sup> was accomplished using THF instead of DMF since THF (which is easier to remove upon reaction completion than DMF) was found to effect similar results. The concentration of NBS was increased to optimize the yield of BrEDOT (spectra 12 and 13).  $^1\text{H}$  NMR results reveal the presence of BrEDOT and EDOT; BrEDOT peaks are chemically shifted to the right. BrEDOT/EDOT thiophene hydrogen peak is around 6ppm while ethylene dioxy hydrogens are around 4ppm. BrEDOT was covered with foil and

stored in the freezer under argon prior to use to prevent degradation, and all efforts were made to ensure the subsequent reaction was conducted as soon as possible.



**Scheme 14.** Bromination of EDOT

Two equivalents of 2-bromoEDOT were coupled  $(\text{SnBu}_3)_2\text{FPz}$  using stille coupling conditions to yield BEFPz. The expected chemical shifts around 9, 7 and 4 ppm are apparent in the  $^1\text{H}$  NMR of the product along with solvent and precursor contaminants. Additional purification is needed before  $^{13}\text{C}$  NMR and electrochemical characterization can be accomplished.



**Scheme 15:** Stille coupling of 2-fluoro-3,6-bis(tributylstannyl)pyrazine with BrEDOT

### Conclusions

Fluorinated bithienylpyrazines were synthesized to stabilize the negative charges that resonate along a polymer backbone by attaching an electron-withdrawing group pendant to the backbone. This monomer design is supposed to provide a competitive environment within the monomer to facilitate efficient charge mobility. Fluorinated bithienyl pyrazines, BTFPz and BEFPz, were successfully synthesized and their electronic properties will be determined after purification.

## CHAPTER IV

### SYNTHESIS OF BISTHIADIAZOLYL BENZENES

#### Background

Thiadiazoles are unique heteroatoms that contain both sulfur and nitrogen atoms. Incorporation of thiadiazoles in EAPs dates back to the 1980s. Wang *et al.*<sup>56</sup> effectively synthesized a donor-acceptor copolymer using benzo-1,2,5-thiadiazole as an acceptor for bulk heterojunction solar cells applications. Conversely, Seo *et al.*<sup>57</sup> used benzo-1,2,5-thiadiazole as donors for similar applications. Bicyclic 1,2,5-thiadiazole was combined with thiophene<sup>57</sup> and tricyclic 1,2,5-thiadiazole was combined with benzene and pyrazine or benzene and another 1,2,5-thiadiazole<sup>58</sup> as high-electron affinity structures.

While 1,2,5-thiadiazoles have been utilized predominantly in solar cell chemistry and organic light emitting diodes (OLEDs), 1,3,4-thiadiazoles<sup>58,59,60,61,62</sup> have been studied as liquid crystals for electroluminescence (EL) and other biological applications. Since thiadiazoles are known to be good acceptors<sup>60,61,62,59,58</sup> and donors,<sup>57</sup> their use as donors is very interesting. 1,2,5-Thiadiazole has successfully been characterized as an efficient charge transfer donor by Seo *et al.*<sup>57</sup> 1,3,4-Thiadiazole's capabilities as a donor have not been explored. Alkoxy benzenes have been studied as donors<sup>57</sup> and acceptors<sup>63</sup>;

their electronaffinities in conjunction with 1,3,4-thiadiazole are still unknown. Alkoxy benzenes are expected to be more electron rich than benzenes due to their electron donating substituents.

The electroluminescence properties of 1,3,4-thiadiazolyldialkoxybenzenes were characterized by Sato and coworkers<sup>60</sup> but the molecule's band gaps and electron affinities with respect to different functional groups were not studied. 1,3,4-Thiadiazolylbenzenes with an alkyne group between the thiazole and benzene rings were studied and 1,3,4-thiadiazoles were determined to be great acceptors for benzenes to make stable n and p-type organic cells.<sup>61,62</sup>

1,4-Dibromobenzene was coupled to 2-bromo-3,4-thiadiazole to form 1,4-bis-(1,3,4-thiadiazol-2-yl) benzene (BTdB, Figure 17) and 1,4-dibromo-2,5-dihexadecyloxybenzene (BBrBC<sub>16</sub>) was coupled to 1,4- dibromobenzene to yield 1,4-bis-(1,3,4-thiadiazol-2-yl)-2,5-bis-hexadecyloxybenzene (BTdBC<sub>16</sub>, Figure 17). These moieties are unique for they contain homocyclic inner rings and high-nitrogen outer rings and therefore are expected to have different optical properties. Unlike the previous two chapters' high-nitrogen content incorporation as high electron-affinity middle rings, this chapter deals with the designing of high-nitrogen content as outer rings. These monomers were synthesized via the Sarandeses protocol.<sup>52</sup> BTdB and BTdBC<sub>16</sub> were attempted to clear any uncertainties.

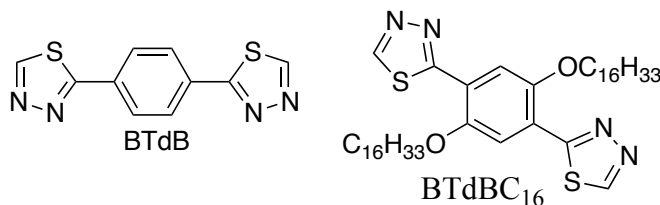


**Figure 17:** Bisthiadiazolylbenzenes

## Experimental

### Materials

1,4-Dibromobenzene was purchased from Acros and recrystallized from ethanol prior use. 2-Bromo-1,3,4-thiadiazole was purchased from Matrix Scientific and used as received. Hydroquinone was purified via sublimation prior to use. 1-Bromohexadecane, potassium hydroxide, and toluene were received from Acros and used as received. All other reagents were procured and purified as described in chapters II and III.

### Instrumentation

Compounds were characterized using melting point determination (MP) and magnetic nuclear resonance (NMR).  $^1\text{H}$  and  $^{13}\text{C}$  NMR were accomplished with Varian INOVA 400 MHz NMR and a Bruker Avance III 400 MHz NMR while MPs were determined using Mel-Temperature Electrochemical with Fluke 51 thermometer detector.

### Synthesis

**1,4-Bis-1,3,4-thiadiazolyl benzene (Td2B):** Following the Mosquera *et al.*<sup>52</sup> protocol, 1,4-dibromobenzene was coupled to 2-bromo-1,3,4-thiadiazole to yield BTdB. A 1000mL 3-neck round bottom flask was fitted with a gas-inlet adapter and two septa and flame dried. 2-Bromo-1,3,4-thiadiazole (4g, 24.2mmol) was dissolved in THF (40mL, 10 wt. %) and added while stirring under positive argon flow. The solution was cooled to  $-78^\circ\text{C}$  with an acetone/dry ice bath and n-BuLi (2.5M in hexanes; 10.6mL, 26.6mmol) was added drop-wise and stirred at  $-78^\circ\text{C}$  for 1 hour to yield a pale orange

solution of lithiated 1,3,4-thiadiazole. A second dry 1000mL 3-neck round bottom flask was fitted with a gas inlet adapter and two septa and dried under vacuum. 1.96g  $\text{InCl}_3$  (88.7mmol) was dissolved in 177.5mL to make 0.05M solution and then added drop wise to the lithiated 1,3,4thiadiazole solution via cannula transfer. Reaction mixture was stirred at  $-78^\circ\text{C}$  for 1 hour and allowed to warm to room temperature for another hour to afford tris(1,3,4-thiadiazolyl)indium. A third 1000mL 3-neck round bottom flask was fitted with an air inlet adapter, a septum and a condenser and flame dried. 1,4-dibromobenzene (1.90g, 8.05mmol) was dissolved in THF (19mL, 10 wt.%) and added to the flask along with  $\text{Pd}(\text{PPh}_3)_4$  (285mg, 0.0130mM) under positive argon flow and stirring. To the 1,4-dibromobenzene, the tris(1,3,4-thiadiazolyl)indium was added drop wise via cannula transfer and heated at reflux for 5 days. Reaction progress was monitored with TLC until the consumption of the starting material. Upon reaction completion, 2mL of methanol was added to quench the reaction and solvent was evaporated under reduced. Resultant solid was dissolved using a large amount of acetonitrile, washed with 5% HCl and the aqueous layer extracted with acetonitrile. The combined organic layers were washed with saturated ammonium chloride and sodium chloride, dried over anhydrous  $\text{MgSO}_4$  and evaporated under reduced pressure. Further purification was halted due to insolubility of the product. Pale yellow solid (3.05g).  $^1\text{H}$  NMR (dimethyl sulfoxid- $\text{d}_6$ )  $\delta$  8.88 (s, 2H), 7.60 (m, 2H) and 7.50 (m,2H).

**2,5-Dibromohydroquinone (DBrHq):** A 250mL 3-neck round bottom flask was fitted with a gas inlet adapter, a septum and a constant pressure addition funnel and flame dried under vacuum. Under positive argon flow, hydroquinone (24.9g, 227mmol)

and glacial acetic acid (125mL) were added to the flask with stirring. Bromine (22.6mL, 440.9mmol) was dissolved in dichloromethane (25mL) and added drop wise to the reaction flask via the addition funnel. The singly brominated hydroquinone was observed to as a light orange solution. Once the rest of the bromine was added over a period of 2 hours, the reaction mixture was stirred for 19 hours. DBrHq precipitated out as white solid. The solid was filtered and dried over NaOH pellets in a desiccator (7.56g, 34.5%). Experimental MP range of 191-192°C was consistent with the literature.<sup>64</sup> <sup>1</sup>H NMR (CD<sub>2</sub>Cl<sub>2</sub>) δ 7.2.0 (s, 2H), 7.16 (s, 2H). (Lit.<sup>64</sup> (acetone-d<sub>6</sub>) δ 8.62 (s, 2H), 7.15 (s, 2H)).

**1,4-Dibromo-2,5-dihexadecacycloxybenzene (DBrC<sub>16</sub>B):** DBrC<sub>16</sub>B was prepared according to a literature procedure.<sup>64</sup> A 500mL 3 neck round bottom flask was fitted with a gas inlet adapter and two septa and flame dried under vacuum. KOH (2.30g, 41.06mmol) was dissolved in excess ethanol in a round bottom flask under argon. A 500mL 3 neck round bottom flask was fitted with a gas inlet adapter, a condenser and a septum and flame dried under a vacuum. Under positive argon flow, DBrHq (5.0g, 18.66mmol) was added and dissolved with THF (50mL) via cannula transfer. While stirring, the KOH solution was added drop wise via cannula transfer and the reaction mixture was stirred at room temperature for 3 hours. 1-Bromohexadecane (12.53g, 41.06mmol) was dissolved in THF (125mL, 10 wt%) and added to the reaction mixture dropwise via cannula transfer. The flask was heated at reflux for 24 hours. After the addition of 800mL of water, the precipitated solid was collected via filtration. Recrystallization using 3:1 ethanol: toluene afforded a white solid (4.0g, 29.90%). Experimental MP range of 87.8-89.1°C was consistent with the range reported in the

literature.<sup>64</sup> <sup>1</sup>H NMR (CDCl<sub>3</sub>) δ 7.08 (s), 3.40 (m), 1.78(m), 1.52(m), 1.45(m) and 0.89(m). (Lit:<sup>64</sup> (acetone-d<sub>6</sub>) δ 6.99 (s), 3.38 (t), 1.55 (q), 1.30 (m) and 0.92 (t)).

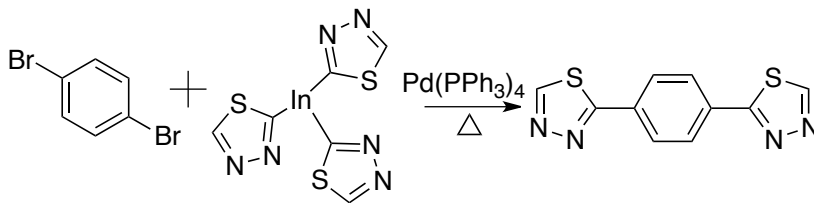
**1,4-Bis-1,3,4-thiadiazolyl-2,5-bis-hexadecyloxybenzene (BTdBC<sub>16</sub>):**

DBrC<sub>16</sub>B was coupled to 2-bromo-1,3,4-thiadiazole using the method described by Mosquera *et al.*<sup>52</sup> to yield BTBC<sub>16</sub>. A 1000mL 3-neck round bottom flask was fitted with a gas inlet adapter and two septa and flame dried under vacuum. 2-Bromo-1,3,4-thiadiazole (1g, 6.06mmol) was dissolved in THF (10mL, 10 wt. %) and added while stirring under positive argon flow. The solution was cooled to -78°C in an acetone/dry ice bath and n-BuLi (2.5M in hexanes; 2.67mL, 6.6mmol) was added drop-wise and stirred at -78°C for 1 hour to yield a pale orange solution of lithiated 1,3,4-thiadiazole. A second dry 1000mL 3-neck round bottom flask was fitted with a gas inlet adapter and two septa and dried under vacuum. InCl<sub>3</sub> (0.49g, 0.222mmol) was dissolved in 177.5mL THF to make a 0.05M solution and then added drop wise to the lithiated 1,3,4-thiadiazole solution via cannula transfer. The reaction mixture was stirred at -78°C for 1 hour and allowed to warm to room temperature for another hour to afford tris(1,3,4-thiadiazolyl)indium. A third 1000mL 3-neck round bottom flask was fitted with an air inlet adapter, a septum and a condenser and flame dried. DBrC<sub>16</sub>B (1.45g, 2.02mmol) was dissolved in THF (14.5mL, 10 wt.%) and added to the flask along with Pd(PPh<sub>3</sub>)<sub>4</sub> (217mg, 0.0130mM) under positive argon flow and stirring. Tris(1,3,4-thiadiazolyl)indium was added drop wise to the BBrC<sub>16</sub>B solution via cannula transfer and heated at reflux for 5 days. Reaction progress was monitored with TLC until consumption of the starting material was evident. Upon reaction completion, 2mL of

methanol was added to quench the reaction, and solvent was evaporated under reduced pressure. The resultant solid was dissolved in dichloromethane and washed with 5% HCl. The aqueous layer was extracted with diethyl ether 3 times. The combined organic layers were washed with saturated ammonium chloride and sodium chloride, dried over anhydrous MgSO<sub>4</sub> and evaporated under reduced pressure. Unreacted started material was precipitated out via precipitation into ethanol to yield a grey-brown liquid (87mg). <sup>1</sup>H NMR (CDCl<sub>3</sub>) δ 9.11 (s), 7.43 (s), 4.15(m), 2.19(m), 2.13(m), 1.76(m), 1.39(m), 1.10(m), and 0.84 (m). <sup>13</sup>C NMR (CDCl<sub>3</sub>) δ 155.7, 139.5, 132.6, 132.1, 132.0, 131.6, 128.5, 99.7, 64.8, 58.3, 34.2, 31.9, 30.3, 29.4, 28.9, 28.0, 22.7, 18.4 and 14.1.

### Results and Discussion

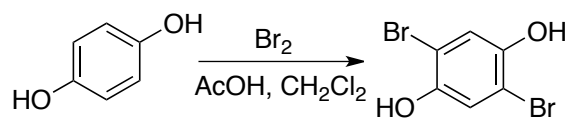
BTdB was prepared by reacting 1,3,4-thiadiazole with 1,4-dibromobenzene (Scheme 16). Unfortunately, the product proved to be insoluble in common organic solvents, and purification was not possible. The solid was slightly soluble in DMSO-d<sub>6</sub> for NMR analysis, revealing a mixture of products. Spectrum 15 shows the presence of the expected product peaks at 8.8, 7.6 and 7.5ppm along with solvent and precursor peaks.



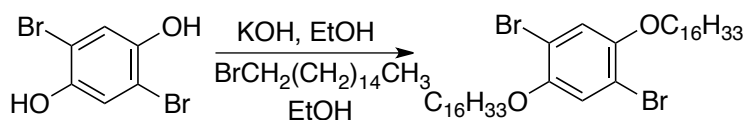
**Scheme 16:** Synthesis of 1,4-bis-(1,3,4-thiadiazol-2-yl)benzene (BTdB)

To improve solubility and solution processability of this compound, long alkyl ether substituents were introduced to the central ring. Etherification was accomplished by

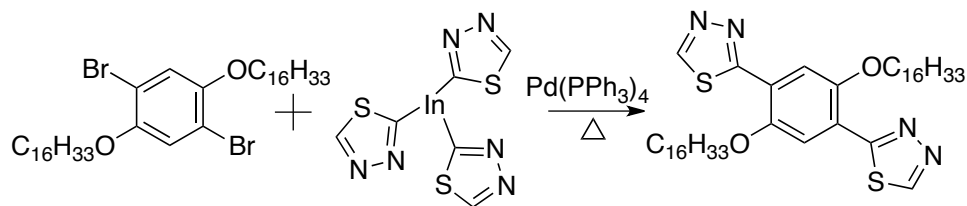
first introducing bromine substituents to hydroquinone (Scheme 17) according to a literature procedure.<sup>64</sup> Brominated hydroquinone (Spectrum 17) was then deprotonated using potassium hydroxide. The resultant diphenoxide was then reacted with two equivalents of 1-bromohexadecane to form the diether 1,4-dibromo-2,5-dihexadecyloxybenzene (Scheme 18), DBrBC<sub>16</sub>, as was previously reported.<sup>64</sup> Spectrum 18 reveals the presence of DBrBC<sub>16</sub> (peaks at 7.1, 3.4 and multiplets from 1.5-0ppm). Lastly, 1,4-dibromo-2,5-dihexadecyloxybenzene was subjected to palladium catalyzed coupling with the organoindium reagent in an attempt to yield the novel monomer BTdBC<sub>16</sub> (Scheme 19). The resultant product proved to be significantly more soluble than BTdB; by precipitation into ethanol and characterization via <sup>1</sup>H NMR and <sup>13</sup>C NMR revealed a complex mixture of products; purification is ongoing. A single peaks at 9.1 ppm and the many aromatic peaks around 7 ppm demonstrate the presence of doubly coupled and unreacted alkoxybenzene precursor (Spectrum 19).



**Scheme 17:** Bromination of hydroquinone



**Scheme 18:** Etherification of 1,4-dibromohydroquinone



**Scheme 19:** Synthesis of 1,4-bis-(1,3,4-thiadiazol-2-yl)-2,5-bis-hexadecyloxybenzene (BTdBC<sub>16</sub>)

### Conclusions

Since 1,3,4-thiadiazole's electronic properties have not been fully studied and its electron affinity or donating abilities have not been established, the goal of this chapter was to couple 1,3,4-thiadiazole with benzene and alkoxy benzenes to decipher each ring's optical properties individually and collectively. BTdB was synthesized but further characterization and isolation ceased due to insolubility. Alkoxy groups were introduced to the benzene to battle solubility problems and BTdBC<sub>16</sub> was realized.

## CHAPTER V

### CONCLUDING REMARKS

#### Conclusions

Monomers were synthesized using palladium catalyzed Stille and Sarandeses couplings. Most of the reactions were allowed to continue more than the published protocol time and stopped after consumption of starting material as confirmed by TLC. Purification of monomers was challenging. Most of the crude products were oils, and column chromatography isolation of product was sometimes impossible due to reactivity with silica. The dichloropyrazine isomers in particular seem to degrade after elution from silica columns; new aliphatic peaks emerged on  $^1\text{H}$  NMR spectrum.

#### Future Work

Purification of synthesized monomers is of the utmost importance for further characterization. Both the fluorinated thienylpyrazines and the thiadiazolyl benzenes need to be isolated and characterized fully. BTBPM synthesis was not completed due to inability to brominate 2,2'-bipyrimidine. Halogenation of the 2,2'-bipyrimidine would enable its coupling to thiophene or EDOT. Another approach would be to start with 5-

bromo-2-chloropyrimidine, halogen exchange the chlorine with iodine and reductively couple 5-bromo-2-iodopyrimidine to yield 5,5'-dibromo-2,2'-bipyrimidine, which would undergo a Sarandese coupling to produce BTBPm and BEBPm. Similarly, a 1:1 donor: acceptor ratio for BTPz, BEPz, BTdB and BTdBC<sub>16</sub> should also be realized to fully compare each monomer's charge transfer effect to increasing acceptor ratio.

To determine n-doping capabilities and optical properties of synthesized monomers, they must be electropolymerized and their electroactivities determined. Cyclic voltammetry experiments should clarify electronic affinity of monomers and n-doping and p-doping capabilities of polymers through reversible oxidation/reduction reactions in the presence of applied voltage. Spectroelectrochemistry (determination of the ultraviolet-visible absorption spectrum of the polymers as a function of applied potential) should be used to determine optical band gap of the polymers. To fully assess the structural and electronic properties such as planarity, aromaticity, and energy and bond length/angle dynamics of neutral versus doped polymer, XRD structures of the monomers should be determined.

Metal coordination of high-nitrogen, conjugated heterocycles enables tunability of optical, chemical, electrochemical and physical properties.<sup>65</sup> In bipyridine-thiophene copolymers bound to ruthenium by Pickup and co-workers, the HOMO was stabilized and electron exchange between metal and polymer was accelerated.<sup>66</sup> Since metal coordination broadens the optical properties of monomers and polymers, coordination with ferromagnetic metals should be considered to achieve super conductivity, electroluminescence and photoluminescence capabilities.<sup>67</sup> Metal coordination should be attempted both before and after electrochemical polymerization. X-Ray structures should

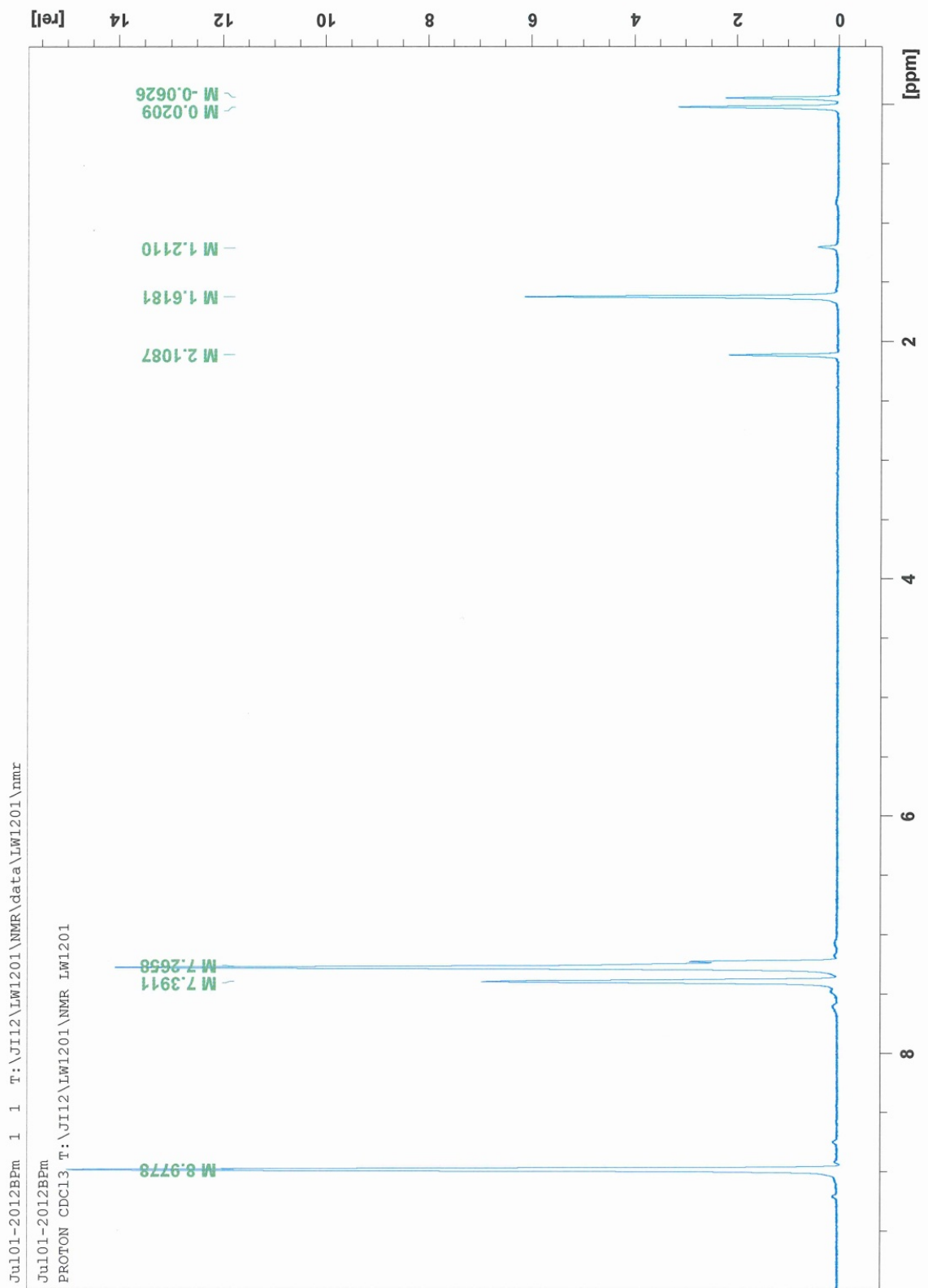
be acquired after synthesis and metal coordination of the monomers. Electrochemical polymerization of metal-coordinated monomers should be attempted and compared to non-metal coordinated monomer polymerization.

## APPENDIX A

### Nuclear Magnetic Spectra

Spectrum	Page
1. 2,2'-Bipyrimidine <sup>1</sup> H NMR .....	56
2. 3-Chloropyrazine 1-oxide <sup>1</sup> H NMR .....	57
3. Dichloropyrazine isomers <sup>1</sup> H NMR .....	58
4. 2,5-BTPz <sup>1</sup> H NMR .....	59
5. BEPz brown <sup>1</sup> H NMR .....	60
6. BEPz yellow <sup>1</sup> H NMR.....	61
7. BEPz brown <sup>13</sup> C NMR .....	62
8. BEPz yellow <sup>13</sup> C NMR.....	63
9. 2-Fluoropyrazine <sup>1</sup> H NMR.....	64
10. (SnBu <sub>3</sub> ) <sub>2</sub> FPz <sup>1</sup> H NMR .....	65
11. BTFPz <sup>1</sup> H NMR .....	66
12. BrEDOT/EDOT <sup>1</sup> H NMR .....	67
13. BrEDOT/EDOT <sup>13</sup> C NMR .....	68
14. BEFPz <sup>1</sup> H NMR .....	69
15. BTdB <sup>1</sup> H NMR.....	70
16. BTdB <sup>13</sup> C NMR .....	71
17. DBrHq <sup>1</sup> H NMR.....	72
18. BBrBC <sub>16</sub> <sup>1</sup> H NMR.....	73

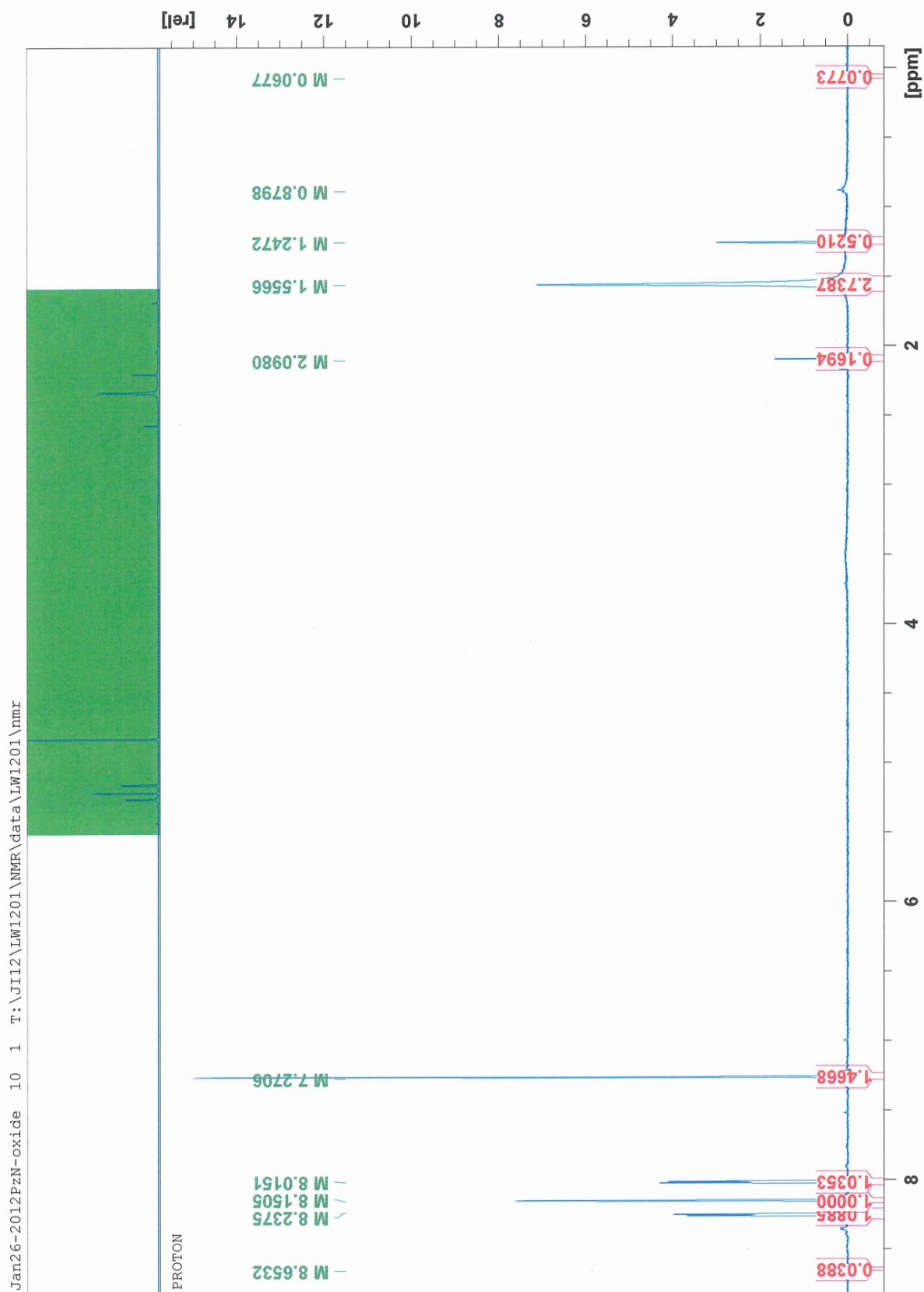
19. BTdBC <sub>16</sub> <sup>1</sup> H NMR.....	74
20.. BTdBC <sub>16</sub> <sup>13</sup> C NMR .....	75

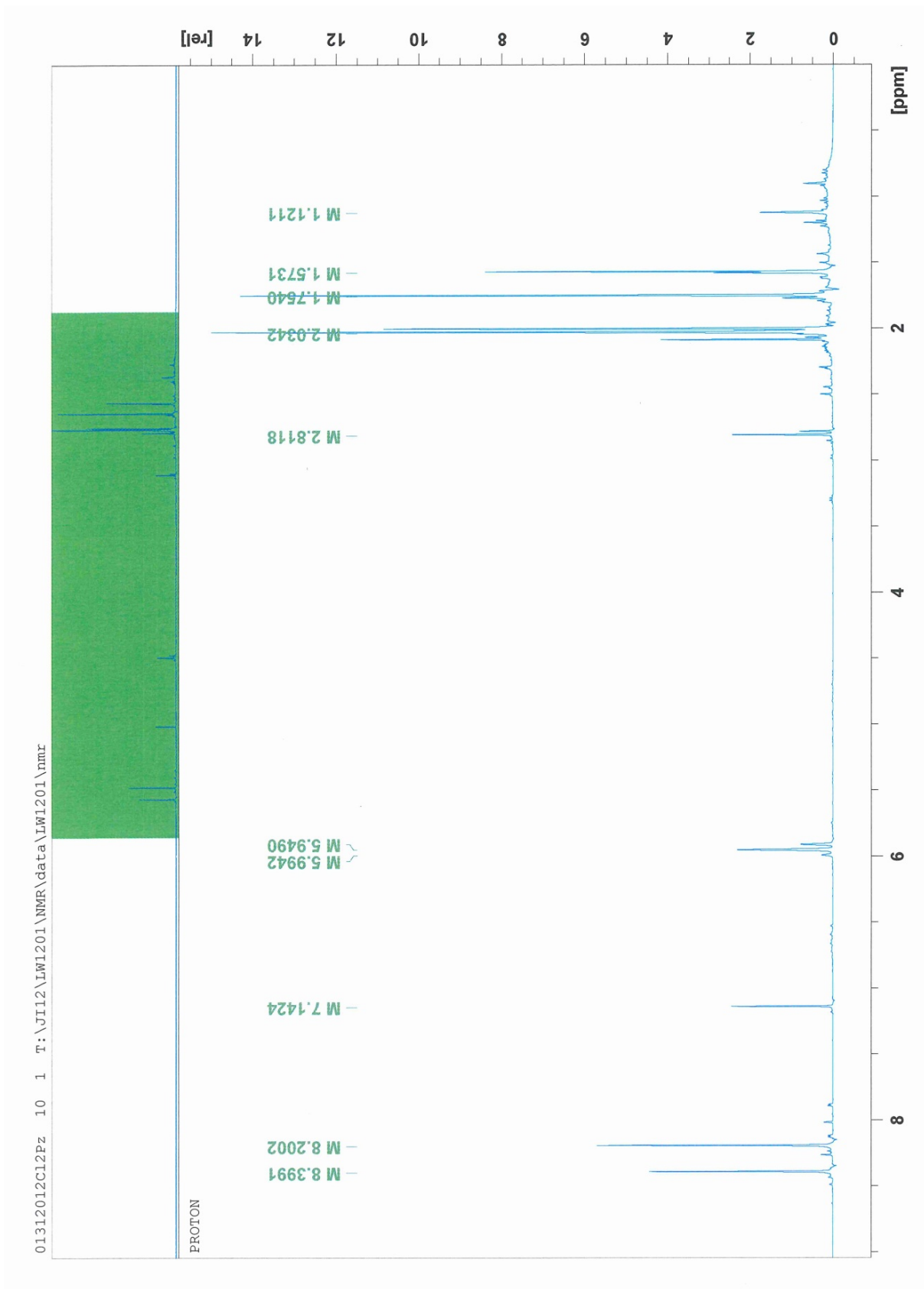


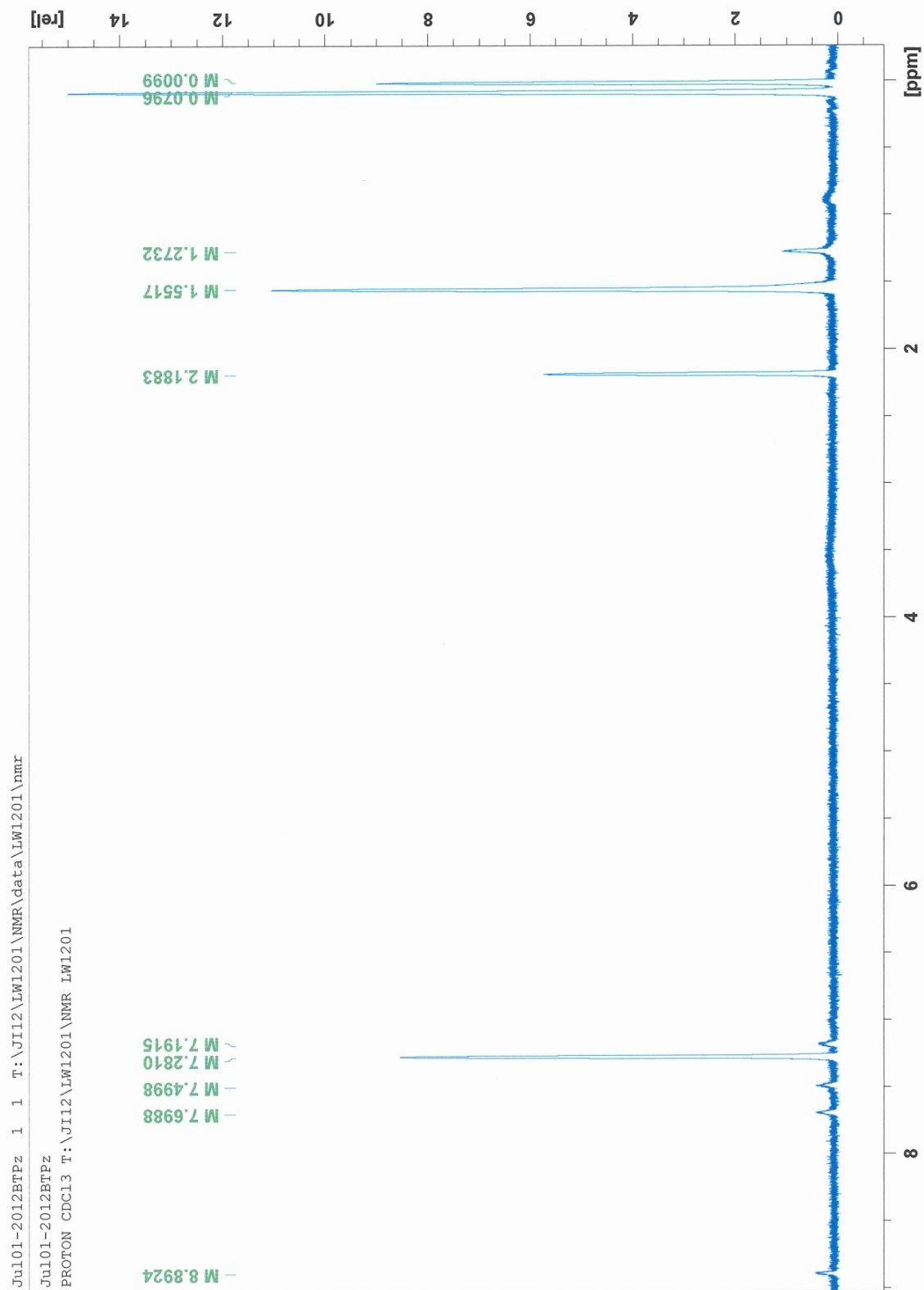
Jul101-2012BPm 1 1 T:\J112\LW1201\NMR\data\LW1201\nmr

Jul101-2012BPm  
PROTON CDCl3 T:\J112\LW1201\NMR LW1201

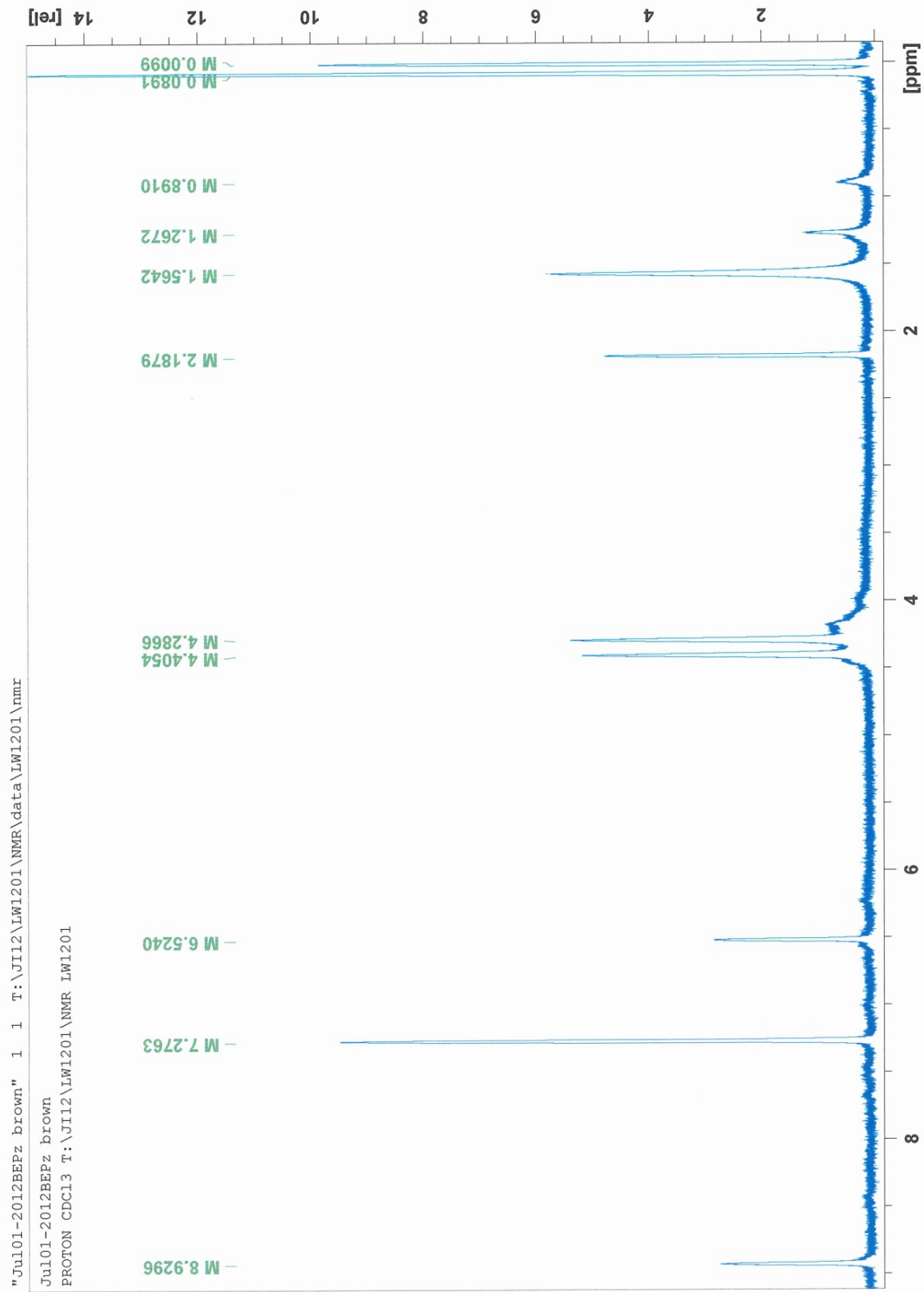
Spectrum 1: 2,2'-Bipyrimidine 1H NMR

Spectrum 2: 3-Chloropyrazine 1-oxide <sup>1</sup>H NMR

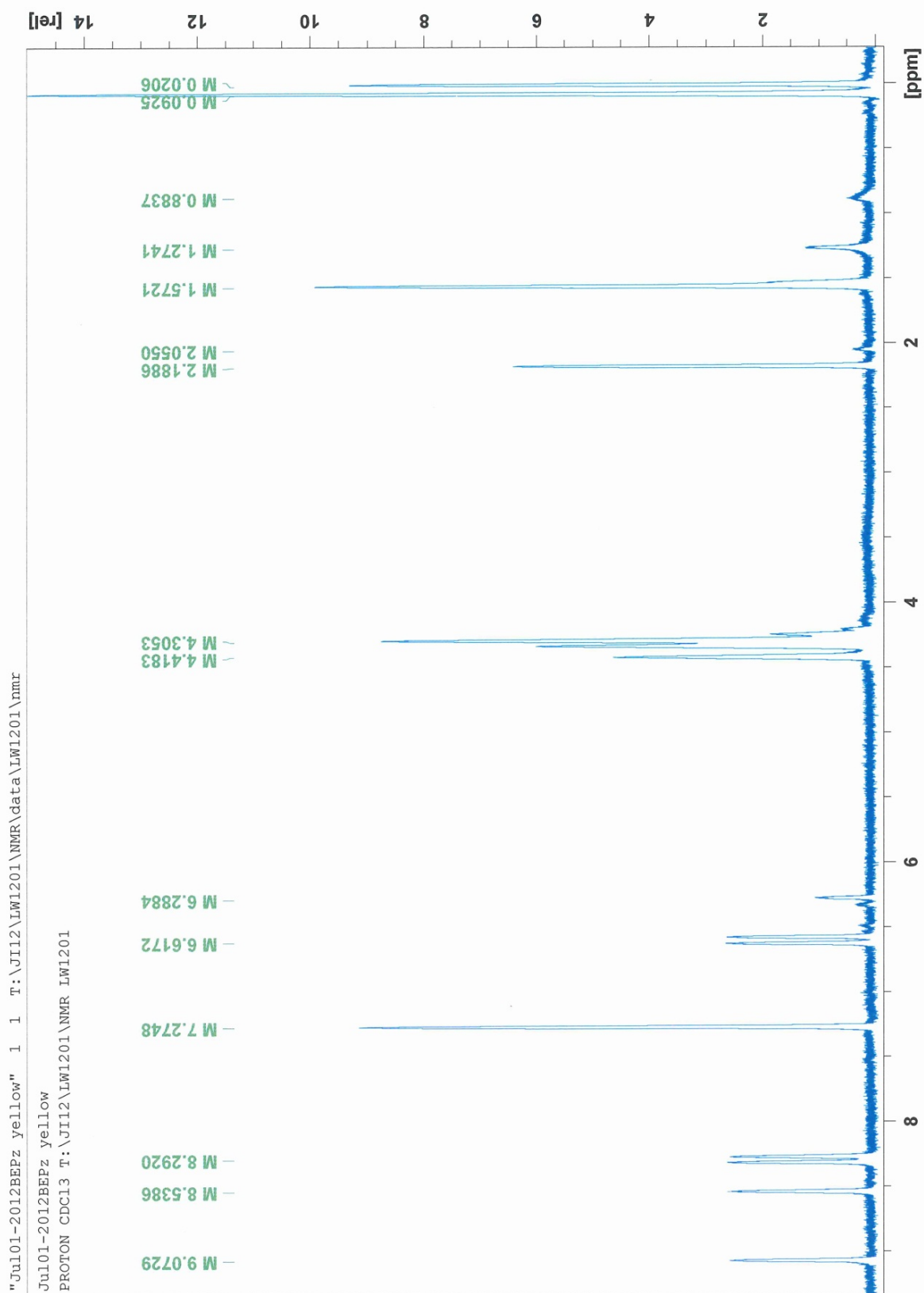
Spectrum 3: Dichloropyrazine isomers  $^1\text{H}$  NMR



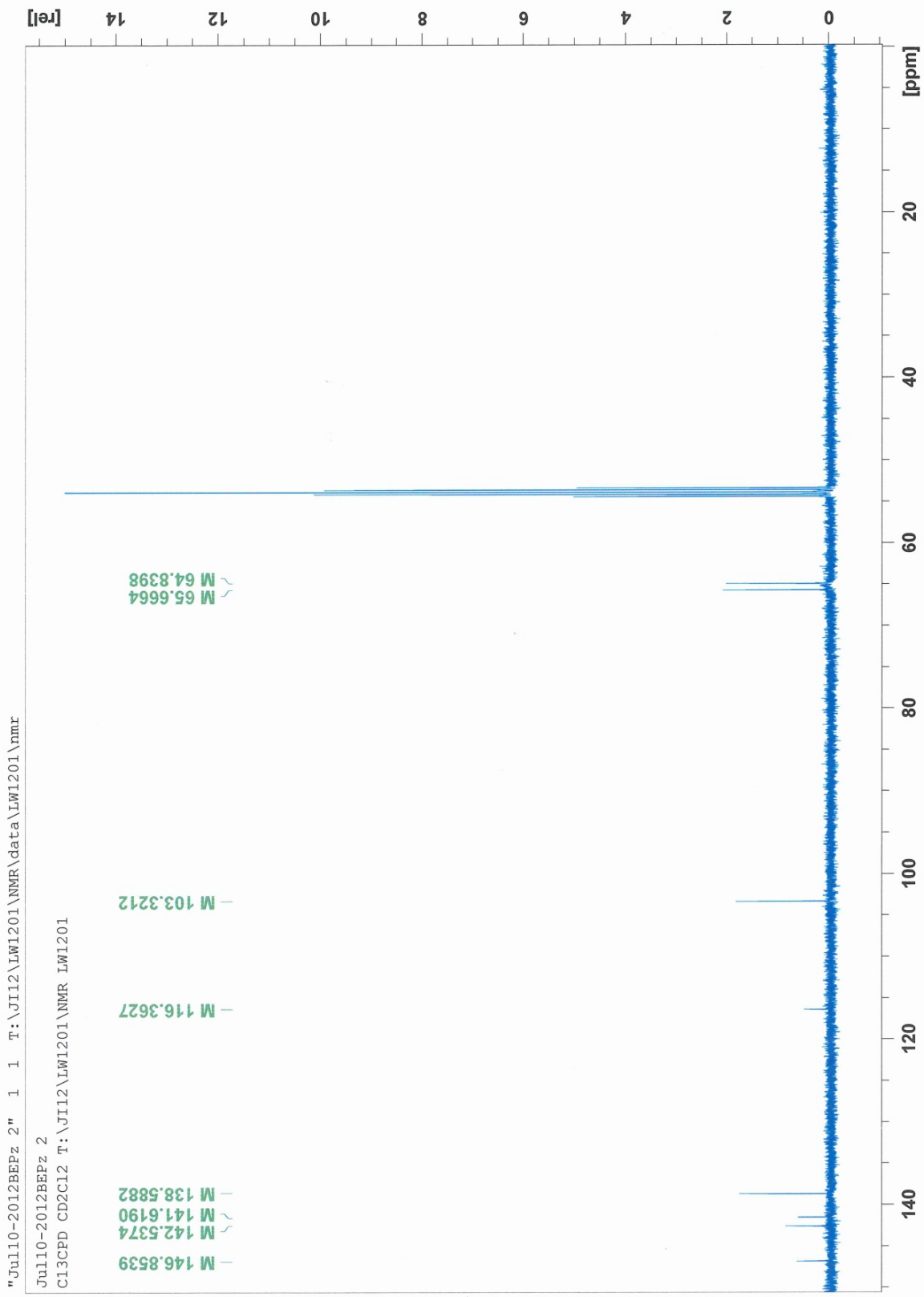
**Spectrum 4: 2,5-BTPz <sup>1</sup>H NMR**



**Spectrum 5: BEPz brown <sup>1</sup>H NMR**



Spectrum 6: BEPz yellow 1H NMR

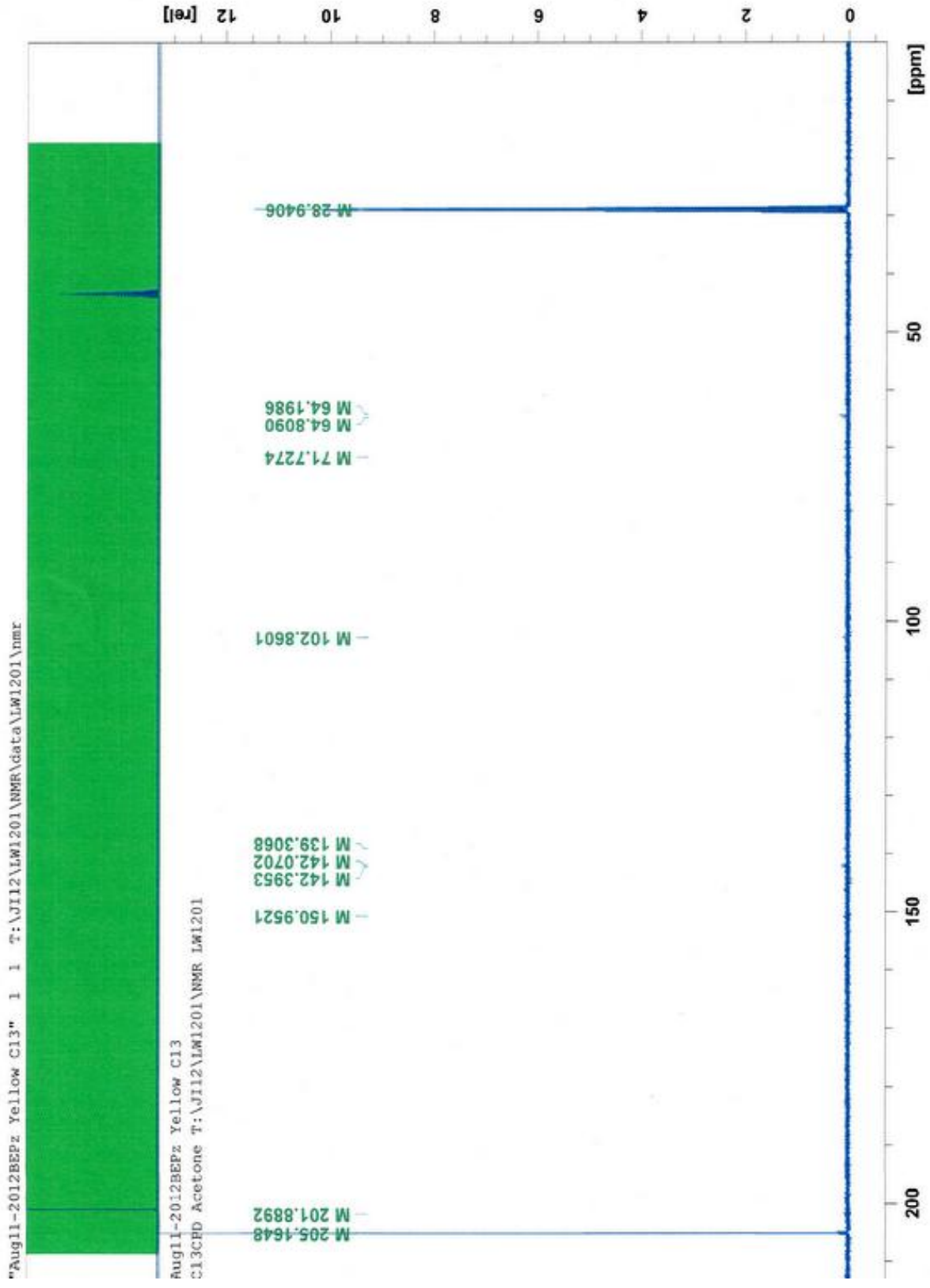


"Jul10-2012BEPz 2" 1 1 T:\JI12\LW1201\NMR\data\LW1201\nmr

Jul10-2012BEPz 2

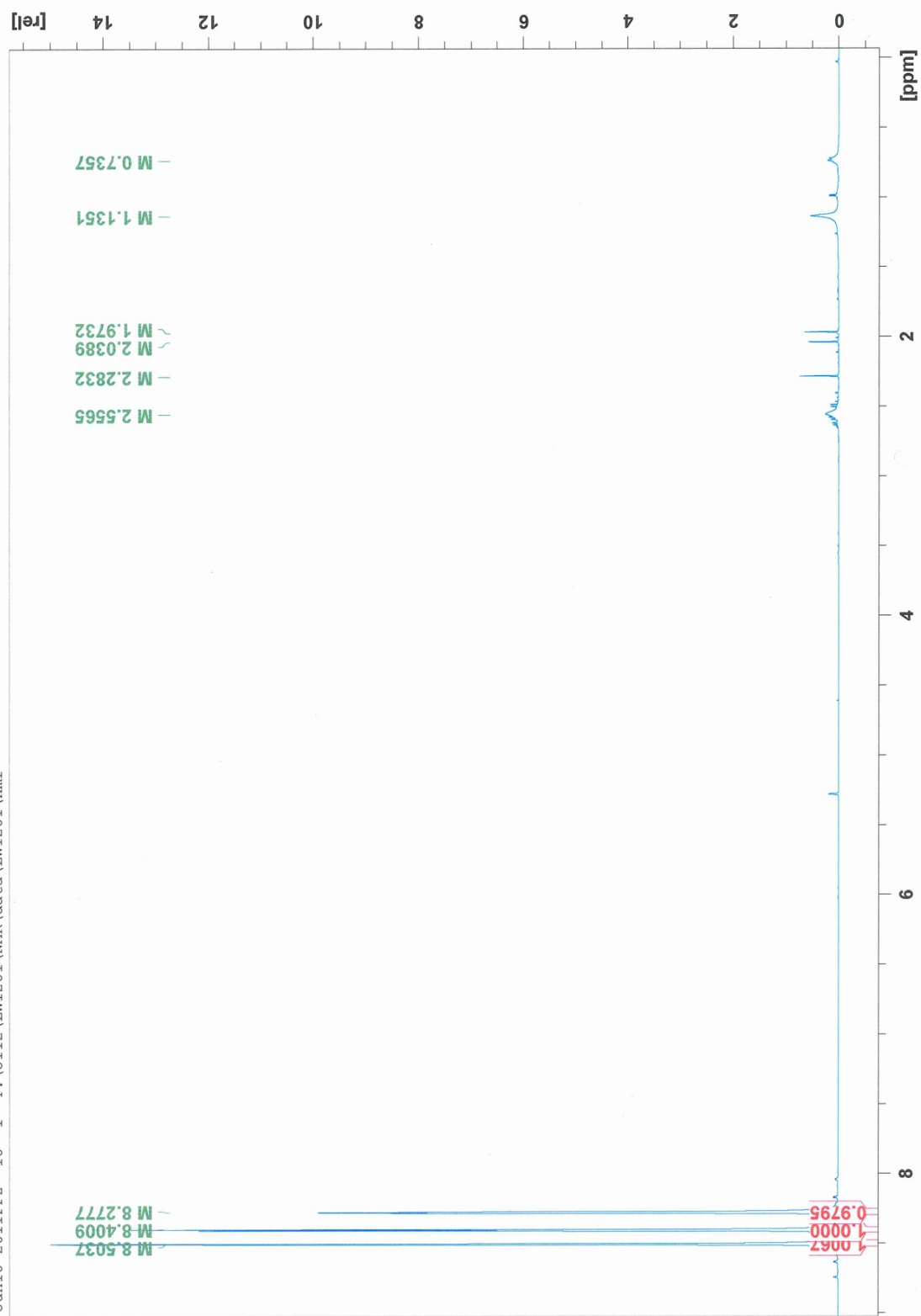
C13CPD CD2C12 T:\JI12\LW1201\NMR LW1201

Spectrum 7: BEPz brown <sup>13</sup>C NMR



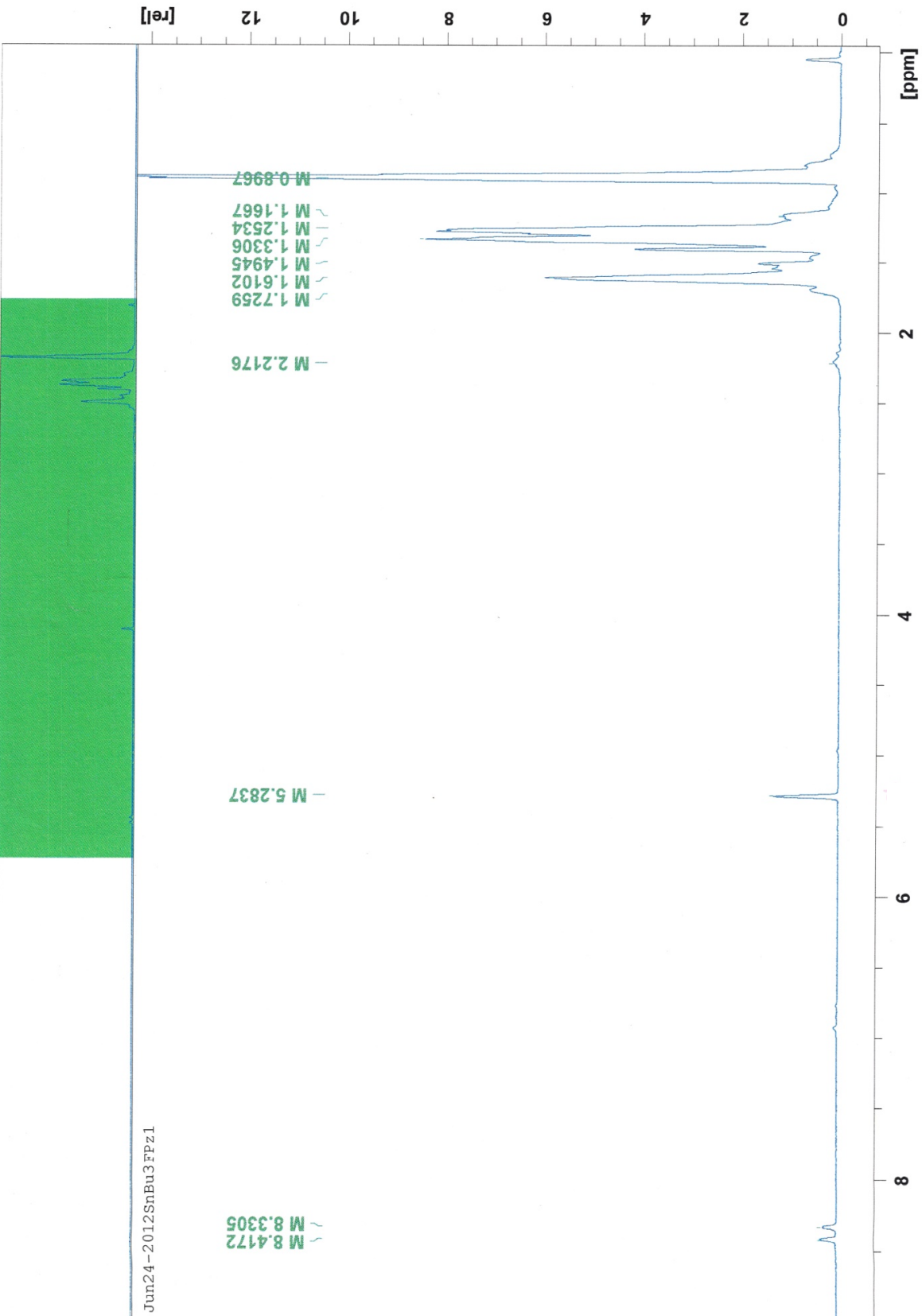
Spectrum 8: BEPz yellow <sup>13</sup>C NMR

Jun10-2011FPz 10 1 T:\J112\LW1201\NMR\data\LW1201\nmr



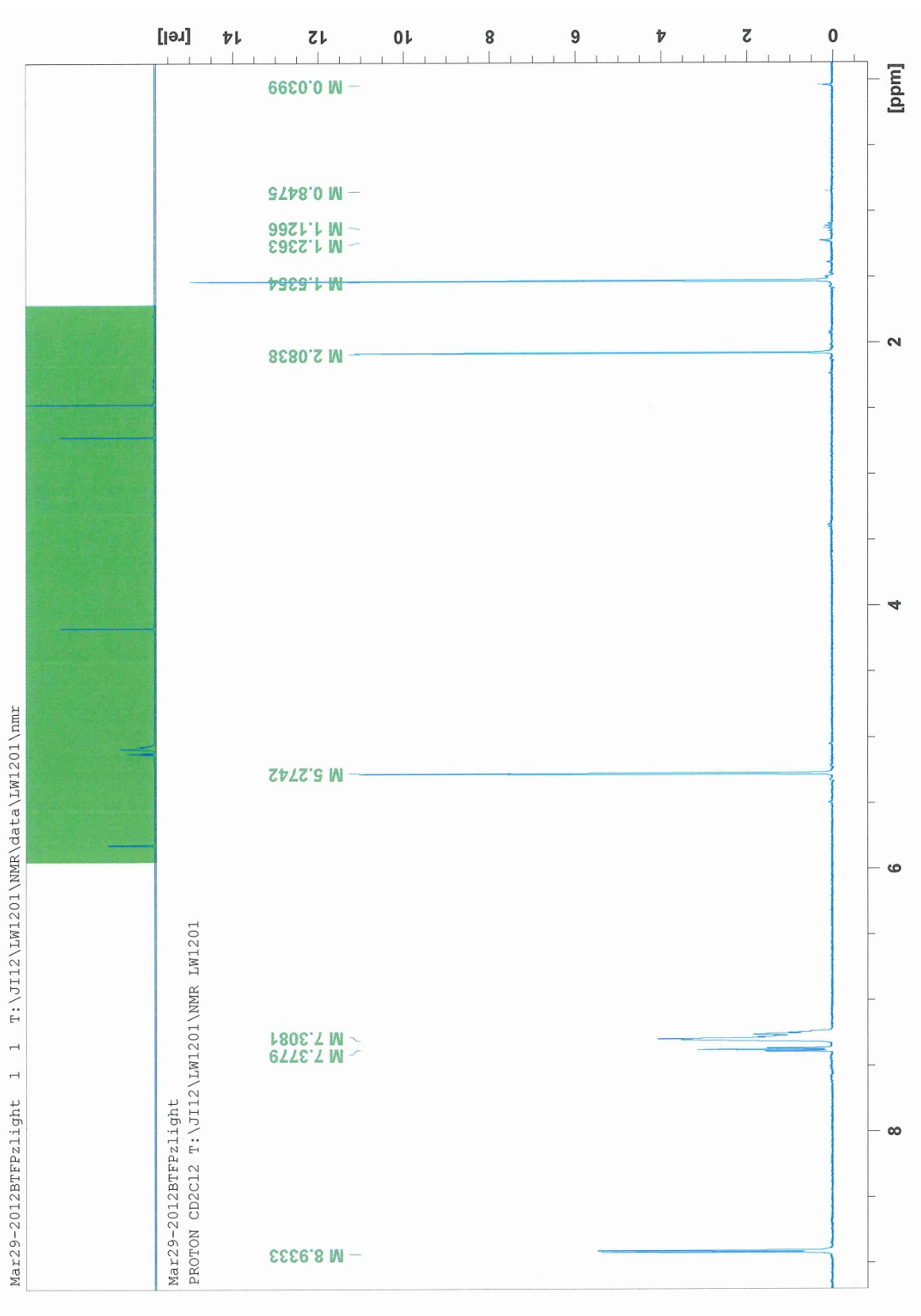
Spectrum 9: 2-Fluoropyrazine 1H NMR

Jun24-2012SnBu3FPz1 1 1 C:\Bruker\TopSpin3.0\examdata

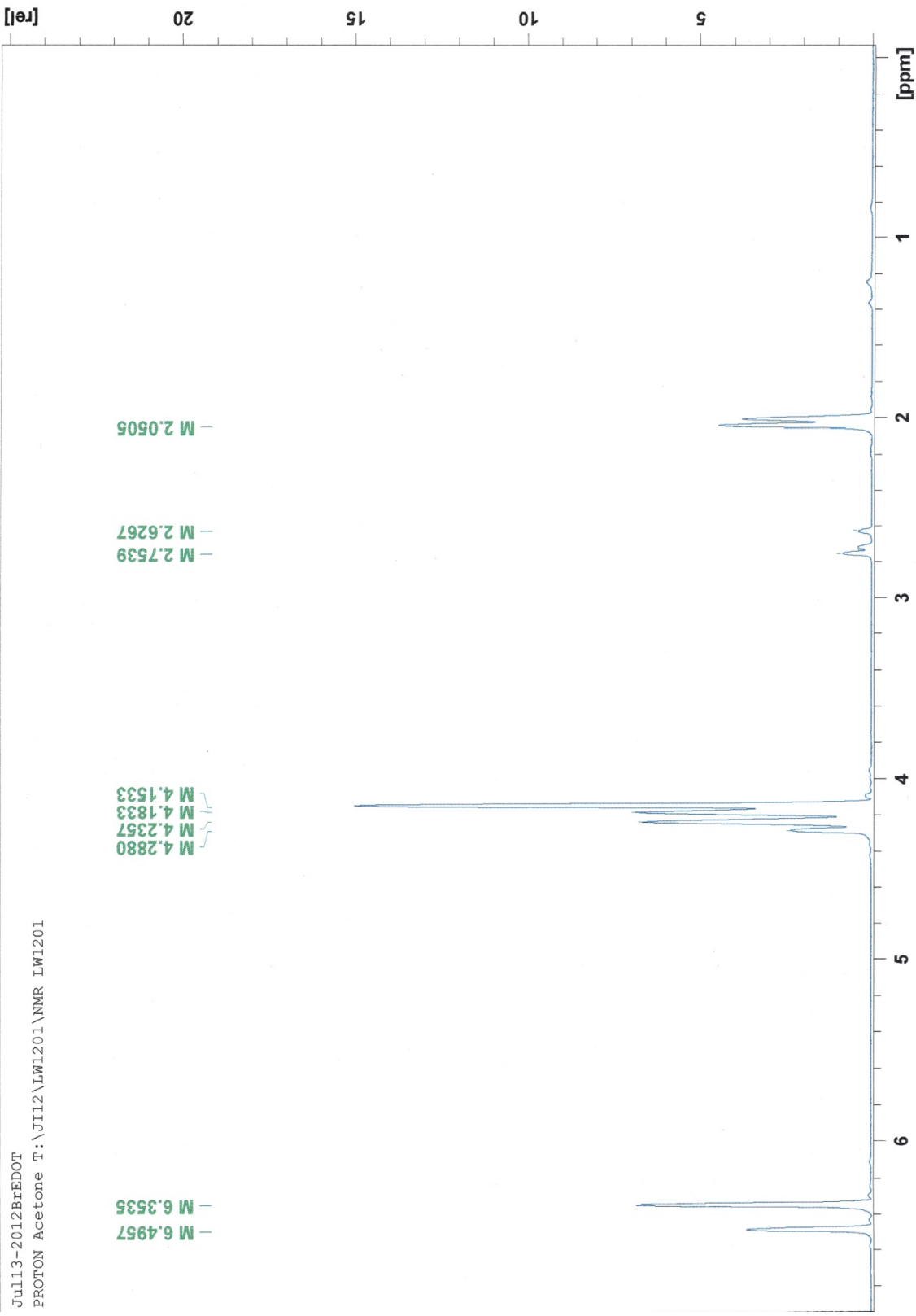


Spectrum 10: (SnBu3)2FPz <sup>1</sup>H NMR

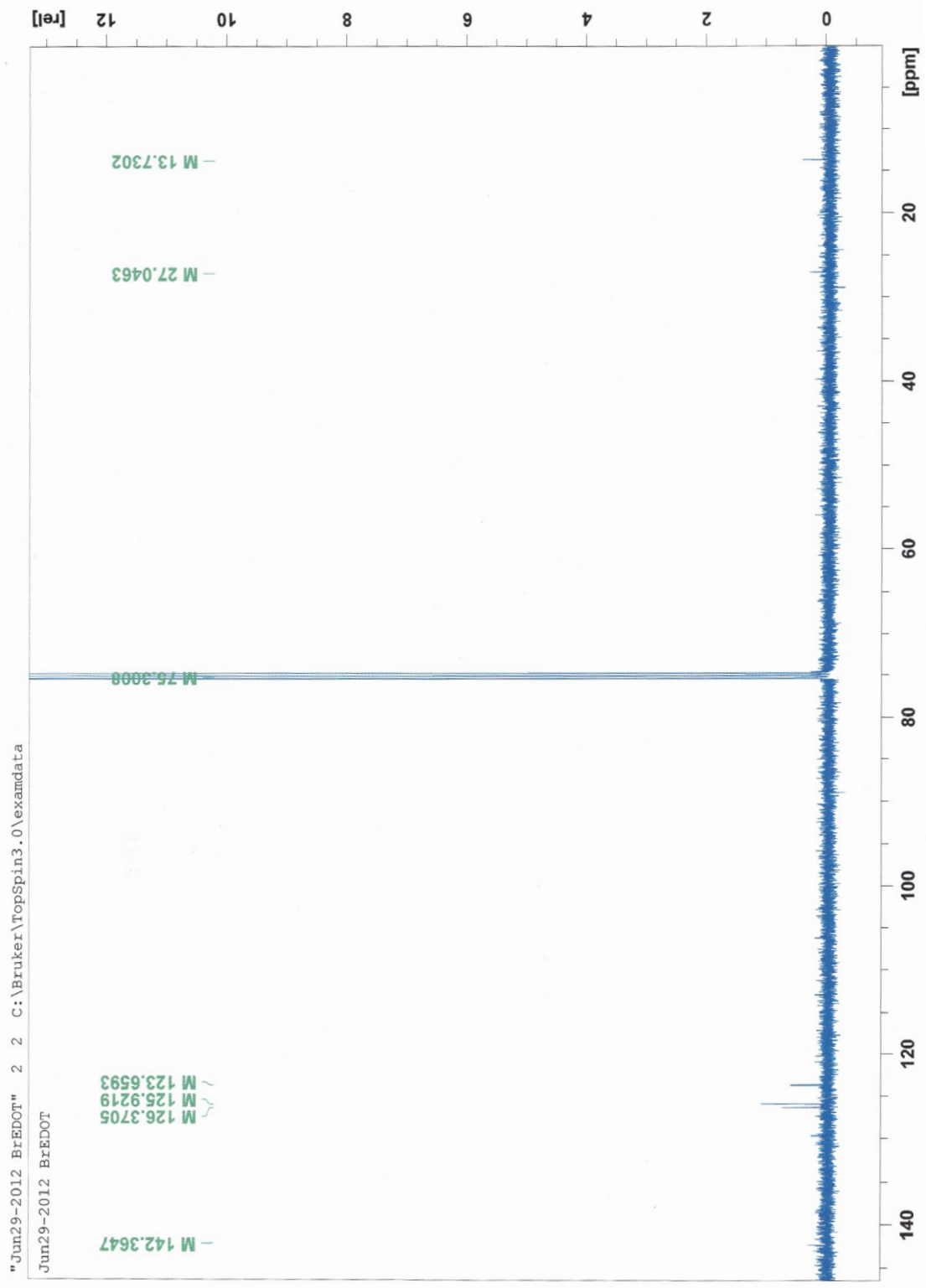
Spectrum 11: BTFPz <sup>1</sup>H NMR



Jul13-2012BrEDOT 1 1 T:\JI12\LW1201\NMR\data\LW1201\nmr  
Jul13-2012BrEDOT  
PROTON Acetone T:\JI12\LW1201\NMR LW1201



Spectrum 12: BrEDOT/EDOT <sup>1</sup>H NMR

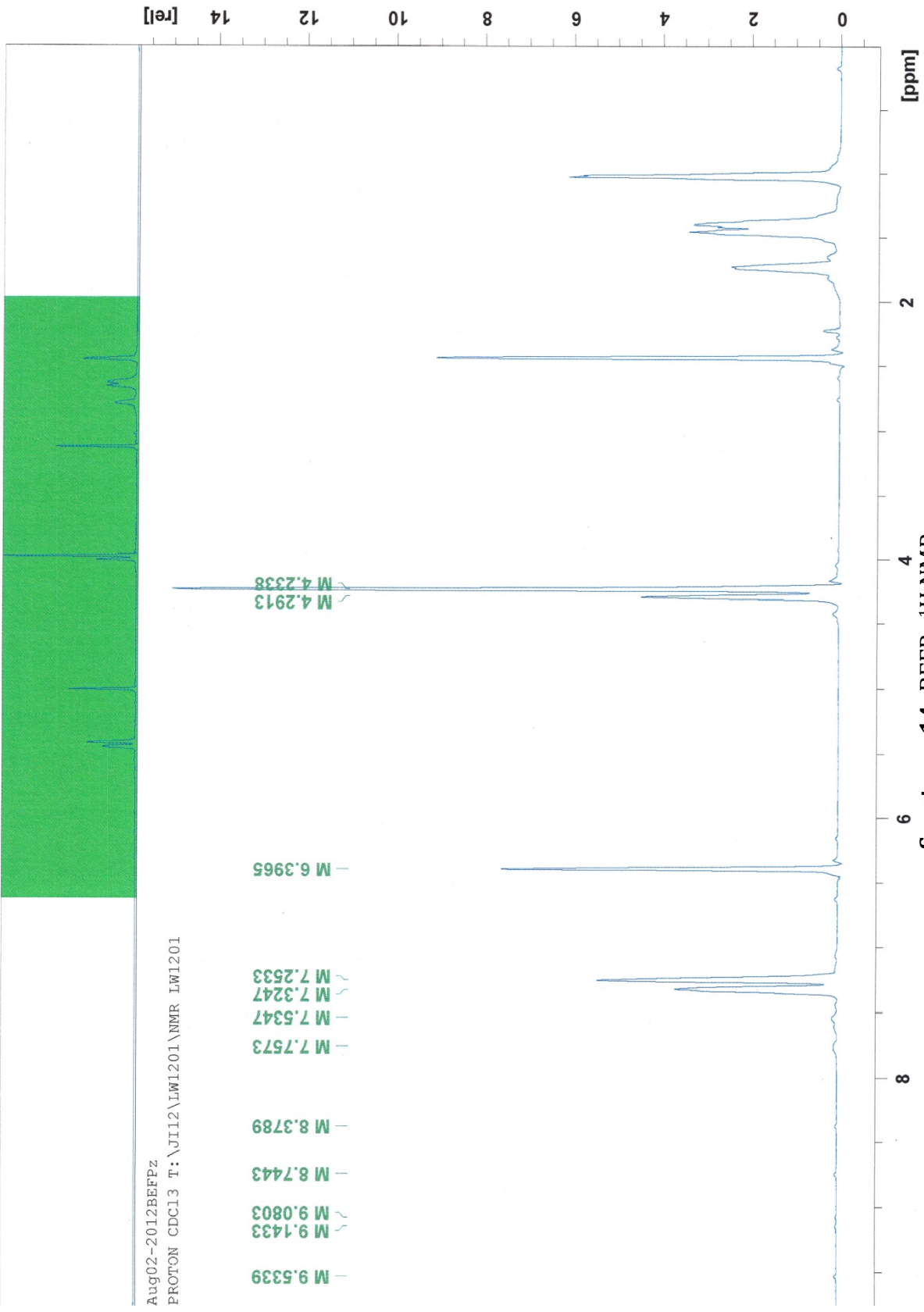


"Jun29-2012 BrEDOT" 2 2 C:\Bruker\TopSpin3.0\examdata  
Jun29-2012 BrEDOT

Spectrum 13: BrEDOT/EDOT <sup>13</sup>C NMR

Aug02-2012BEFPz 1 1 T:\J112\LW1201\NMR\data\LW1201\nmr

Aug02-2012BEFPz  
PROTON CDC13 T:\J112\LW1201\NMR LW1201

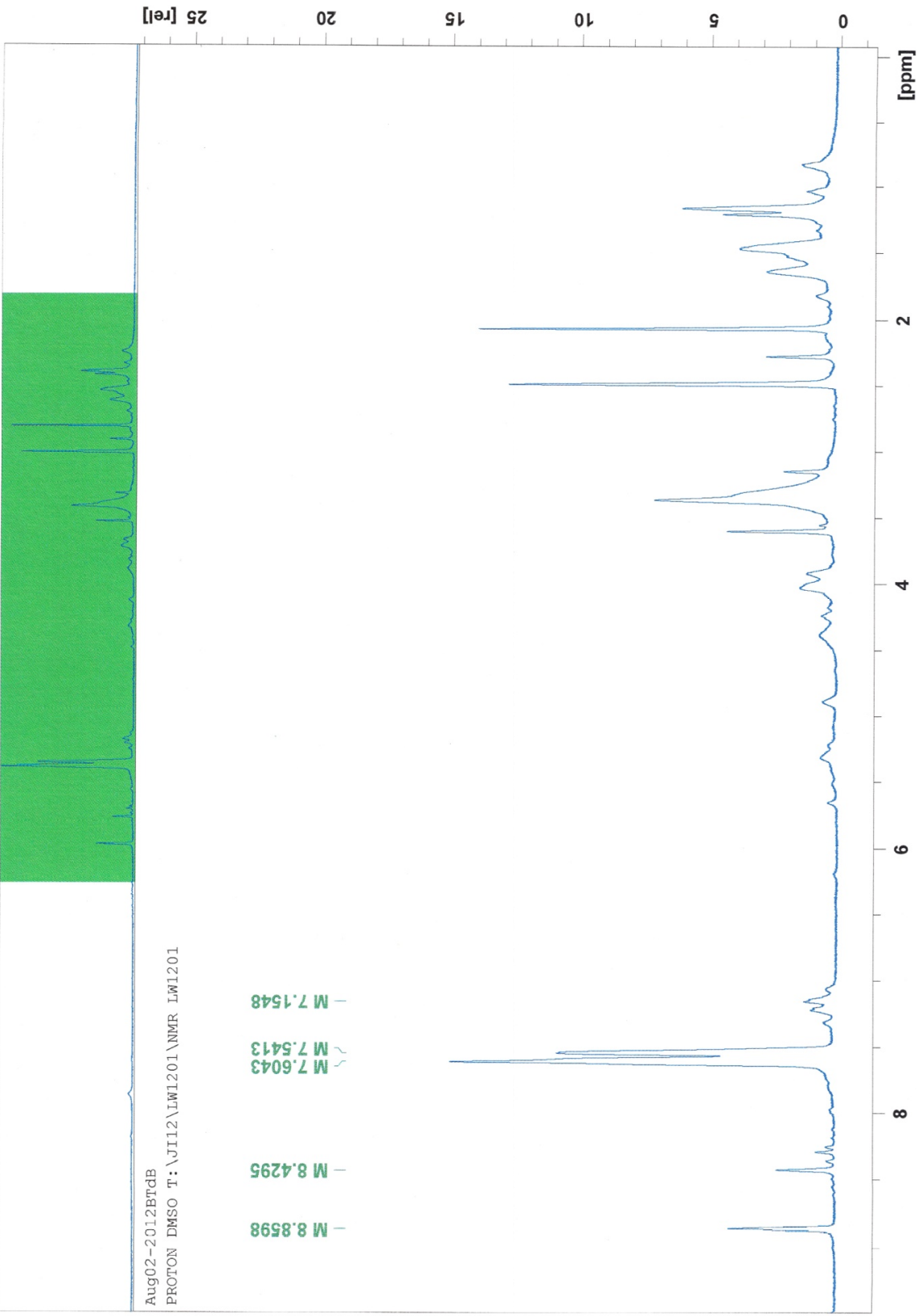


Spectrum 14: BEFPz 1H NMR

Aug02-2012BTdB 1 1 T:\JI12\LW1201\NMR\data\LW1201\nmr

Aug02-2012BTdB  
PROTON DMSO T:\JI12\LW1201\NMR LW1201

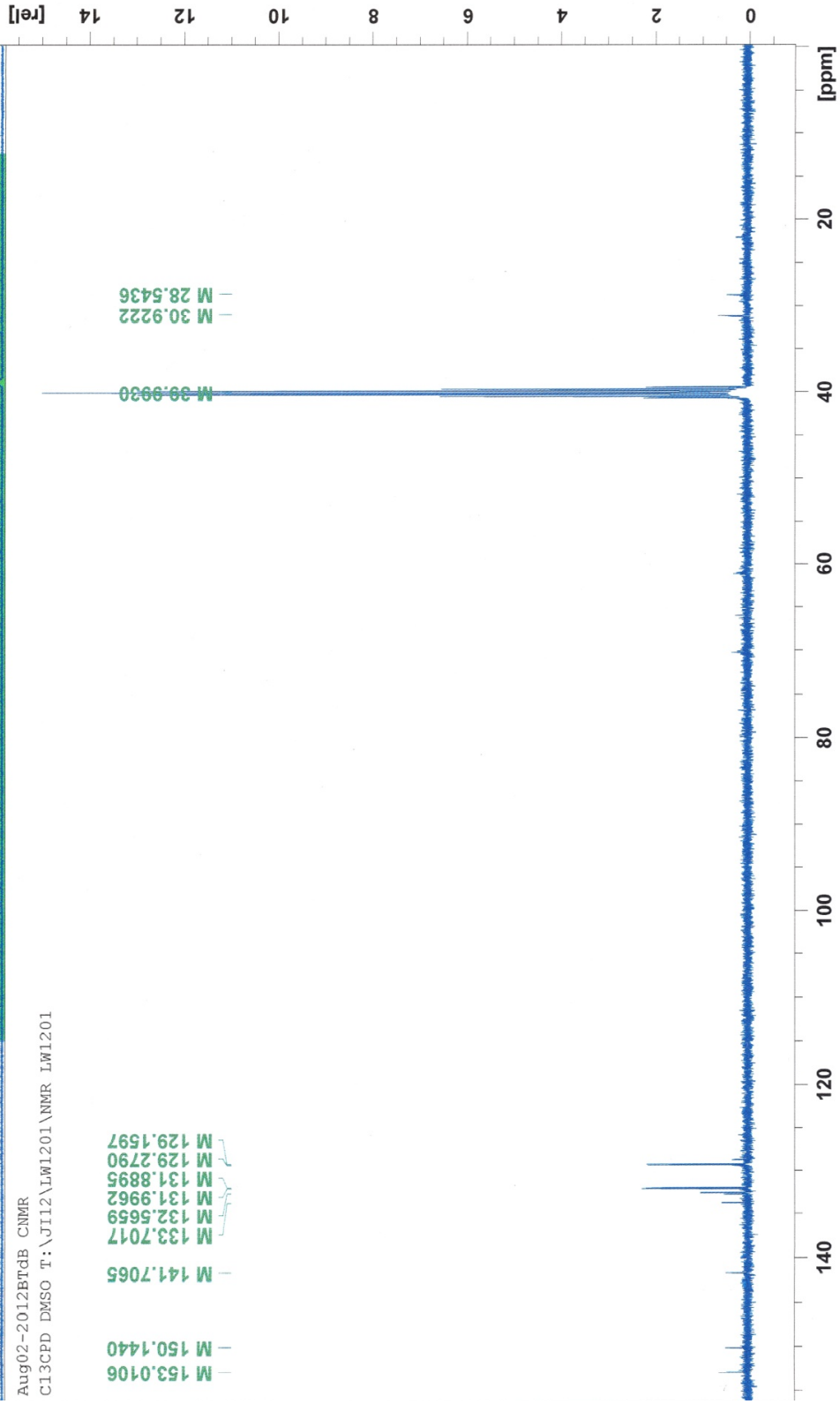
M 7.1548  
M 7.5413  
M 7.6043  
M 8.4295  
M 8.8598



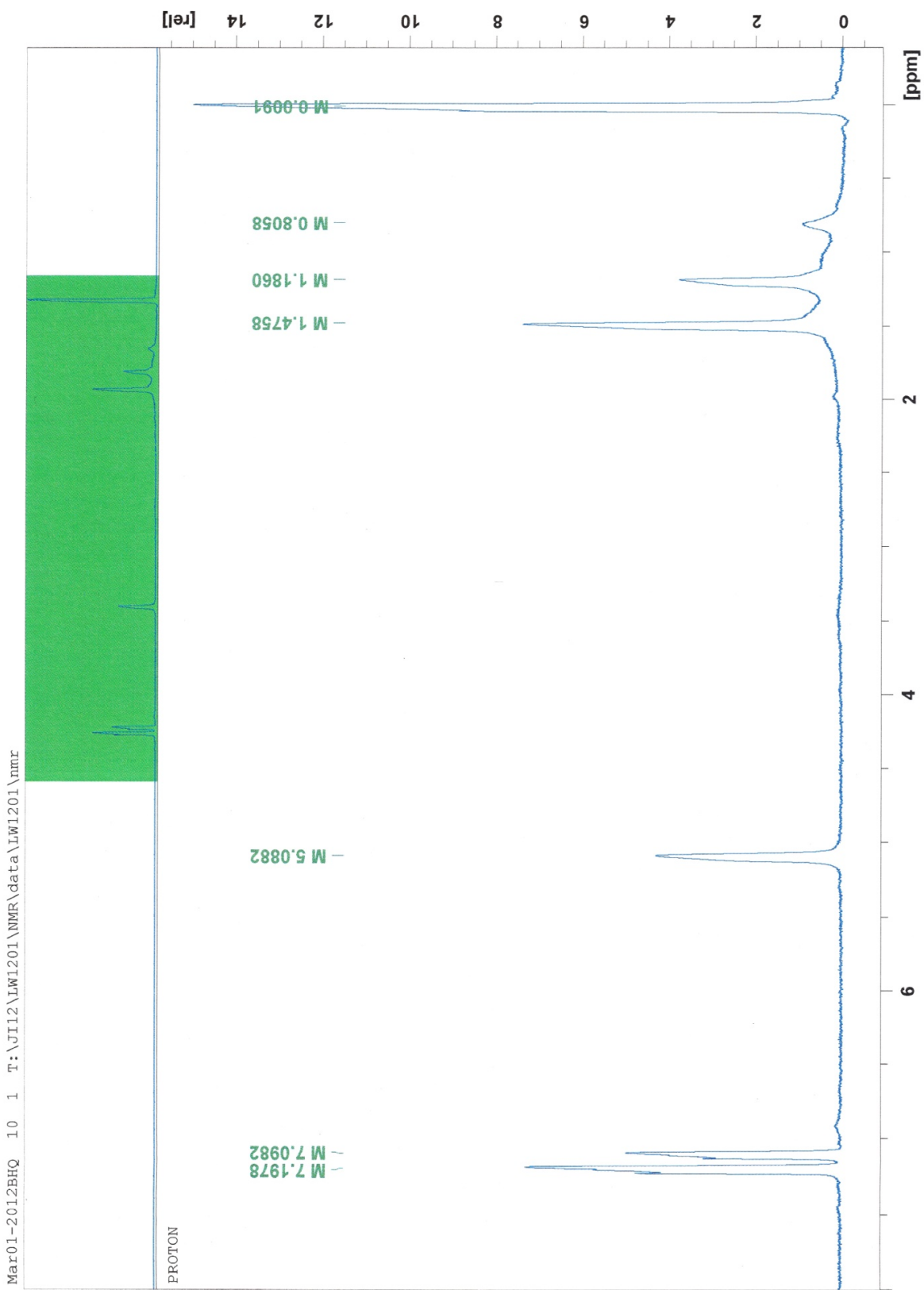
Spectrum 15: BTdB 1H NMR

"Aug02-2012BTdB CNMR" 1 1 T:\J112\LW1201\NMR\data\LW1201\nmr

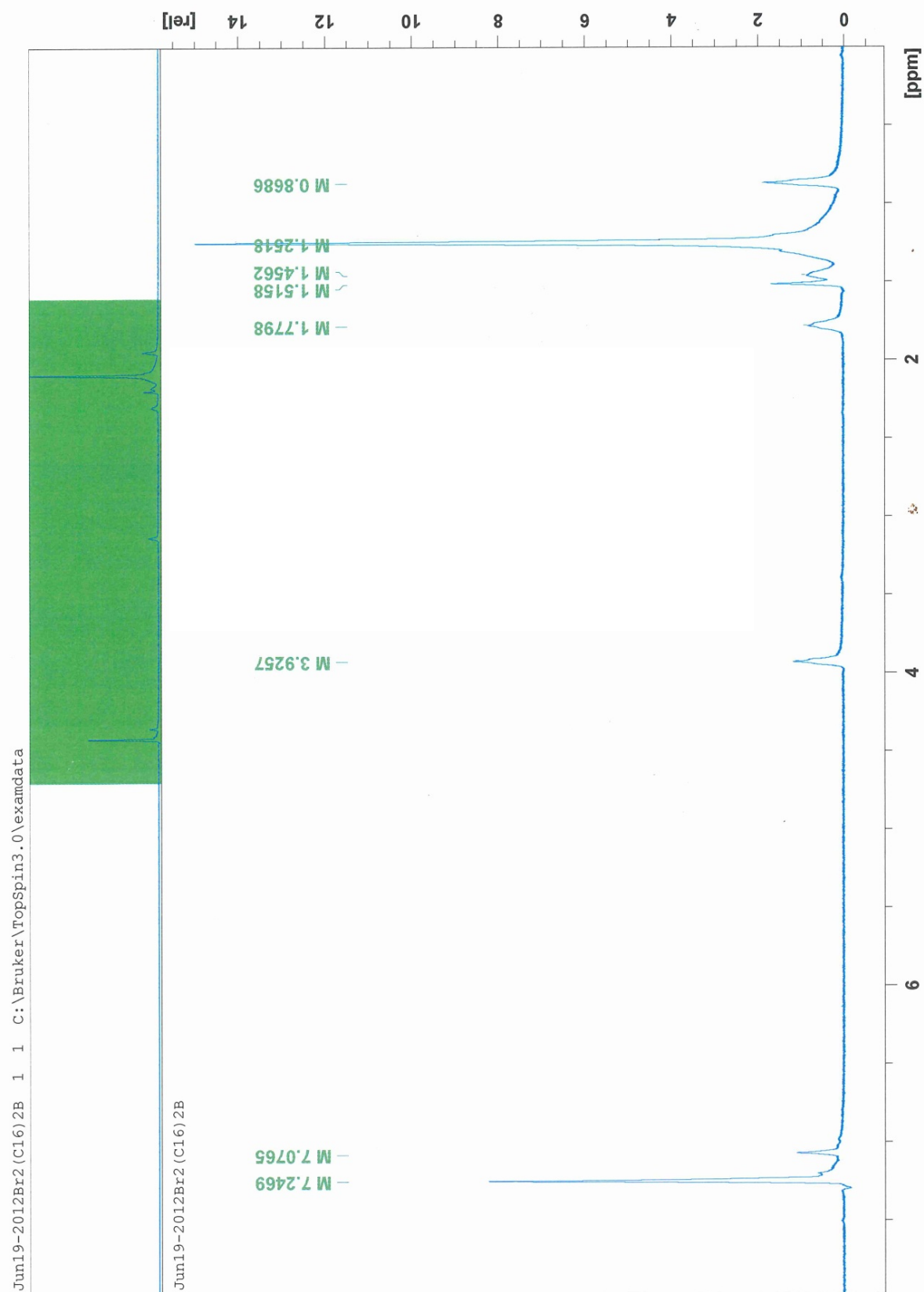
Aug02-2012BTdB CNMR  
C13CPD DMSO T:\J112\LW1201\NMR LW1201

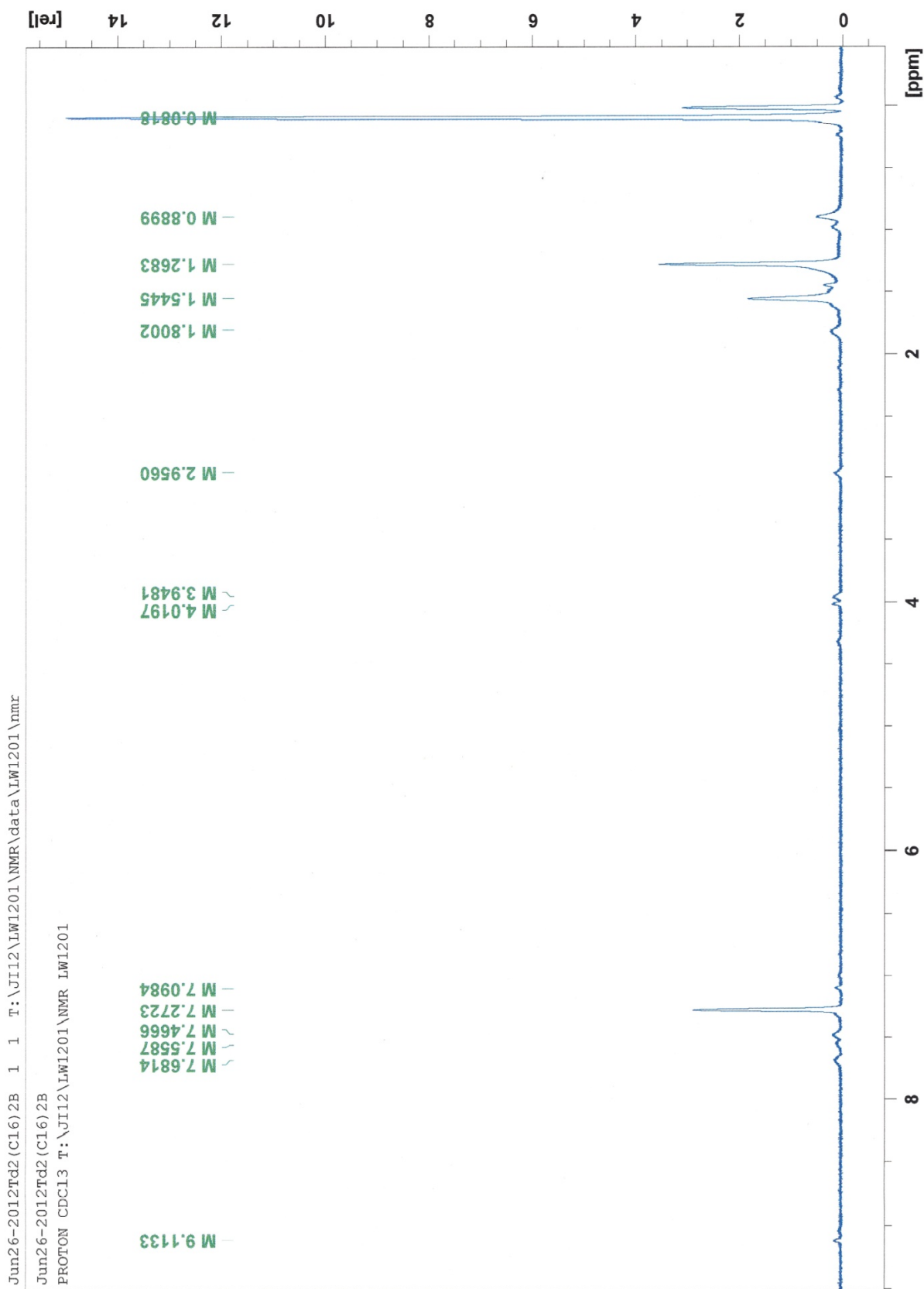


Spectrum 16: BTdB <sup>13</sup>C NMR

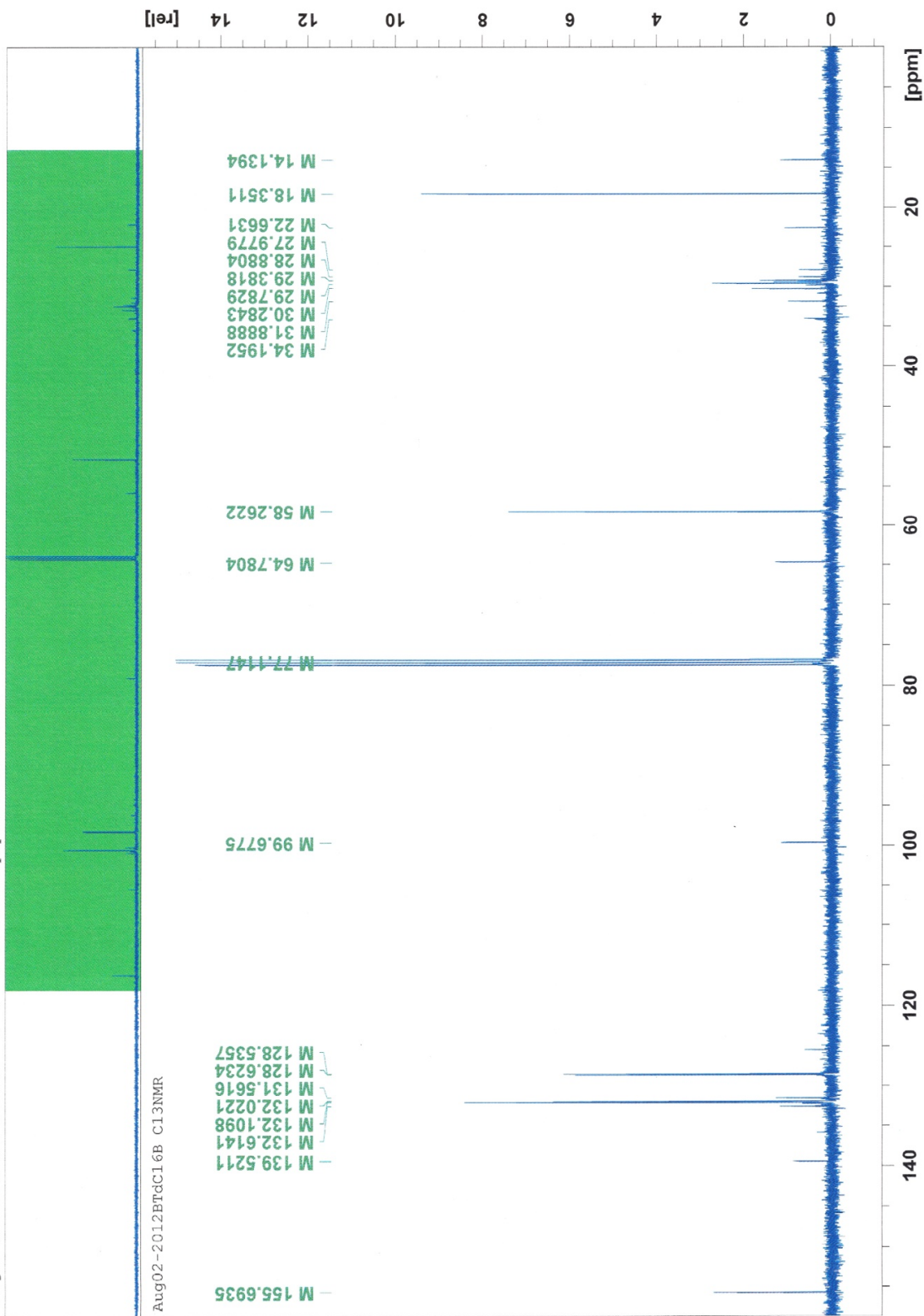


Spectrum 17: DBrHq <sup>1</sup>H NMR

Spectrum 18: DBrBC<sub>16</sub> <sup>1</sup>H NMR

Spectrum 19: BTdBC<sub>16</sub> <sup>1</sup>H NMR

"Aug02-2012BTdC16B C13NMR" 1 1 C:\Bruker\TopSpin3.0\examdata



Spectrum 20: BTdBC<sub>16</sub> <sup>13</sup>C NMR

## APPENDIX B

### X-ray Structure Data

Table	Page
1. Atomic parameters of BTPm .....	77
2. Anisotropic displacement parameters, in Å <sup>2</sup> (BTPm) .....	78
3. Selected geometric informations of BTPm (A) .....	78
4. Selected geometric informations of BTPm (B) .....	79
5. Selected geometric informations of BTPm(C) .....	80

**Table 1:** Atomic parameters of BTPm

Atomic parameters								
Atom	Ox.	Wyck.	Site	S.O.F.	x/a	y/b	z/c	U [ $\text{\AA}^2$ ]
N2		2a	1		0.5572(3)	0.8236(5)	0.8728(2)	
N1		2a	1		0.5771(3)	0.7333(6)	0.6676(2)	
C9		2a	1		0.4150(3)	0.4896(7)	0.7213(3)	
C12		2a	1		0.4797(3)	0.5486(7)	0.6374(3)	
H9		2a	1		0.4536	0.4546	0.5566	0.04
C10		2a	1		0.4618(3)	0.6386(8)	0.8408(3)	
H11		2a	1		0.4233	0.6053	0.9013	0.043
C11		2a	1		0.6115(3)	0.8644(7)	0.7844(3)	
S1		2a	1	0.71	0.79642(19)	1.1287(3)	0.71660(16)	
C1		2a	1	0.71	0.7173(3)	1.0673(6)	0.8169(3)	
C2		2a	1	0.71	0.7712(8)	1.2468(16)	0.9268(7)	
H2		2a	1	0.71	0.7427	1.245	0.9964	0.051
C3		2a	1	0.71	0.8646(15)	1.418(3)	0.9257(12)	
H3		2a	1	0.71	0.905	1.5488	0.9912	0.056
C4		2a	1	0.71	0.8938(11)	1.380(2)	0.8183(9)	
H4		2a	1	0.71	0.9584	1.478	0.8015	0.056
S2		2a	1	0.764	0.22293(15)	0.2229(3)	0.78225(15)	
C5		2a	1	0.764	0.3069(3)	0.2877(6)	0.6855(3)	
C6		2a	1	0.764	0.2483(9)	0.1264(18)	0.5698(7)	
H6		2a	1	0.764	0.2758	0.138	0.4997	0.056
C7		2a	1	0.764	0.1514(11)	-0.044(2)	0.5648(8)	
H7		2a	1	0.764	0.11	-0.1686	0.496	0.055
C8		2a	1	0.764	0.1211(7)	-0.0141(16)	0.6726(5)	
H8		2a	1	0.764	0.0535	-0.1098	0.6855	0.053

**Table 2:** Anisotropic displacement parameters, in  $\text{\AA}^2$  (BTPm)

<b>Anisotropic displacement parameters, in <math>\text{\AA}^2</math></b>						
<b>Atom</b>	<b>U<sub>11</sub></b>	<b>U<sub>22</sub></b>	<b>U<sub>33</sub></b>	<b>U<sub>12</sub></b>	<b>U<sub>13</sub></b>	<b>U<sub>23</sub></b>
N2	0.0388(15)	0.0431(18)	0.0315(14)	-0.0018(14)	0.0197(13)	0.0005(15)
N1	0.0365(14)	0.0370(17)	0.0288(13)	-0.0009(13)	0.0157(11)	0.0016(14)
C9	0.0303(16)	0.0255(18)	0.0298(15)	0.0025(13)	0.0156(13)	0.0031(15)
C12	0.0387(18)	0.039(2)	0.0242(15)	0.0001(15)	0.0145(14)	-0.0017(16)
C10	0.0382(17)	0.046(2)	0.0317(16)	-0.0008(17)	0.0230(14)	0.0006(18)
C11	0.0305(17)	0.038(2)	0.0295(16)	0.0020(15)	0.0133(14)	0.0017(17)
S1	0.0454(8)	0.0423(9)	0.0405(8)	-0.0047(7)	0.0282(6)	-0.0010(6)
C1	0.0347(17)	0.035(2)	0.0325(17)	0.0060(14)	0.0156(14)	0.0068(17)
C2	0.045(3)	0.055(4)	0.042(3)	0.007(3)	0.032(3)	-0.006(3)
C3	0.043(3)	0.039(3)	0.051(3)	-0.0050(18)	0.0140(19)	-0.005(2)
C4	0.036(3)	0.044(3)	0.058(3)	-0.0041(19)	0.019(3)	0.007(3)
S2	0.0467(7)	0.0524(10)	0.0417(8)	-0.0105(7)	0.0299(6)	-0.0059(7)
C5	0.0328(16)	0.034(2)	0.0354(17)	0.0057(15)	0.0153(15)	0.0061(17)
C6	0.077(4)	0.042(3)	0.037(4)	-0.005(3)	0.042(3)	-0.010(3)
C7	0.052(3)	0.028(3)	0.052(3)	-0.0106(19)	0.016(2)	0.000(3)
C8	0.036(4)	0.040(3)	0.060(4)	-0.006(2)	0.023(4)	0.010(3)

**Table 3:** Selected geometric information of BTPm (A)

<b>A) Selected geometric informations</b>			
<b>Atoms 1,2</b>	<b>d 1,2 [<math>\text{\AA}</math>]</b>	<b>Atoms 1,2</b>	<b>d 1,2 [<math>\text{\AA}</math>]</b>
N2—C10	1.3168(46)	C2—C3	1.3263(185)
N2—C11	1.3362(50)	C2—H2	0.9300(93)
N1—C12	1.3317(45)	C3—C4	1.3465(200)
N1—C11	1.3368(41)	C3—H3	0.9308(132)
C9—C12	1.3946(55)	C4—H4	0.9306(122)
C9—C10	1.3961(46)	S2—C5	1.6843(43)
C9—C5	1.4652(45)	S2—C8	1.7119(68)
C12—H9	0.9303(33)	C5—C6	1.4018(81)
C10—H11	0.9297(39)	C6—C7	1.3316(150)
C11—C1	1.4548(45)	C6—H6	0.9298(98)
S1—C1	1.6730(45)	C7—C8	1.3527(132)
S1—C4	1.7124(94)	C7—H7	0.9316(87)
C1—C2	1.4113(79)	C8—H8	0.9303(80)

**Table 4:** Selected geometric information of BTPm (B)

<b>B) Selected geometric informations</b>			
<b>Atoms 1,2,3</b>	<b>Angle 1,2,3 [°]</b>	<b>Atoms 1,2,3</b>	<b>Angle 1,2,3 [°]</b>
C10—N2—C11	116.572(305)	C1—C2—H2	121.693(661)
C12—N1—C11	116.680(268)	C2—C3—C4	111.848(1226)
C12—C9—C10	114.414(280)	C2—C3—H3	124.079(1427)
C12—C9—C5	122.204(315)	C4—C3—H3	124.073(1232)
C10—C9—C5	123.383(299)	C3—C4—S1	111.222(805)
N1—C12—C9	123.033(324)	C3—C4—H4	124.328(1195)
N1—C12—H9	118.485(315)	S1—C4—H4	124.450(918)
C9—C12—H9	118.482(304)	C5—S2—C8	93.001(258)
N2—C10—C9	123.844(309)	C6—C5—C9	129.948(432)
N2—C10—H11	118.092(352)	C6—C5—S2	107.114(381)
C9—C10—H11	118.065(303)	C9—C5—S2	122.863(262)
N2—C11—N1	125.448(270)	C7—C6—C5	116.979(735)
N2—C11—C1	117.908(307)	C7—C6—H6	121.522(956)
N1—C11—C1	116.643(283)	C5—C6—H6	121.499(665)
C1—S1—C4	93.146(389)	C6—C7—C8	111.432(892)
C2—C1—C11	130.639(414)	C6—C7—H7	124.300(996)
C2—C1—S1	107.195(369)	C8—C7—H7	124.267(809)
C11—C1—S1	122.152(264)	C7—C8—S2	111.330(501)
C3—C2—C1	116.556(832)	C7—C8—H8	124.382(759)
C3—C2—H2	121.751(1007)	S2—C8—H8	124.288(633)

**Table 5:** Selected geometric information of BTPm (C)

<b>C) Selected geometric informations</b>			
<b>Atoms 1,2,3,4</b>	<b>Tors. an. 1,2,3,4 [°]</b>	<b>Atoms 1,2,3,4</b>	<b>Tors. an. 1,2,3,4 [°]</b>
C11—N1—C12—C9	-0.140(491)	C11—C1—C2—C3	-177.331(814)
C10—C9—C12—N1	-0.634(495)	S1—C1—C2—C3	1.303(999)
C5—C9—C12—N1	179.282(312)	C1—C2—C3—C4	-2.010(1517)
C11—N2—C10—C9	-0.774(501)	C2—C3—C4—S1	1.742(1449)
C12—C9—C10—N2	1.123(509)	C1—S1—C4—C3	-0.866(943)
C5—C9—C10—N2	-178.793(319)	C12—C9—C5—C6	-0.875(707)
C10—N2—C11—N1	-0.129(500)	C10—C9—C5—C6	179.034(556)
C10—N2—C11—C1	-179.93(30)	C12—C9—C5—S2	-177.317(273)
C12—N1—C11—N2	0.572(503)	C10—C9—C5—S2	2.592(483)
C12—N1—C11—C1	-179.625(295)	C8—S2—C5—C6	1.777(486)
N2—C11—C1—C2	-3.663(667)	C8—S2—C5—C9	178.924(357)
N1—C11—C1—C2	176.518(516)	C9—C5—C6—C7	179.320(643)
N2—C11—C1—S1	177.878(255)	S2—C5—C6—C7	-3.807(905)
N1—C11—C1—S1	-1.940(441)	C5—C6—C7—C8	4.238(1198)
C4—S1—C1—C2	-0.202(532)	C6—C7—C8—S2	-2.596(1038)
C4—S1—C1—C11	178.573(443)	C5—S2—C8—C7	0.386(648)

## LITERATURE CITED

- <sup>1</sup> Liu, Y.; Li, Y.; Schanze, K.A. Photophysics of  $\pi$ -conjugated oligomers and polymers that contain transition metal complexes. *J. Photochem. Photobio. C: Photochem. Rev.* **2002**, 3, 1-23.
- <sup>2</sup> Wong, C. T.; Chan, W.K. Yellow light-emitting poly(phenylenevinylene) incorporated with pendant ruthenium bipyridine and terpyridine complexes. *Adv. Mat.* **1999**, 11, 6, 455-459.
- <sup>3</sup> MacDiarmid, A.G. Synthetic Metals: A Novel Role For Organic Polymers. *Angew. Chem. Int. Ed.* **2001**, 40, 2581-2590.
- <sup>4</sup> Zotti, G.; Schiavon, G. Electrochemical n-doping of poly(dithienylvinylene). A comparison of cyclovoltammetric and conductive properties in n- and p-doping. *Synth. Met.* **1994**, 63, 53-56.
- <sup>5</sup> Fu, Y.; Wang, H.; Chen, M.; Shen, W. A DFT study of the effects of donor-to-acceptor ratio on the electronic properties of copolymers based on tricyclic non-classical thiophene. *Mol. Sim.* **2011**, 37, 6, 478-87.
- <sup>6</sup> Pozo-Gonzalo, C.; Pomposo, J.A.; Rodriguez, J.; Schmidt, E.Y.; Vasiltssov, A.M.; Zorina, N.V.; Ivanov, A.V.; Trofimov, B.A.; Mikhaleva, A.I.; Zaitsev, A.B. Synthesis and electrochemical study of narrow band gap conducting polymers based on 2,2'-dipyrroles linked with conjugated aza-spacers. *Synth. Met.* **2007**, 157, 60-65.
- <sup>7</sup> Yamaguchi, I.; Mitsuno, H. Synthesis of n-Type  $\pi$ -Conjugated Polymers with Pendant Crown Ether and Their Stability of n-Doping State Against Air. *Macromolecules.* **2010**, 43, 9348-9354.
- <sup>8</sup> Eiji, I.; Takanori, Y.; Keiichi, M. Injection control and thermally stimulated current in ionic polarized polymer based light emitting diode. *Thin Solid Films.* **2003**, 438-439, 142-146.
- <sup>9</sup> Moliton, A.; Hiorns, R.C. Review of electronic and optical properties of semiconducting  $\pi$ -conjugated polymers: applications in optoelectronics. *Polym Int.* **2004**, 53, 1397-1412.
- <sup>10</sup> Tanaka, S.; Yamashita, Y. Synthesis of narrow band gap heterocyclic copolymer of aromatic-donor and quinonoid-acceptor units. *Synth, Met.* **1995**, 69, 599-600.

- <sup>11</sup> Surjan, P.; Karoly, N. Quinoid-aromatic competition as a tool for band structure design for conjugated polymers. *Synth. Met.* **1993**, 4261-4265.
- <sup>12</sup> Irvin, D.J.; Stenger-Smith, J.D.; Yandek, G.R.; Carberry, J.; Currie, D.A.; Theodoropoulou, N.; Irvin, J. A. Enhanced Electrochemical Response of Solution-Deposited n-Doping Polymer via Co-Casting with Ionic Liquid. *J. Appl. Polym. Sci. B: Polym. Phys.* **2012**, 50, 1145-1150.
- <sup>13</sup> de Leeuw, D.M.; Simenon, M.M.J.; Brown, A.R.; Einerhand, R.E.F. Stability of n-type doped conducting polymers and consequences for polymeric microelectronic devices. *Synth. Met.* **1997**, 87, 53-59.
- <sup>14</sup> Zotti, G.; Schiavon, G.; Zecchin, S. Irreversible processes in the electrochemical reduction of polythiophenes. Chemical modifications of the polymer and charge-trapping phenomena. *Synth. Met.* **1995**, 72, 3, 275-281.
- <sup>15</sup> Zotti, G.; Schiavon, G.; Zecchin, S.; Berlin, A.; Pagani, G. Electrochemical reduction of 4-ylidene-substituted polycyclopentadithiophenes. Polythiophene chain bridging by electrohydrodimerization. *Synth. Met.* **1994**, 66, 149-155.
- <sup>16</sup> Beaujuge, P.M., Reynolds, J.R. Color Control in  $\pi$ -Conjugated Organic Polymers for Use in Electrochromic Devices. *Chem. Rev.* **2010**, 110, 268–320.
- <sup>17</sup> Mishra, S.P.; Akshaya, K.; Manorian, P. Synthesis and characterization of soluble narrow gap polymers based on diketopyrrolopyrrole and propylenedioxythiophenes. *Synth. Met.* **2010**, 160, 2422–2429.
- <sup>18</sup> Heck, R.F. Acylation, methylation, and carboxyalkylation of olefins by Group VIII metal derivatives. *J. Am. Chem. Soc.* **1968**, 90, 5518-5526.
- <sup>19</sup> Negishi, E.I.; King, A. O.; Okukado, N. Selective carbon-carbon bond formation via transition metal catalysis. 3. A highly selective synthesis of unsymmetrical biaryls and diarylmethanes by the nickel- or palladium-catalyzed reaction of aryl- and benzylzinc derivatives with aryl halides. *J. Org. Chem.* **1977**, 42, 1821-1823.
- <sup>20</sup> Bäckvall, J.E. Scientific Background on the Nobel Prize in Chemistry 2010: Palladium-catalyzed cross couplings in organic synthesis. *Kungl. Vetenskaps-akademien*. November, **2008**, 1-12.
- <sup>21</sup> Miyaura, N.; Yamada, K.; Suzuki, A. A new stereospecific cross-coupling by the palladium-catalyzed reaction of 1-alkenylboranes with 1-alkenyl or 1-alkynyl halides. *Tetrahedron Lett.* **1979**, 20, 3437-40.
- <sup>22</sup> Kosugi, M.; Shimizu, Y.; Migita, T. Reactions of allyltin compounds of aromatic halides with allyltributyltin in the presence of tetrakis(triphenylphosphine)palladium(0). *Chem. Lett.* **1977**, 6, 3, 301-302.

- <sup>23</sup> Nobel Prizes in Chemistry.  
[http://www.nobelprize.org/nobel\\_prizes/chemistry/laureates/](http://www.nobelprize.org/nobel_prizes/chemistry/laureates/)(accessed 07/22/2012), part of Nobel Prize. <http://www.nobelprize.org/> (accessed 07/22/2012).
- <sup>24</sup> Toudic, F.; Heynderickx, A.; Plé, N.; Turck, A.; Quéguiner, G. Regioselective synthesis and metallation of tributylstannylfluoropyrazines. Application to the synthesis of some new fluorinated liquid crystals diazines. Paart 34. *Tetrahedron*. **2003**, *59*, 6375-6384.
- <sup>25</sup> Schaffer, M.A.; Marchildon, M.A.; McAuley, E.K.; Cunningham, M.F. Thermal nonoxidative degradation of nylon 6,6. *Rev. Macromol. Chem. Phys.* **2000**, *C40*, 4, 233–272.
- <sup>26</sup> Malinauskas, A. Chemical Deposition of Conducting Polymers. *Polymer*. **2001**, *42*, 3957-3972.
- <sup>27</sup> Stefan, M.C.; Javier, A.E.; Osaka, I.; McCullough, R.D. Grignard Metathesis Method (GRIM): Toward a Universal Method for the Synthesis of Conjugated Polymers. *Macromolecules*. **2009**, *42*, 30-32.
- <sup>28</sup> Facchetti, A.  $\pi$ -Conjugated Polymers for Organic Electronics and Photovoltaic Cell Applications. *Chem. Mater.* **2011**, *23*, 733–758.
- <sup>29</sup> Winter, M.; Brodd, R. J. What are batteries, fuel cells, and supercapacitors? *Chem. Rev.* **2004**, *104*, 4245.
- <sup>30</sup> Irvin, J.; Irvin, D.; Stenger-Smith, J.D. Electrically Active Polymers for Use in Batteries and Supercapacitors. In *Handbook of Conducting Polymers*; 3rd Ed., T. Skotheim and J. R. Reynolds, eds., Taylor & Francis: Boca Raton, FL, **2007**; pp 9.1-9.29.
- <sup>31</sup> Arbizzani, C.; Catelani, M.; Mastragostino, M.; Mingazzini, C. n- And p-Doped Polythieno[3,4-B:3',4'-D] Thiophene: A Narrow Band Gap Polymer for Redox Supercapacitors. *Electrochim. Acta*. **1995**, *40*, 12, 1871-1876.
- <sup>32</sup> Bernede, J.C. Organic photovoltaic cells: history, principle and techniques. *J. Chil. Chem. Soc.* **2008**, *53*, 3, 1549-1564.
- <sup>33</sup> Anthony, J. E. Small-Molecule, Nonfullerene Acceptors for Polymer Bulk Heterojunction Organic Photovoltaics. *Chem. Mater.* **2011**, *23*, 583–590.
- <sup>34</sup> Chaignaud, M.; Gillaizeau, I.; Ouhamou, N.; Coudert, G. New highlights in the synthesis and reactivity of 1,4-dihydropyrazine derivatives. *Tetrahedron*. **2008**, *64*, 8059-8066.
- <sup>35</sup> Yamamoto, T.; Fujiwara, Y.; Fukumoto, H.; Nakamura, Y.; Koshihara, S.; Ishikawa, T. Preparation of a new poly( p-phenylene) type polymer, poly(pyrazine-2,5-diyl), with a

coplanar structure. *Polymer*. **2003**, 44, 4487–4490.

<sup>36</sup> Tanaka, S.; Kaeriyama, K.; Hirajde, T. Properties of poly[2,5-bis(2-thienyl)thiazole] and poly[bis(2-thienyl)pyridine]s. *Die Makromolekulare Chemie, Rapid Communications*. **1988**, 9, 11, 743-748.

<sup>37</sup> Dubois, C.J.; Reynolds, J.R. 3,4-Ethylenedioxythiophene-Pyridine-Based Polymers: Redox or n-Type Electronic Conductivity? *Adv. Mater.* **2002**, 14, 1844-1847.

<sup>38</sup> Process-Auto: Automatic Data Acquisition and Processing Package for Imaging Plate and CCD Diffractometers, Rigaku Corporation, 3-9-12 Matsubara, Akishima, Tokyo 196-8666, JAPAN, 2006.

<sup>39</sup> SHELXL97, Sheldrick, G. M., University of Gottingen, Germany, 1997.

<sup>40</sup> Winkel, K. Low band gap donor-acceptor strategies for stable n-doping. Master Thesis, Texas State University, San Marcos, Texas, August 2011.

<sup>41</sup> Jenks, W.S.; Matsunaga, N.; Gordon, M. The Effects of Conjugation and Aromaticity on the Sulfoxide Bond. *J. Org. Chem.* **1996**, 61, 1275-1283.

<sup>42</sup> Amaral, S.S.; Campos, P.T.; dos Santos, J.M.; Fernandes, L.S.; Martin, M.A.P.; Bonacorso, H.G.; Zanatta, N. Crystal Structure, Aromatic Character and AM1 Calculations of 2-(N'-Benzylidenehydrazino)-4-trifluoromethyl-pyrimidine and 2-(N'-Methylbenzylidenehydrazino)-5-methyl-4-trifluoromethyl-pyrimidine. *The Open Crystallography Journal*. **2010**, 3, 59-66.

<sup>43</sup> Liu, J.Q.; Wang, Y.Y.; Zhang, Y.N.; Liu, P.; Shi, Q.Z.; Batten, S.R. Topical diversification in metal-organic frameworks: secondary ligand and metal effects. *Eur. J. Inorg. Chem.* **2009**, 147-154.

<sup>44</sup> Sotzing, G.A.; Reynolds, J.R.; Steel, P.J. Electrochromic Conducting Polymers via Electrochemical Polymerization of Bis(2-(3,4-ethylenedioxy)thienyl) Monomers. *Chem. Mater.* **1996**, 8, 882-889.

<sup>45</sup> Irvin, J.A.; Schwendeman, I.; Lee, K. A. Abboud, Y.L.; Reynolds, J.R. Low Oxidation Potential Conducting Polymers Derived from 3,4-Ethylenedioxythiophene and Dialkoxybenzenes. *J. Polym. Sci. A: Polym. Chem.* **2001**, 39, 13, 2164-2178.

<sup>46</sup> Schwab, P.F.; Fleischer, F.; Michl, J. Preparation of 5-brominated and 5,5'-dibrominated 2,2'-bipyridines and 2,2'-biprimidines. *J. Org. Chem.* **2002**, 67, 2, 443-449.

<sup>47</sup> Zissel, R.; Stroh, C. Segmented multitopic ligands constructed from bipyrimidine, phenanthroline, and terpyridine modules. *Tetrahedron Letters*. **2004**, 45, 4051-4055.

<sup>48</sup> Song, B.; Wu, G.; Wang, Z.; Zhang, X. Metal-Ligand Coordination-Induced Self-

- Assembly of Bolaamphiphiles Bearing Bipyrimidine. *Langmuir Let.* **2009**, 25 (23), 13306-13310.
- <sup>49</sup> Dillow, G.W.; Kebarle, P. Electron affinities of aza-substituted polycyclic aromatic hydrocarbons. *Can. J. Chem.* **1989**, 67, 1628-1631.
- <sup>50</sup> Klein, B.; Hetman, N.E.; O'Donnel, M.E. Pyrazines. 111. The Action of Phosphoroyl Chloride on Pyrazine N-Oxides. *J. Org. Chem.* **1963**, 28, 6, 1682-1686.
- <sup>51</sup> Zarras, P.; Irvin, J. Electrically Active Polymers. In *Encyclopedia of Polymer Science and Technology*, 3rd ed.; Wiley Interscience: New York, NY, 2004.
- <sup>52</sup> Mosquera, A.; Riveiros, R.; Sestelo, J.P.; Sarandeses, L.A. Cross-Coupling Reactions of Indium Organometallics with 2,5-Dihalopyrimidines: Synthesis of Hyrtinadine A. *Org. Lett.* **2008**, 10, 17, 3745-3748.
- <sup>53</sup> Witker, D.L.; Clancy, S.O.; Irvin, D.J.; Stenger-Smith, J.D.; Irvin, J.A. Electrochemical Deposition of a New n-Doping Polymer Based on Bis(thienyl)isopyrazole. *J. Electrochem. Soc.* **2007**, 154, G95-G98.
- <sup>54</sup> Belletête, M.; Beaupre, S.; Bouchard, J.; Blondin, P.; Leclerc, M.; Durocher, G. Theoretical and Experimental Investigations of the Spectroscopic and Photophysical Properties of Fluorene-Phenylene and Fluorene-Thiophene Derivatives, Precursors of Light Emitting Polymers. *J. Phys. Chem. B.* **2000**, 104, 39, 118-125.
- <sup>55</sup> Sun, H.; DiMugno, S.G. Room-Temperature Nucleophilic Aromatic Fluorination: Experimental and Theoretical Studies. *Angew. Chem. Int. Ed.* **2006**, 45, 2720-2725.
- <sup>56</sup> Wang, H.; Cheng, P.; Liu, Y.; Chen, J.; Zhan, X.; Hu, W.; Shuai, Z.; Li, Y.; Zhu, D. A Conjugated polymer based on 5,5'-bibenzo[c][1,2,5]thiadiazole for high-performance solar cells. *J. Mat. Chem.* **2012**, 22, 8, 3432-3439.
- <sup>57</sup> Soe, Y.H.; Lee, W.H.; Park, J.H.; Bae, C.; Hong, Y.; Park, J.W.; Kang, I.N. Side-Chain Effects on Phenothiazine-Based Donor-Acceptor Copolymer Properties in Organic Photovoltaic Devices. *J. Polym. Sci. A: Polym. Chem.* **2012**, 50, 649-658.
- <sup>58</sup> Yang, Z.; Yang, S.; Zhang, J. Ground- and Excited-State proton Transfer and Rotamerism in 2-(2-Hydroxyphenyl)-5-Phenyl-1,3,4-oxadiazole and Its O'/NH or S'-Substituted Derivatives. *Appl. Phys. Lett.* **2008**, 93, 111, 6354-6360.
- <sup>59</sup> Yasuda, T.; Imase, T.; Nakamura, Y.; Yamamoto, T. New Alternative Donor-Acceptor Arranged Poly(Aryleneethynylene)s and Their Related Compounds Composed of Five-Membered Electron-Accepting 1,3,4-Thiadiazole, 1,2,4-Triazole, or 3,4-Dinitrothiophene Units: Synthesis, Packing Structure, and Optical Properties. *Macromolecules.* **2005**, 38, 11, 4687-4697.
- <sup>60</sup> Sato, M.; Yamauchi, M.H.; Kasuga, K. Synthesis and optical properties of new

conjugated polymers composed of 1,3,4-thiadiazole and 2,5-dialkoxybenzene rings. *Macromol. Rapid Commun.* **2000**, 21, 1234-1237.

<sup>61</sup> Granadino-Roldán, J.M.; Garzón, A.; García, G.; Moral, M.; Navaroo, A.; Fernández-Lienres, M.P.; Peña-Ruiz, T.; Fernández-Gómez, M. Theoretical Study of the Effect of Alkyl and Alkoxy Lateral Chains on the Structural and Electronic Properties of  $\pi$ -Conjugated Polymers Consisting of Phenylethynyl-1,3,4-thiadiazole. *J. Phys. Chem. C.* **2011**, 115, 2865–2873.

<sup>62</sup> Garzón, A.; Granadino-Roldán, J.M.; Moral, M.; García, G.; Fernández-Lienres, M.P.; Navaroo, A.; Peña-Ruiz, T.; Fernández-Gómez, M. Density functional theory study of the optical and electronic properties of oligomers based on phenyl-ethynyl units linked to triazole, thiadiazole, and oxadiazole rings to be used in molecular electronics. *J. Chem. Phys.* **2010**, 132, 064901, 1-11.

<sup>63</sup> Hennrich, G.; Omenat, A.; Asselberghs, I.; Foerier, S.; Clays, K.; Verbiest, T.; Serrano, J.L. Liquid Crystals from C<sub>3</sub>-Symmetric Mesogens for Second-Order Nonlinear Optics. *Angew. Chem. Int. Ed.* **2006**, 45, 4203-4206.

<sup>64</sup> Irvin, J.A. Low-oxidation-potential-conducting polymers: alternating substituted para-phenylene and 3,4-ethyldioxythiophene repeat units. *Polymer.* **1998**, 39, 11, 2339-2347.

<sup>65</sup> Abd-El-Aziz, A. S.; Shipman, P. O.; Boden, B.N.; McNeil, W.S. Synthetic methodologies and properties of organometallic and coordination macromolecules. *Prog. Polym. Sci.* **2010**, 35, 714-836.

<sup>66</sup> Pickup, P. G. Conjugated metallopolymers. Redox polymers with interacting metal based redox sites. *J. Mater. Chem.* **1999**, 9, 1641-1653.

<sup>67</sup> Ng, P. K.; Gong, X.; Chan, S.H.; Lam, L.S.; Chan, W.K. The role of ruthenium and rhenium diimine complexes in conjugated polymers that exhibit interesting opto-electronic properties. *Chem. Eur. J.* **2001**, 7, 20, 4358-4367.

## VITA

Makda Tesfaselassie Araya was born in Asmara, Eritrea, on September 27, 1984, the daughter of Dr. Tesfaselassie Araya and Zafu Mebrahtu Habte. After graduation from Robert Leon Turner High School, Carrollton, Texas, in August of 2003, she obtained her Bachelor of Science in Biochemistry and Biology from University of Texas at Dallas in December 2007. She worked as a microbiologist in Grand Prairie, Texas for a few years and entered Texas State University-San Marcos in August 2010 to pursue a Master of Science in Chemistry.

Permanent address: Makdaal@yahoo.com

This thesis was typed by Makda T. Araya.